AD_____

Award Number: DAMD17-03-1-0081

TITLE: The Role of the Y-Located TSPY Gene in Prostatic Oncogenesis

PRINCIPAL INVESTIGATOR: Yun-Fai Chris Lau, Ph.D.

CONTRACTING ORGANIZATION: Northern California Institute for Research and Education
San Francisco, CA 94121

REPORT DATE: February 2006

TYPE OF REPORT: Annual

PREPARED FOR: U.S. Army Medical Research and Materiel Command
Fort Detrick, Maryland 21702-5012

REPORT DOCUMENTATION PAGE

Form Approved
OMB No. 0704-0188

1. REPORT DATE	2. REPORT TYPE	3. DATES COVERED
01-02-2006	Annual	1 Feb 2005 – 31 Jan 2006

4. TITLE AND SUBTITLE

The Role of the Y-Located TSPY Gene in Prostatic Oncogenesis

5a. CONTRACT NUMBER

5b. GRANT NUMBER
DAMD17-03-1-0081

5c. PROGRAM ELEMENT NUMBER

6. AUTHOR(S)

Yun-Fai Chris Lau, Ph.D.

5d. PROJECT NUMBER

5e. TASK NUMBER

5f. WORK UNIT NUMBER

7. PERFORMING ORGANIZATION NAME(S) AND ADDRESS(ES)

Northern California Institute for
Research and Education
San Francisco, CA 94121

8. PERFORMING ORGANIZATION REPORT NUMBER

9. SPONSORING / MONITORING AGENCY NAME(S) AND ADDRESS(ES)
U.S. Army Medical Research and Materiel Command
Fort Detrick, Maryland 21702-5012

10. SPONSOR/MONITOR'S ACRONYM(S)

11. SPONSOR/MONITOR'S REPORT NUMBER(S)

12. DISTRIBUTION / AVAILABILITY STATEMENT
Approved for Public Release; Distribution Unlimited

13. SUPPLEMENTARY NOTES
Original contains colored plates: ALL DTIC reproductions will be in black and white.

14. **ABSTRACT**

The TSPY gene is the only functional gene within the critical region harboring the gonadoblastoma locus on the Y chromosome (GBY). Expression studies demonstrated that it is aberrantly expressed in prostate cancer. This project is designed to address the role of this putative oncogene on the Y chromosome in this male-specific cancer. The objectives are: 1) to identify the oncogenic or tumor promoting domain in TSPY, and 2)to correlate TSPY over-expression with prostatic oncogenesis in transgenic mice. For the past year, we have examined the TSPY expression in additional 61 cases of prostate cancer and demonstrated that its expression is proportional to the degrees of malignancy of these clinical samples. Similar study of a tissue recombination model of prostate cancer demonstrated the same results, suggesting TSPY expression is intimately associated with prostate cancer. Significantly, studies of a line of transgenic mice harboring 50 copies of the human TSPY gene on their Y chromosome demonstrated that TSPYis expressed in hyperplasic regions of the prostates of old mice, resembling those of latent cancer in old men. These findings are significant, supporting the role of TSPY in the initiation of prostatic oncogenesis. For the next 12-month period, we plan to continue our characterization of our transgenic mice to confirm TSPY as an oncogene.

15. SUBJECT TERMS
Y chromosome gene, prostate cancer, transgenic mouse, molecular

16. SECURITY CLASSIFICATION OF:			17. LIMITATION OF ABSTRACT	18. NUMBER OF PAGES	19a. NAME OF RESPONSIBLE PERSON
					USAMRMC
a. REPORT	b. ABSTRACT	c. THIS PAGE			19b. TELEPHONE NUMBER *(include area code)*
U	U	U	UU	74	

Standard Form 298 (Rev. 8-98)
Prescribed by ANSI Std. Z39.18

Table of Contents

INTRODUCTION

The TSPY gene is a tandemly repeated gene on he short arm of the human Y chromosome. Genetic mapping and complete sequencing of the human Y chromosome demonstrated that TSPY is located in the critical region harboring the only oncogenic or tumor promoting locus, termed gonadoblastoma on Y (GBY), on this male-specific chromosome. TSPY is postulated serve a function in spermatogonia by directing their division in spermatogenesis. When it is aberrantly expressed in tissues, such as the epithelial cells of the prostate, incapable of entering spermatogenesis, it exerts an oncogenic or tumor promoting effects, and in collaboration with other oncogenic events, leading to oncogenesis. The majority of our efforts for the third year are focused on the two specific aims proposed in the original application.

BODY

Task 1. To identify the oncogenic and/or tumor promoting properties of TSPY

In order to substantiate TSPY as an oncogene or tumor promoter, we have examined its expression in about 60 more cases of prostate cancers of different clinical stages. The results showed that TSPY expression increases with increasing Gleason grades, supporting the postulation that TSPY is a putative oncogene on the human Y chromosome.

Expression of TSPY in Human Prostate Cancer

Previously, we have investigated the role of the Y chromosome in prostate cancer by examining the expression of 31 Y chromosome genes in prostate cancer of various degrees of malignancy and prostatic cell lines [1]. The results from this initial survey identified the TSPY gene to be a strong candidate gene from the male-specific chromosome that could potentially contribute to prostatic oncogenesis. TSPY was expressed at heterogeneous levels in prostatic samples of various degrees of malignancy. Its expression could be stimulated by androgen in the prostatic cell line, LNCaP.

We further studied the TSPY expression by in situ mRNA hybridization and immunostaining on prostatic sections from 11 patients suffering from prostate cancer of various Gleason grades [2]. Both RNA and protein studies corroborated with each others, demonstrate a

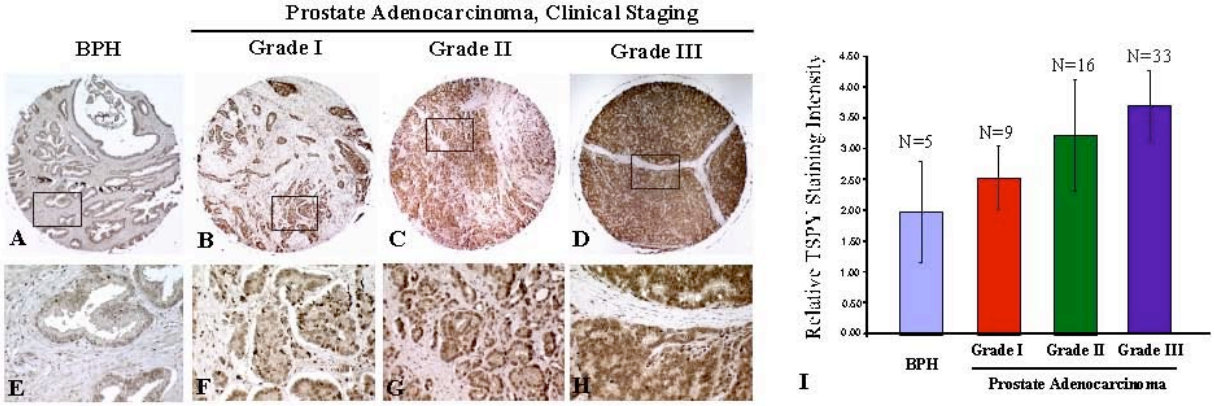

Figure 1. Immunostaining of BPH and various grades of prostate adenocarcinoma with TSPY antibody in a tissue array consisting of 63 samples. **A-D** show samples of BPH, grade I, II, and III prostate adenocarcinoma, boxed areas are represented in **E-H** respectively. **I** shows the relatively immunostaining intensity of TSPY in these samples. Grade I = well differentiated, Gleason score 6 or less; II = intermediate, Gleason ~ 7; III = high grade, Gleason > 8.

low-level expression of TSPY gene in morphologically normal epithelia, an elevated level in hyperplastic and cancer epithelia of low Gleason grades and the highest levels on cancer cells of

high Gleason grades. Hence, there is a parallel increase in TSPY expression with malignancy in prostate cancer.

Recently, we had performed a similar immunostaining study on a tissue array consisting of 63 specimens of BPH and prostate cancer of various clinical stages (i.e. I, II and III). The intensity of TSPY was scored on an arbitrary scale of 1 to 5, i.e. light to intense staining (Figure 1). Our results clearly confirm those of previous studies, establishing the fact that TSPY expression increases with the degree of malignancy among these prostate cancer samples.

Task 2. To Correlate TSPY Over-Expression with Prostatic Oncogenesis in Transgenic Mice

Expression of TSPY in a Tissue Recombination Model of Prostate Cancer

In adult prostate, homeostasis is maintained via reciprocal stromal and epithelial interactions [3, 4]. During carcinogenesis, following genetic damage to the epithelium, such reciprocal interactions are disrupted, favoring proliferation for the epithelial cells. Recently, excellent tissue recombination models of stromal-epithelial interactions have been established pirmarily in Dr. Gerald Cunha's laboratory at UCSF and used to study the hormonal and genetic determinants involved in normal and malignant prostatic growth. One such model utilizes an SV40 T antigen-immortalized non-tumorigenic human prostatic epithelial cell line, BPH-1, and stromal cells from various sources [3, 5, 6]. The BPH-1 cells were initially developed by Dr. Simon Hayward, a Collaborator in this project, while he was in Dr. Cunha's laboratory at UCSF. In general, such tissue recombinants with normal stromal cells, when transplanted to the kidney capsule of nude mice, produce solid branched epithelial cords and ductal structures with a benign histology. In testosterone and estradiol ($T+E_2$) treated hosts, such recombinants develop focally invasive carcinomas. Similarly, when human carcinomas-associated fibroblasts (CAFs) from prostate cancer patients are used as stromal donors, large aggressively malignant tumors develop [5]. The oncogenic processes are dependent on genetic damage to the epithelium. Such damage can result from specific genetic targeting, such as the knockout of the RB tumor suppressor gene [7]; or by the more general genetic damage caused, for

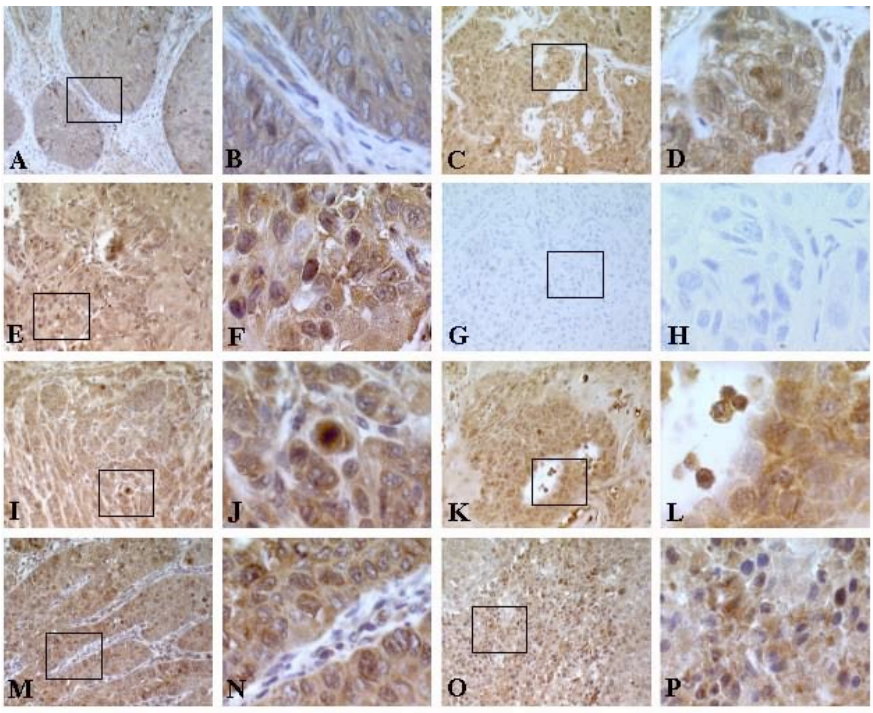

Figure 2. TSPY expression in BPH-1-rUGM prostatic tissue recombinants. A-B) Normal; C-D) $T+E_2$ treated; G-H) staining without primary antibody, negative control of C-D; E-F) BPH-1-CAF recombinant; and derivative BPH-1 lines from BPH-1-CAF recombinants showing oncogenic growth with rUGM (without CAF) recombination. I-J) BPH-1 ^{CAFTD}-03; K-L) BPH-1 ^{CAFTD}-04; M-N) BPH-1 ^{CAFTD}-05; O-P)BPH-1 ^{CAFTD}-08. Boxed areas are enlarged in corresponding figures on the right .

example by the expression of viral oncogenes [6]. These studies emphasize the importance of stromal microenvironment, genetic and hormonal influence in the carcinogenic transformation of the epithelial (BPH-1) cells.

In collaboration with Dr. Simon Hayward, now at Vanderbilt University, we have examined the TSPY expression in recombinant transplants consisting of either BPH-1 and rat urogenital sinus mesenchyme (rUGM) or BPH-1 and CAFs. Our results demonstrated that TSPY proteins were expressed only at low levels in the epithelial cells (i.e. BPH-1) in the benign BPH-1+rUGM recombinants (Figure 2A, B) and significantly in the tumor cells induced by $T+E_2$ treatment with the hosts (Figure 2C,D). For the BPH-1 and CAFs recombinants, TSPY is widely expressed and is localized in the carcinoma and cancerous BPH-1 cells (Figure 2E,F). Several BPH-1 derivative lines (Figure 2I–P) have been obtained from sequential grafting of the tumor cells from the initial BPH-1/CAF recombinants. When they are recombined with normal rat UGM, these BPH-1 derivative lines give rise to prostatic carcinoma without the needs of CAF nor hormonal treatment. Hence, they have been selected and sequentially enriched for acquiring additional mutational steps towards the spontaneous oncogenic phenotypes. TSPY stained positively with these tumor cells (Figure 2I-P). These results are in agreement with those observed in $T+E_2$ induced prostate cancer in the Noble rats and further support the postulation that TSPY participates in prostatic oncogenesis. The abundant expression of TSPY in the CAF-induced BPH-1 derivative cells in these recombinants suggests that TSPY activation could be one of the events leading to the tumorigenic properties of these derivative BPH-1 cells. If TSPY is involved in oncogenesis in these models, the observations also suggest that TSPY might be needed to maintain an oncogenic phenotype for such tissue recombinants.

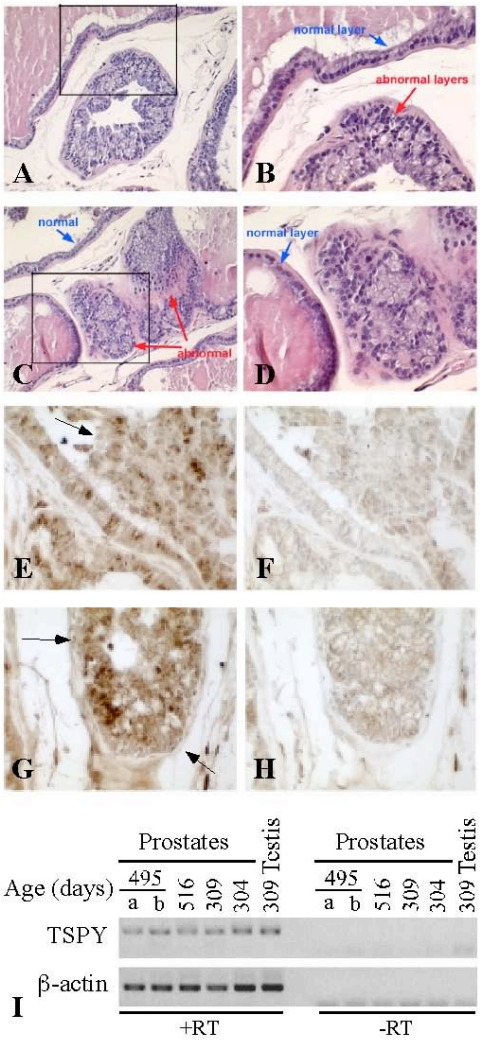

Figure 3. Expression of TSPY transgene in prostates of old transgenic mice. A-D) Detection of PIN-like structures by H&E staining in the prostate of a 516-day old mouse. Boxed areas in A and C correspond to those in B and D respectively. E-H) Immunostaining of TSPY protein in the prostates of old mice (E, G, samples; F and H, no primary antibody). I) RT-PCR analysis of total RNAs derived from old prostates showing TSPY specific transcripts (+RT) and its absence in controls (-RT).

Prostatic Hyperplasia and TSPY Expression in Old TSPY Transgenic Mice

In collaboration with Jörg Schmitke, we have obtained a line of transgenic mice harboring about 50 copies of an 8.5-kb human DNA fragment containing the 2.8-kb functional human TSPY gene [8]. The transgene is tandemly integrated on the Y chromosome of the host, suggesting that the transgene is analogous to the human natural gene that is also tandemly repeated on the Y chromosome. By and large, this transgene is properly regulated and is expressed appropriately in the spermatogonial cells of the host testis, similar to the human situation [8]. Among young transgenic mice, the TSPY transgene is not expressed in their morphologically normal prostates [8]. Recently, we were able to obtain several old male animals (from 309 to 516 days old) from this transgenic line and analyze the expression of their human TSPY transgenes in the prostates with morphology, immunostaining and RT-PCR analyses (Figure 3). Our results showed that various foci of abnormal multi-cell

layer tubular structures, resembling hyperplasia or prostatic intraepithelial neoplasia (PIN), were observed among the prostates of these old transgenic mice (Figure 3, A-D). Preliminary immunostaining experiments showed that these PIN like-structures were positive for the human TSPY protein (Figure 3, E, G). To confirm the expression of the human TSPY transgene, we conducted a RT-PCR experiment with total RNA derived from parallel prostatic tissues. Our results showed that human TSPY specific transcripts were detected with this technique (Figure 3, I), suggesting that the tandemly repeated human TSPY transgene could be dysregulated in prostates of its aging host animals.

Although preliminary in nature, these results suggest that TSPY gene dysregulation could play a significant role in prostatic oncogenesis. Latent cancers have been demonstrated in the prostates of elderly men [9, 10]. The mechanism leading to the development of such non-clinical cancer foci is uncertain. Our results in aged transgenic mice suggest that TSPY could potentially be expressed and contribute to the development of latent prostate cancer foci in elderly men. We are currently exploring this possibility through collaborations with clinical urologists and pathologists by examining TSPY expression in this type of latent prostate cancer specimens, and comparing those from clinical specimens. If TSPY is expressed specifically in foci of latent cancer, it raises the possibility that it might play an important role in the initiation and/or early stages of prostatic oncogenesis.

FUTURE DIRECTIONS

Currently, we have several lines of transgenic mice harboring a TSPY transgene directed by a prostate-specific human kallikrein 2 promoter [11, 12]. Our preliminary studies, described above, clearly suggest that ectopic TSPY expression is intimately associated with early stages of prostatic oncogenesis. Hence, it will be important to complete the analysis of these transgenic mouse lines in terms of TSPY expression and prostatic oncogenesis. According, we have requested a 12-month no cost extension of the present project and hope to be able to accomplish this additional study in the coming year.

KEY RESEARCH ACCOMPLISHMENTS

- Establish TSPY to be the putative gonadoblastoma gene.
- Demonstrate TSPY expression is proportional to the severity of the prostate cancer.
- Demonstrate Tspy gene expression in a tissue recombinant model of prostate cancer.
- Show the human TSPY transgene is expressed in hyperplasic regions in the prostates of old transgenic mice.

REPORTING COTCOMES

1. Williams K, Fernandex S, Stien X, Ishii K, Love HD, Lau Y-FC, Roberts RL and Hayward SW (2005). Unopposed c-MYC expression in benign prostatic epithelium causes a cancer phenotype. Prostate, 63:369-384.
2. Kido T and Lau Y-FC (2005). A Cre gene directed by a human TSPY promoter is specific for germ cells and neurons. Genesis, 42:263-275.
3. Kersemaekers AM, Honecker F, Stoop H, Cools M, Molier M, Wolffenbuttel K, Bokemeyer C, Li Y, Lau Y-FC, Oosterhuis JW, Looijenga LH (2005). Identification of germ cells at risk

for neoplastic transformation in gonadoblastoma: an immunohistochemical study for OCT3/4 and TSPY. Hum Pathol. 36:512-21.

4. Cools M, Honecker F, Stoop H, Veltman JD, de Krijger RR, Steyerberg E, Wolffenbuttel KP, Bokemeyer C, Lau Y-FC, Drop SL, Looijenga LH (2006). Maturation delay of germ cells in fetuses with trisomy 21 results in increased risk for the development of testicular germ cell tumors. Hum Pathol. 37:101-11.
5. Honecker F, Stoop H, Mayer F, Bokemeyer C, Castrillon DH, Lau Y-FC, Looijenga LH, Oosterhuis JW (2006). Germ cell lineage differentiation in non-seminomatous germ cell tumours. J Pathol. 208:395-400.
6. Hoei-Hansen C, Sehested A, Juhler M, Lau Y-FC, Skakkebaek NE, Laursen H and Rajpert-De Meyts E (2006). New evidence for orgin of intracranial germ cell tumors from primordial germ cells: Analysis of c-Kit, Oct-3/4, AP-2γ, TSPY and others. J Path, in press.

CONCLUSION

We have now established strong evidence supporting TSPY to be the gene for GBY, the only oncogenic locus on the human Y chromosome. Its expression in prostate cancer suggests that it might play a significant role in the multistep oncogenic process in prostate cancer. We have examined additional cases of prostate cancer of different clinical grades and demonstrated that TSPY expression is proportional to the severity of the cancer. We demonstrated TSPY expression increased with malignancy of a tissue recombination model of prostate cancer. Significantly, we also demonstrated that TSPY is expressed in the hyperplasic regions in the prostates of old transgenic mice, suggesting that TSPY might play an important role in the initiation of prostatic oncogenesis.

SO WHAT

GBY is the only oncogenic locus on the Y chromosome. Equating TSPY to be the gene for GBY is significant in establishing a role for this chromosome in male-specific cancers, such as TGCTs and prostate cancer. Our results, so far, demonstrate a direct relationship between TSPY expression and prostatic oncogenesis, thereby supporting its putative role in this cancer. Successful implementation of the transgenic mouse studies in this project will be critical in establishing TSPY as an oncogene in prostate cancer.

REFERENCES

1. Lau, Y.F. and J. Zhang, *Expression analysis of thirty one Y chromosome genes in human prostate cancer*. Mol Carcinog, 2000. **27**(4): p. 308-21.
2. Lau, Y.F., H.W. Lau, and L.G. Komuves, *Expression pattern of a gonadoblastoma candidate gene suggests a role of the Y chromosome in prostate cancer*. Cytogenet Genome Res, 2003. **101**(3-4): p. 250-60.
3. Cunha, G.R., et al., *Hormonal, cellular, and molecular regulation of normal and neoplastic prostatic development*. J Steroid Biochem Mol Biol, 2004. **92**(4): p. 221-36.
4. Hayward, S.W., et al., *Malignant transformation in a nontumorigenic human prostatic epithelial cell line*. Cancer Res, 2001. **61**(22): p. 8135-42.

5. Olumi, A.F., et al., *Carcinoma-associated fibroblasts direct tumor progression of initiated human prostatic epithelium*. Cancer Res, 1999. **59**(19): p. 5002-11.
6. Wang, Y., et al., *Development and characterization of efficient xenograft models for benign and malignant human prostate tissue*. Prostate, 2005.
7. Day, K.C., et al., *Rescue of embryonic epithelium reveals that the homozygous deletion of the retinoblastoma gene confers growth factor independence and immortality but does not influence epithelial differentiation or tissue morphogenesis*. J Biol Chem, 2002. **277**(46): p. 44475-84.
8. Schubert, S., et al., *Generation and characterization of a transgenic mouse with a functional human TSPY*. Biol Reprod, 2003. **69**(3): p. 968-75.
9. Greene, D.R. and T.M. Wheeler, *Clinical relevance of the individual prostate cancer focus*. Cancer Invest, 1994. **12**(4): p. 425-37.
10. Liavag, I., T.B. Harbitz, and O.A. Haugen, *Latent carcinoma of the prostate*. Recent Results Cancer Res, 1972. **39**: p. 131-7.
11. Xie, X., et al., *The EZC-prostate model: noninvasive prostate imaging in living mice*. Mol Endocrinol, 2004. **18**(3): p. 722-32.
12. Xie, X., et al., *Robust prostate-specific expression for targeted gene therapy based on the human kallikrein 2 promoter*. Hum Gene Ther, 2001. **12**(5): p. 549-61.

The Prostate 63:369–384 (2005)

Unopposed c-MYC Expression in Benign Prostatic Epithelium Causes a Cancer Phenotype

Karin Williams,[1]* Suzanne Fernandez,[1] Xavier Stien,[1] Kenichiro Ishii,[1] Harold D. Love,[1] Yun-Fai (Chris) Lau,[5] Richard L. Roberts,[1,2,4] and Simon W. Hayward[1,3,4]

[1]*Department of Urologic Surgery, Vanderbilt University Medical Center, Nashville, Tennessee*
[2]*Department of Pathology, Vanderbilt University Medical Center, Nashville, Tennessee*
[3]*Department of Cancer Biology, Vanderbilt University Medical Center, Nashville, Tennessee*
[4]*Department of Vanderbilt-Ingram Comprehensive Cancer Center, Vanderbilt University Medical Center, Nashville, Tennessee*
[5]*Department of Medicine, VA Medical Center, University of California, San Francisco, California*

BACKGROUND. We have sought to develop a new in vivo model of prostate carcinogenesis using human prostatic epithelial cell cultures. Human prostate cancers frequently display DNA amplification in the 8q24 amplicon, which leads to an increase in the copy number of the c-MYC gene, a finding that suggests a role for c-MYC in human prostate carcinogenesis. In addition overexpression of c-MYC in transgenic mouse models results in prostatic carcinogenesis.
METHODS. We took advantage of the ability of retroviruses to integrate foreign DNA into human prostatic epithelium (huPrE) to generate cell lines that overexpress the c-MYC protooncogene. These cells were recombined with inductive rat urogenital sinus mesenchyme and grafted beneath the renal capsule of immunocompromised rodent hosts.
RESULTS. The resultant tissue displayed a phenotype consistent with a poorly differentiated human prostatic adenocarcinoma. The tumors were rapidly growing with a high proliferative index. The neoplastic cells in the tumor expressed both androgen receptors (AR) and prostate-specific antigen (PSA), both characteristic markers of human prostate cancers. Microarray analysis of human prostatic epithelial cells overexpression c-MYC identified a large number of differentially expressed genes some of which have been suggested to characterize a subset of human cancers that have myc overexpression. Specific examples were confirmed by Western blot analysis and include upregulation of c-Myb and decreased expression of PTEN. Control grafts using either uninfected huPrE or using huPrE cells infected using an empty vector expressing a green fluorescent protein tag gave rise to well differentiated benign prostatic glandular ducts.
CONCLUSIONS. By using a retroviral infection strategy followed by tissue recombination we have created a model of human prostate cancer that demonstrates that the c-MYC gene is sufficient to induce carcinogenesis. *Prostate 63: 369–384, 2005.* © 2004 Wiley-Liss, Inc.

KEY WORDS: **myc; tissue recombination; retroviral gene transfer; prostate cancer**

Grant sponsor: University of California, San Francisco Prostate Cancer Center; Grant sponsor: DAMD; Grant number: 17-01-1-0037; Grant sponsor: NIH; Grant number: CA96403; Grant sponsor: Davis Foundation; Grant sponsor: Vanderbilt Ingram Cancer Center; Grant number: P30 CA68485; Grant sponsor: Vanderbilt Diabetes Research and Training Center; Grant number: P60 DK20593.

*Correspondence to: Karin Williams, Department of Urologic Surgery, A1302 MCN, Vanderbilt University Medical Center, Nashville, TN 37212-2765. E-mail: karin.williams@vanderbilt.edu
Received 25 May 2004; Accepted 7 September 2004
DOI 10.1002/pros.20200
Published online 21 December 2004 in Wiley InterScience (www.interscience.wiley.com).

INTRODUCTION

Prostate cancer is the single most diagnosed cancer in men and a major cause of mortality/morbidity within North America and Europe [1–3]. The introduction of routine PSA testing has resulted in earlier detection of prostate cancer and appears to be resulting in a decrease in disease-specific death rates [4]. While certain proteins such as TSPY have been found to display altered expression in very early cancer [5], there has not been sufficient characterization of PCa to identify many potential progression pathways that characterize prostate cancer [6]. Therefore, unlike the well-characterized pathway of acquired mutations displayed by colon cancer, there is not a clearly defined pathway for the progression and development of malignant disease in the prostate.

c-MYC is a transcription factor that belongs to the myc/mad/max family of Basic-helix-loop-helix-zipper (bHLHZ) proteins. Three closely related members make up the MYC family (c-MYC, L-MYC, N-MYC) and although they have very distinct patterns of expression, evidence exists that the proteins are able to compensate, to some extent, for the loss of one family member [7]. However, both c-MYC and N-myc knockout mice exhibit embryonic lethality [8,9].

Myc forms a heterodimeric transcription factor complex with its partner Max [10]. In this state Myc/Max is capable of binding to its DNA recognition site, the so-called E-box [core sequence (CACGTG)]. Max/Mad heterodimers also bind the E-box and act as transcriptional repressors presumably repressing genes induced by Myc/Max [11]. Like myc, both Max and Mad have related family members, capable of modulating this pattern of induction/repression by binding to each other and modulating the availability of the E-box. Myc also appears to be capable of binding and sequestering several other regulatory factors such as Sp-1 and Miz-1, causing transcriptional modulatory effects not associated with E-box binding [12–14].

Cell proliferation, differentiation, and apoptosis are all responses regulated by myc expression. The Myc protein acts as a cell activator that relies on other accessory proteins to specify the nature of the response. The proliferation pathway is mediated by Myc's ability to activate several cyclins, including cyclin E [15] and cyclin D2 [16,17]. The activation of cyclin D2 causes sequestering of $p27^{kip}$ from cyclin E and driving the cell into S phase. Myc also indirectly reduces expression of $p21^{WAF1}$ and $p15^{ink4b}$ [18,19], both of which are involved in cell cycle arrest.

Myc overexpression/deregulation has been implicated in numerous neoplastic transformations both in human disease and transgenic mouse models [20–28]. Furthermore, inactivation of the myc gene has been shown to elicit regression of Myc-induced tumors in the absence of novel mutations [23,29,30].

c-MYC was the first oncogene to be recognized as being overexpressed in human prostate cancer [28]. However, the precise role played by c-MYC in human prostate cancer is unclear in part due to the amplification of the 8q24 amplicon. This amplicon is particularly rich in genes, several of which [e.g., c-MYC [31], NOV [nephroblastoma overexpressed gene], EIF3S3 [eukaryotic translation initiation factor 3 subunit 3], HAS2 [hyaluronan synthase2] [32], KIAA0196 [33], and PSCA [34]] are expressed in prostate and have either oncogenic or tumor suppressor potential. FISH analysis has identified amplification of the 8q24 amplicon [32,35–37] in a large percentage of human adenocarcinomas [38,39] and some prostate intraepithelial neoplasias (PIN) [37].

Mouse models of prostatic neoplasia have been generated in which the c-MYC gene was expressed from either the probasin promoter [20] or C(3)1 promoter [22]. Two probasin promoter variants were used in one study; these promoters share the same prostate specificity but differ in promoter activity. Both the Hi-Myc (ARR_2PB-myc) and Low-Myc (sPB-myc) animals develop mouse PIN (mPIN) and invasive carcinoma but the time to development and progression differs by approximately 6 months [20]. While these probasin-Myc transgenic mice apparently progress from mPIN to prostatic adenocarcinoma the relationship of PIN to adenocarcinoma in humans remains unsubstantiated. The C(3)1 promoter is a weaker promoter than the probasin constructs. Mice carrying the C(3)1-Myc transgene fail to develop adenocarcinoma within their lifetime although they do develop mPIN-like lesions [22]. These data suggest that a low level of myc expression correlates with mPIN development while the progression to adenocarcinoma requires elevated c-MYC levels.

Given that c-MYC is reported to be overexpressed and the gene amplified in human prostate cancer, and because transgenic mouse models overexpressing c-MYC in the prostate have a dose related progression towards malignancy, we decided to test the ability of cMYC to transform human prostatic epithelium. To do so in vivo a tissue recombination model was used to follow prostatic carcinogenesis in response to overexpression of c-MYC.

MATERIALS AND METHODS

Human Cell Culture

Human prostate tissue samples were obtained from the Vanderbilt Tissue Acquisition Core via the Department of Pathology in accordance with Vanderbilt IRB protocols. Cores 6 mm in diameter were removed from

radical prostatectomy samples and were sampled by histologic analysis on frozen sections to determine the nature (benign vs. malignant vs. severe inflammation) of the tissue contained within the core.

Benign tissue was cut into 2 mm cubes using sterile scalpels. After washing in RPMI (Gibco, Carlsband, CA) 5% FCS (Atlanta Bioscience Atlanta, GA) the tissue was plated on Primaria™ tissue culture flasks with sufficient medium to wet the plate and create a strong surface tension (1.2 ml/25 cm^2). After cell attachment had taken place (~12 hr) the volume of medium was increased. Tissue obtained from tissue recombination grafts was reintroduced into culture in an identical manner.

Tissue Culture Medium

Tissue culture medium for human prostatic epithelial cells (huEpi mix) consisted of: [RPMI 1640, 1% ITS (Insulin Transferrin Selenium), 1% Antibiotic/Antimycotic (all from Gibco)], 2.5% charcoal stripped serum (Atlanta Bioscience), BPE (Bovine Pituitary Extract) 1:250 (Hammond Cell Tech, Winsor CA), Cholera toxin (1 μg/ml), and Epidermal Growth Factor (0.01 μg/ml) (Sigma, St. Louis, MO).

LZRS Retroviral Plasmid Construct

The plasmid LZRS c-MYC/EGFP (Fig. 1) was constructed utilizing the LZRS-EGFP backbone (Nolan Laboratory, Stanford, CA). The CMV promoter was excised from pIRES-EGFP (Clontech, Palo Alto, CA) as a BglII/BamHI fragment. The fragment was ligated into the BamHI site of the LZRS-EGFP backbone to give C7Δ.

The human c-MYC cDNA clone (BC000917) was obtained from ATCC (Rockville, MD) and amplified by PCR using a 5′ primer specific to translational start site and a 3′ primer containing an XhoI restriction site and the consensus sequence for the translational stop site with subsequent deletion of any polyadenylation sites. After PER amplification, the product was gel purified, and cloned into poem T-Easy (ProtÕgÕ, Madison, WI). Following DNA sequence verification of the cloned product the c-MYC coding region was excised using EcoRI/XhoI and sub cloned into the EcoRI/XhoI sites of pLZRS-EGFP to give C7-Myc.

Viral Production

Amphotrophic ϕNXA packaging cells were obtained from ATCC [under an MTA from the Nolan laboratory Stanford (www.stanford.edu/group/nolan)]. These cells were maintained in 5% FCS/RPMI 1,640 with antibiotic surveillance. The ϕNX packaging cell lines were reselected with both hygromycin B and diphtheria toxin (Sigma) every 3–4 months. The LZRS retroviral constructs were transfected into ϕNX cells that were 70%–80% confluent. Routine transfection took place using 25 cm^2 flasks. Lipofectamine 2000 (Invitrogen, Grand Island, NY) was optimally used at a

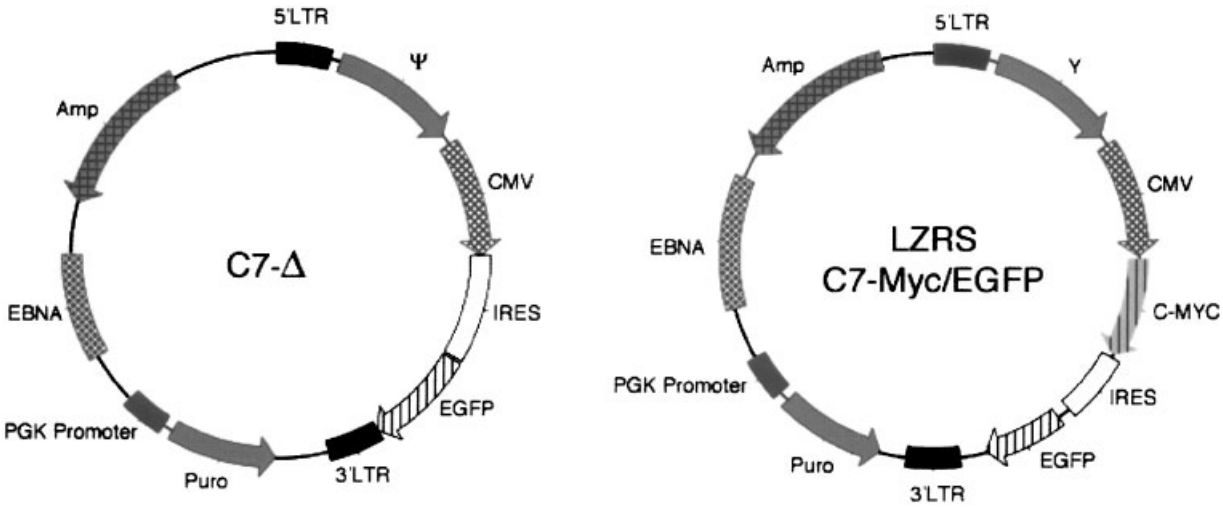

Fig. 1. Retroviral constructs, control vector C7Δ and LZRS C7-MYC/EGFP. pLZRS is a retroviral vector derived from the Moloney murine Leukemia virus (MoMuLV). The gene of interest (c-MYC) and the Enhanced Green Fluorescent Protein (EGFP) are expressed from a bicistronic message under the control of the cmv promoter. The 5′ viral LTR controls expression of the transcript that contains Ψ (the extended viral packaging signal). The retroviral particle contains, and integrates into the genome, only the genetic information between and including the 5′ and 3′ LTRs'. pLZRS does not contain the structural genes necessary for viral formation and replication, these are provided by the packaging cell line ϕNX. Other components of pLZRS such as the puromycin resistance gene and EBNA (EBV episomal functions) contribute to stability and selection of the plasmid in the packaging cell line. pLZRS also includes the pUC origin of replication and E. coli Amp gene for propagation and antibiotic selection in bacteria.

final concentration of 3 μl/ml according to manufacture's protocols. Eight hours post transfection the ϕNX cells were given fresh RPMI/5% FCS and incubated overnight at 37°C. Viral supernatant was removed in the morning and the cells split if necessary and moved to a 32°C incubator to ensure greater viral stability. The viral supernatant was spun at 3,000 rpm and passed through a 45 μm filter to ensure the absence of contaminating ϕNX cells. The viral supernatant was then supplemented with 4 μg/ml Polybrene (hexadimethrine bromide, Sigma) and either stored at −70°C or used immediately.

Viral Infection

The viral supernatant containing the c-MYC/EGFP or C7-delta control retrovirus was diluted 1:1 with huEpi mix that was double strength with respect to the added constituents and the polybrene concentration was corrected to 4 μg/ml. The viral medium was then placed on the huPrE cells (three patients from which both TZ and PZ cores were put into independent culture dishes in duplicate) in culture and replaced 8 hr later. Primary cells were incubated at 37°C as their rate of cell division was severely compromised at 32°C, the increased stability of the viral particles at 32°C therefore could not be utilized when working with huPrE but proved useful when certain immortal cell lines were infected, data not shown. Successive rounds of infection over 5 days were employed to generate infected cells. Owing to the growth patterns of the huPrE we found that daily infection would ensure the presence of virus during the initial outgrowth of cells and therefore generate the maximum number of infected cells. Infection rates were monitored using fluorescence microscopy of the bicistronic EGFP tag. After infection the cells were maintained in culture until use. The cells were examined by a clinical pathologist to assess any phenotypic differences in the infected cells.

Culture of Infected Cells

Following infection, a proportion of the cells were used as a source of epithelium in tissue recombinants. The remaining cells were maintained in culture for a further 16 passages with batches frozen in liquid nitrogen at different points. All remaining cells were frozen after passage 16. Cells were examined for the continued expression of the EGFP tag using fluorescence microscopy; expression of AR, PSA, and c-MYC was monitored using Western blot analysis.

Tissue Recombination

Tissue recombinants were prepared, as previously described [40,41]. Briefly, pregnant rats were obtained from Harlan (Harlan, Indianapolis). Rat urogenital sinus mesenchyme (UGM) was prepared from 18-days embryonic fetuses (plug date denoted as day 0). Urogenital sinuses were dissected from fetuses and separated into epithelial and mesenchymal components by tryptic digestion, as previously described. UGM was then further reduced to single cells by a 90 min digestion at 37°C with 187 U/ml collagenase (Gibco). Following digestion, the cells were washed extensively with RPMI-1640 tissue culture medium. Viable cells were then counted using a hemacytometer, with viability determined by trypan blue exclusion. Epithelial cells were released from tissue culture plates using trypsin. Trypsin was neutralized and the cells washed and counted using a hemacytometer. Cell recombinants were prepared by mixing 100,000 epithelial cells with 300,000 stromal cells. Cells were pelleted and resuspended in 50 μl of neutralized type 1 rat tail collagen prepared as, previously described [42]. The recombinants were allowed to gel at 37°C for 15 min and were then covered with growth medium and cultured overnight. They were then grafted beneath the renal capsule of adult male severe combined immunodeficient (SCID) mice [C.B.17/IcrHsd-scid mice (Harlan)].

Subcutaneous Grafting

Epithelial cells (100,000) were pelleted and resuspended in 50 μl of neutralized type 1 rat tail collagen prepared, as described previously [42] and placed under the skin of adult male SCID mice [C.B.17/IcrHsd-scid mice (Harlan)]. Some of these subcutaneus grafts were surrounded in matrigel (BD Biosciences, Bedford, MA) at the time of grafting.

Tissue Recovery, Fixation, and Processing

Mice were sacrificed by Isoflurane inhalation followed by cervical dislocation according to Vanderbilt animal care protocols. The kidney and attached graft together with internal organs were removed and examined at the gross level. The c-MYC grafts owing to their substantial size were divided into several pieces. Those fragments containing the kidney were fixed in 10% neutral buffered formalin, as were the internal organs of the host. The remaining tissue was then divided to give representative portions for (1) RNA extraction, (2) Protein extraction, and (3) for further tissue culture. Tissue destined for RNA extraction was cut into small pieces and immersed in RNA LATER (Ambion, Austin, TX) according to manufacturer's instructions. Tumor tissue for protein extraction was snap frozen on dry ice and stored at −70°C until required. The third portion of the tumor was removed

for tissue culture or frozen [43] to allow extraction of viable cells.

Culture of Tumor-Derived Epithelial Cells

Tumor tissue was minced and placed in culture in a minimal volume of tissue culture medium (as per primary culture). Cells were passaged using trypsin and then frozen. Continued transduced gene expression in these cells was confirmed by fluorescence microscopy to detect the expression of EGFP and by Western blotting to confirm continued expression of c-MYC.

Antibodies

For immunolocalization studies the following antisera were used. Androgen receptors (AR) were detected using a rabbit polyclonal antibody (*sc*-816) raised against a peptide within the N-terminal domain of hAR, EGFP was detected using a mouse monoclonal to the full length GFP that detects all GFP variants (*sc*-9996). c-Myb (*sc*-8412), PTEN (*sc*-7974*sc*-9996), p63 (*sc*-8343) (Santa Cruz Biotechnology, Santa Cruz, CA). c-MYC was detected using a mouse monoclonal (NCL-c-MYC) raised against full-length recombinant human protein obtained from Novocastra (Burlingam, CA). Ki67 (M-7240), PSA (A-0562), broad-spectrum Keratin antibodies (Z-0622) were obtained from DAKO (Carpinteria, CA), and keratin 8, 14, and 18 [clones LE41, LL001, and LE61 gifts from Prof. E.B.Lane, Dundee University, UK [44,45]].

Protein Extraction

Tissue extracts of human prostate epithelial cells maintained in tissue culture for one passage, and c-MYC infected huPrE cells were prepared by homogenization in 400 μl cold buffer A (10 mM HEPES pH 7.9; 10 mM KCl: 0.1 mM EDTA; 0.1 mM EGTA; 0.1 mM DTT; 1× protease complete (Roche, Indianapolis, IN). The cells were allowed to swell on ice for 15 min, after which 25 μl of a 10% solution of Nonidet NP-40 (Sigma) was added and the tube vortexed vigorously for 10 sec. The homogenate was then centrifuged for 30 sec in a Microfuge. The supernatant was snap frozen and stored at −70°C.

Western Blotting Analysis

Tissue extracts from huPrE epithelial cells grown in culture and their c-MYC infected counterparts as well as extracts from the BPH1 prostatic epithelial cell line were run on denaturing mini gels containing an acrylamide gradient from 4%–20% (w/v) polyacrylamide (Invitrogen). Gels were run in MOPS/SDS running buffer (50 mM 3-[*N*-morpholino] propane sulfonic acid [MOPS], 50 mM Tris base, 0.1% SDS, 1.025 mM EDTA [pH 7.7] for 35 min at 200 mA. Samples were blotted onto PVDF membrane (Invitrogen) using transfer buffer (25 mM bicine, 25 mM Bis-Tris, 1.025 mM EDTA, 50 nM chorobutanol [pH 7.2] (Invitrogen) in the mini gel tank according to the manufacturers instructions. Thereafter, membranes were blocked for 2–3 hr at room temperature in BLOTTO (5% nonfat dried milk powder [Difco]) dissolved in Phosphate buffered saline (Sigma) containing 0.1% Tween-20 (PBST). Membranes were incubated overnight in Blotto with the any one of the antibodies (anti c-MYC 1:800, AR 1:1,000, c-Myb 1:600, GFP 1:2,000, E-Cad 1:1,000, PTEN 1:800). Bound antibodies were detected using appropriate secondary antibodies (1:4,000 peroxidase conjugated Donkey anti rabbit/Sheep anti mouse [Amersham Pharmacia Biotech, Piscataway, NJ] and 1:2,000 rabbit anti goat [Santa Cruz]) and the enhanced chemiluminescence visualization system (Amersham Pharmacia Biotech) according to the manufacturer's instructions.

Immunohistochemistry

Deparaffinized, slide mounted sections were rehydrated and then subjected to heat induced antigen retrieval using the commercial retrieval buffer (H-3300) from Vector Laboratories, Brlingham, CA. The sections were microwaved for 15 min at a power that ensured continuous but not excessive boiling. Slides were permitted to cool to room temperature prior to incubation with 3% hydrogen peroxide in methanol for 15 min to block endogenous peroxidase. After washing in PBS the slides were blocked in Clean Vision™ from ImmunoVision Technologies for 15 min. This blocking optimized the use of monoclonal antibodies on tissue recombinants in which an immunocompromised mouse host was the graft host. The antibodies towards GFP (Santa Cruz,), Ki67, PSA, and broad spectrum Keratin (DAKO) were all used at 1:200 (p63 used at 1:1,000) [diluted in 1:4 normal swine serum (broad spectrum Keratin, PSA, p63) or normal rabbit serum (GFP, Ki67, keratins 8, 14, 18) in PBS/5% BSA]. All antibodies were incubated on sections overnight at 4°C. Sections were then incubated with the appropriate biotinylated secondary antibodies for 1 hr. [Broad spectrum Keratin, p63 and PSA, swine anti rabbit (DAKO), and for GFP, keratin 8, 14, 18 and Ki67 rabbit anti mouse, (DAKO), both of which were diluted 1:500 in the appropriate normal serum (see above)]. After appropriate washing steps the sections were incubated in ABC-HRP complex (Vector) for 30 min and washed extensively. Bound antibodies were then visualized by incubation with 3,3′-diaminobenzidine tetrahydrochloride (liquid DAB, DAKO). Sections were counter-

stained with hematoxylin. Images were captured onto a computer using a Zeiss microscope equipped with an AxioCam camera (Zeiss) and software.

Identification in Histological Sections of Species Origin of Cells in a Tissue Graft

Staining with the Hoechst 33258 dye (Sigma) was performed, as previously described [46]. The Hoechst dye Sections were examined by fluorescence microscopy. Host mouse cells contain several small discrete intranuclear fluorescent bodies, which are absent in cells from either rat or human allowing us to confirm that the tumor is not derived from the host mouse.

RNA Isolation

Tissue was rapidly excised from the outer portions of the graft and placed in 10x v/v RNA LATER (Ambion, Austin, TX). The tissue was then refrigerated prior to use 1–5 days after removal from the host. The tissue was dissected in a Petri dish containing RNA LATER to remove any kidney tissue (none was actually visible in any of the tissues) or obviously necrotic tissue (this tissue was very soft and white, resembling cotton candy).

RNA was isolated using the Qiagen mini RNA Easy kit according to the manufacturers instructions (Qiagen, Valencia, CA). The RNA was DNAse treated again using Qiagen reagents as detailed in the RNA easy protocol. The RNA concentration was then determined spectrophotometrically and the RNA aliquoted and snap frozen at −70°C.

RNA Labeling and Hybridization

All RNA and cDNA manipulations and cDNA array hybridizations were undertaken by technical support staff within the Vanderbilt Microarray Shared Resource (http://array.mc.vanderbilt.edu) using the protocols outlined on their website http://array.mc.vanderbilt.edu/support/protocols.htm. The use of tissue culture cells permitted the use of the standard cDNA labeling without amplification of the RNA. The microarray used for our experiments was the human 11K comprised of the Research Genetics human clone set.

cDNA Array Analysis

Data was normalized by Lowess sub grid and Gene Pix Pro Software was used to analyze differentially expressed genes between the two analysis groups. The groups consisted of huPrE grown in culture and infected with the LZRS-myc virus.

RESULTS

Infection of Hupre With a Retrovirus Containing C-Myc/Egfp Elicits Phenotypic Changes In Vitro

The huPrE cells grown on tissue culture plastic have a characteristic cobblestone appearance (Fig. 2). The presence of high levels of cholera toxin severely suppressed fibroblastic growth resulting in an almost pure epithelial cell population, as determined by visual examination. The rate of emergence of epithelial cell sheets from individual tissue fragments was highly variable both with respect to 'flask to flask' variation-using tissue from a single patient and with respect to

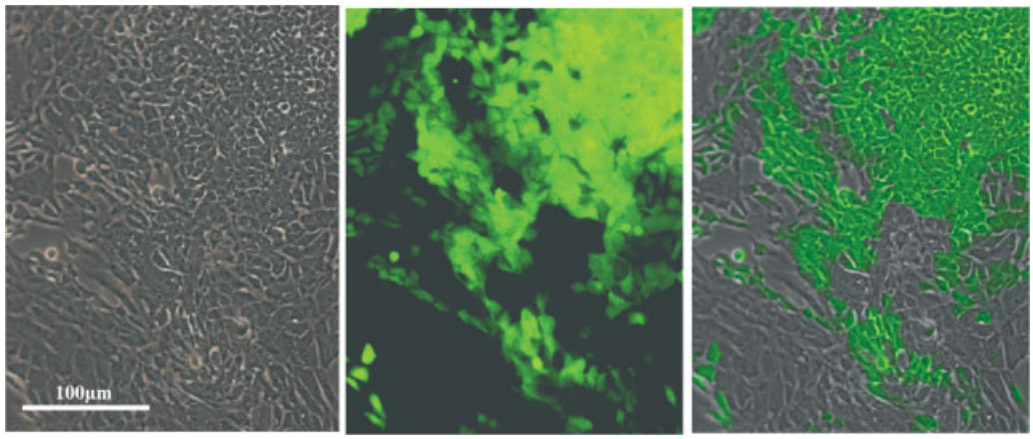

Fig. 2. Phase contrast photomicrograph of human prostate epithelium in cell culture 4 days after infection (Left panel). Note the typical cobblestone morphology in lower left hand side compared to the denser cells present in the upper right hand side. (Middle panel) Fluorescent image of human prostate epithelium culture 4 days post infection. Note that approximately one half of the cultured cells strongly express EGFP due to infection by the C7-Myc retrovirus. (Right panel) overlay, confirming that the small densely packed cells express EGFP while those with the cobblestone morphology do not.

'patient to patient' variation. Infection was started on day 2 in culture regardless of the presence/absence of visible epithelial cell outgrowths. After 2–5 rounds of infection a very large number of cells (20%–40%) on the margins of the growing sheet of epithelial cells expressed EGFP, suggesting an extremely efficient infection. At this point, infection was halted and the cells allowed to proliferate for 72 hr. The cultured cells displayed an altered morphology. Instead of a uniform monolayer of epithelial cells with a cobblestone appearance, there were discreet nests of tightly packed cells. The nests had well defined borders and were surrounded by cells displaying the expected normal phenotype (Fig. 2). When visualized on an inverted fluorescent microscope the nests displayed uniform EGFP fluorescence while the surrounding cells did not express EGFP.

All of the c-MYC/EGFP infected cell cultures observed (three patients from which both TZ and PZ cores were put into independent culture dishes in duplicate, a total of 12 independent cultures) exhibited similar morphological changes. The cells were irregular in shape and markedly smaller, the cytoplasm to nuclear ratio was decreased, and the nucleus was in many cases irregular in shape with prominent nucleoli. The cells also formed multiple layers within the nests, and many non-adherent viable cells were observed. The 'nest' phenomenon was observed until the cultures were trypsinized and split. Subsequent cultures initially displayed both phenotypes of cells but the morphologically normal cells were rapidly lost as the EGFP-expressing epithelial cells rapidly colonized the tissue culture plates. Within 10 days the entire culture consisted of EGFP expressing cells that varied widely in their fluorescence (and by subsequent analysis c-MYC expression). Over time the EGFP expression became more uniform but a range of EGFP expression has always been observed throughout the cultures. This suggests that the cultures represent a variety of clones resulting from multiple initial infections.

HuPrE infected with the LZRS C7Δ (the 'empty vector') exhibited normal cobblestone morphology and typically infect with relatively low efficiency $\leq$1% at low passage number, the control infections are less efficient than infections with the C7-Myc retrovirus. The Green EGFP infected cells were indistinguishable from their uninfected neighbors under phase contrast and could only be identified by EGFP expression. The C7Δ-infected cells could be passaged a maximum of five times before they became senescent.

The C7 Myc infected cells were maintained through 16 passages and showed no signs of senescence during this period. They continued to express both EGFP and c-MYC as well as prostatic epithelial markers including AR and PSA.

Hupre/C-Myc-Egfp Plus RugmTissue Recombinants Form Rapidly Growing Adenocarcinomas Expressing Human Prostatic Markers

Tissue recombinants of huPrE and rUGM were prepared. Control grafts contained either uninfected or C7-Δ-infected epithelium. Recombinants using C7-myc contained different percentages of c-MYC-infected cells (from 10% to 50% dependent on the time post infection that the cells were grafted). All grafts were composed of 100,000 epithelial cells and 300,000 rUGM cells. Host mice carrying myc-expressing grafts were sacrificed after 28 days due to the large size of the graft, which exceeded the size of the normal kidney (Fig. 3). Recombinants composed of C7Δ PrE and rUGM grafted to the contralateral kidneys of experimental hosts were very small and poorly developed at 28 days post grafting. In separate experiments, using a 3-month time point fully differentiated prostatic structures expressing PSA and AR were seen. Control grafts maintained a benign histology throughout (Fig. 3). The phenotype and timing of developmental events in these control grafts is consistent with previously published results using human prostatic epithelial organoids [47].

Initial inspection of the large c-MYC expressing grafts, indicated several very large blood vessels located on the surface of the graft and areas of white necrotic tissue in areas devoid of obvious blood vessels (Fig. 3). The kidney tissue was readily apparent upon subsequent dissection and was essentially normal.

C7-Myc cells grafted subcutaneously into the flank of SCID mice developed large tumors after 6 weeks (data not shown) that were indistinguishable from C7-Myc recombined with rUGM. The slightly longer time frame probably reflects the slower recruitment of blood vessels to a subcutaneous graft site compared to the sub renal graft site.

Thin smears of surface cells from the tumors expressed EGFP when exposed to fluorescent light (data not shown). These cells were placed into tissue culture to confirm EGFP expression and their human origin.

Expression from the CMV promoter is maintained throughout the growth of the graft. We have previously observed promoter downregulation (unpublished data) in cells carrying genes under the CMV promoter introduced via retroviral integration possibly via methylation events consistent with those described in transgenic mice [48,49]. The EGFP levels within the cells placed into reculture maintained a range of EGFP expression consistent with cultures prior to grafting suggesting that such repression had not occurred in these tumors.

In all the huPrE/c-MYC tumors the grafts consisted of cells strongly staining with hematoxylin. The cells characteristically exhibited large irregular nuclei, pro-

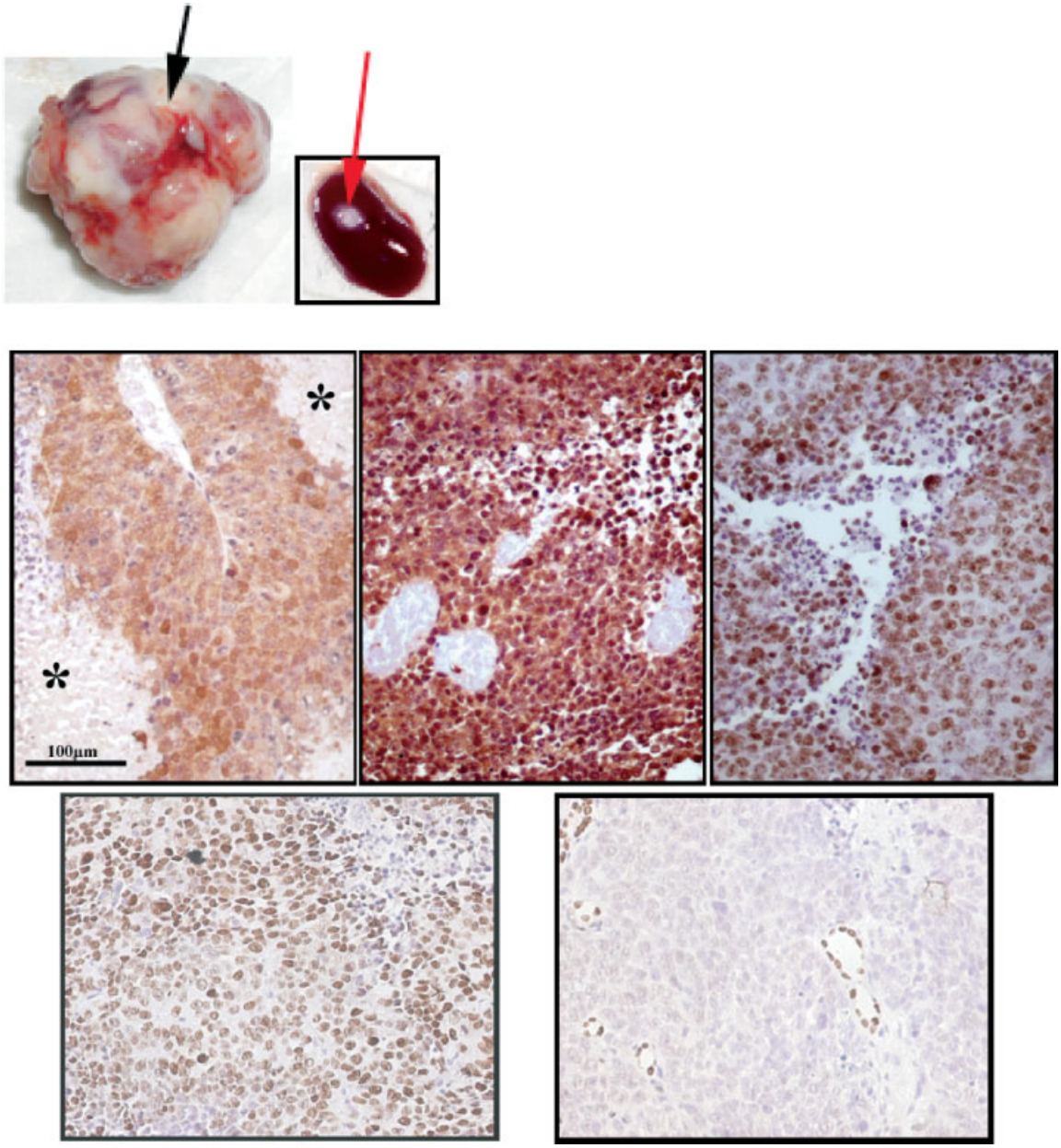

Fig. 3. Gross anatomy of mouse kidney with a c-MYC overexpressing prostate epithelial cell recombinant xenograft (top left). Note the encasement of the kidney by the tumor (black arrow). The control kidney carrying the C7Δ PrE/rUGM graft is displayed on the right, the small xenograft is barely visible (red arrow). Photomicrograph showing the poorly differentiated c-MYC expressing human prostatic tumors (middle/bottom panel) strongly express enhanced green fluorescent protein (middle left) PSA [(center)* indicates necrotic tissue]. The high mitotic rate observed in the tumor was confirmed by a very high index of statining with Ki67 (middle right). Bottom panel (left to right) AR, and p63.

minent nucleoli, and dense cytoplasm. A large number of dividing cells were present in a single field and many of the mitotic figures were clearly abnormal (Fig. 3). No fibromuscular stroma was present in the grafts nor was any apparent at the graft extremities. Irregular areas of necrotic tissues extended throughout the grafts and predominated in the interior, but did not interfere with the kidney. Areas of living tissue surrounded the few blood vessels that populated the graft interior. Immunohistochemical analysis of the C7-myc induced tumors revealed that these retained expression of two key markers of prostate tissue, AR and PSA. In addition the tumors expressed EGFP confirming their origin. Tumors expressed keratins 8 and 18 and lacked p63 and keratin 14 staining suggesting a luminal rather than basal cell origin. This is consistent with the profile seen

in human prostate cancer. The proliferation rate of the cells was extremely high as indicated by the almost universal presence of Ki67 in the nuclei (Fig. 3). This was consistent with the observation of extremely rapid tumor growth.

No infiltration was observed into the kidney, a well dealinated border was observed and the kidney morphology was normal with no obvious compression or damage (Fig. 3). Hoechst 33258 staining confirmed that none of the epithelial cells observed were of mouse origin and that no 'non mouse' cells were present in the kidney (data not shown). Some areas displaying p63 positive cells were observed within the graft, these were determined (by a trained pathologist) to be mouse kidney structures caught in cross section, providing a good internal positive control for the tumor cells, which were universally negative for basal cell markers (Fig. 3).

Molecular Characteristics of Tumor-Derived Cells

A microarray analysis comparison of the cells derived from the C7-myc tumors and of primary epithelial cultures from the same patient revealed a number of changes (Table 1). As might be expected many genes were seen to be regulated in response to c-MYC overexpression. Attention in this analysis was focused upon genes known to be regulated in tumors. Of particular note was the observation that PTEN and E-cadherin expression was seen to be suppressed and c-Myb expression was observed to be upregulated in the tumorigenic cells. This observation was confirmed by Western blotting to examine expression of these proteins (Fig. 5). Western blotting analysis also confirmed the continued overexpression of c-MYC, and the expression of both AR and EGFP.

DISCUSSION

The present study demonstrates that c-MYC overexpression is sufficient to drive normal human prostatic epithelium to a metastatic tumor within a tissue recombination model. Retroviral infection of normal prostate epithelium with the EGFP expressing empty vector resulted in benign prostatic architecture indicating that MYC overexpression not infection/integration

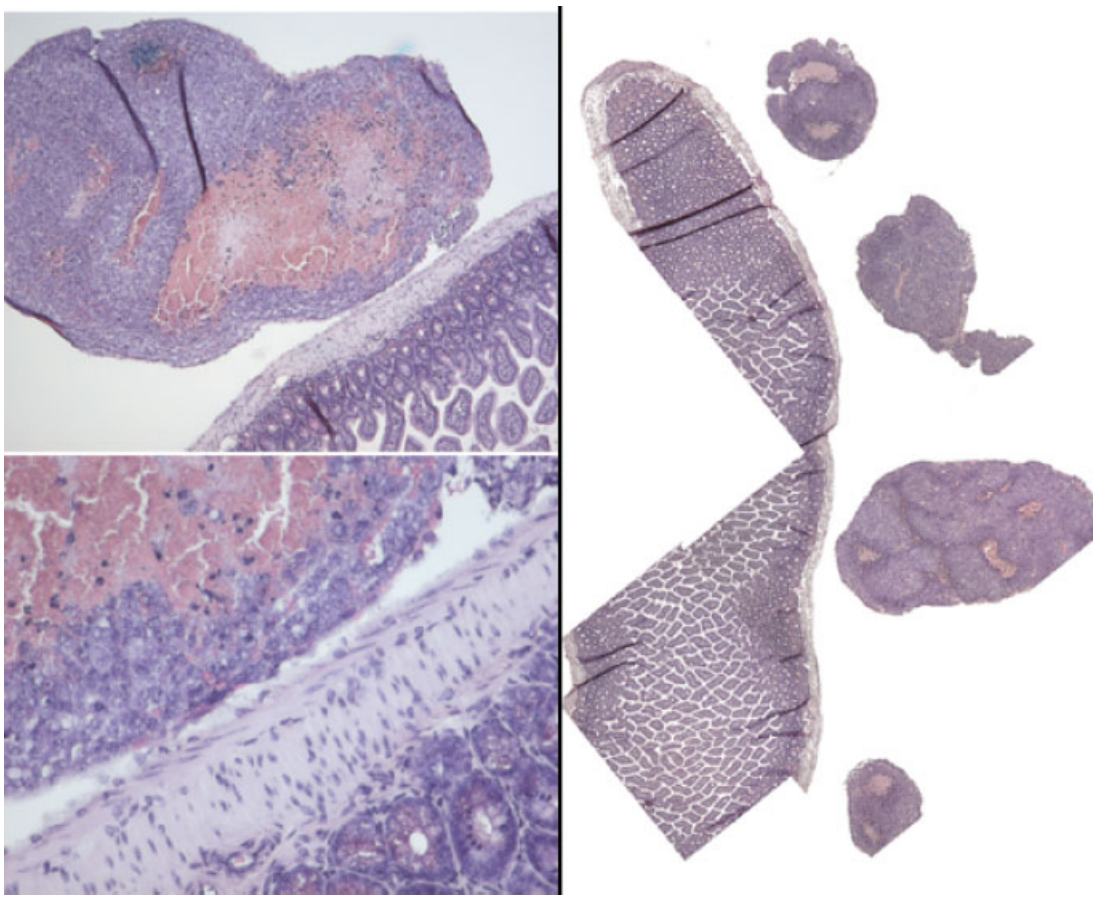

Fig. 4. Histopathologic appearance of metastatic lesions. Multiple metastatic lesions were found in mice as focal growths predominantly following the line of the intestinal tract. H&E high magnification of tumor immediately adjacent to the intestine (left panel top & bottom). Low magnification composite (right panel) showing three metastatic nodules that were attached to the host mouse intestine.

TABLE I. Microarray Data Set of mRNA Showing 2-fold Differences in Levels Between C7-Myc PrE and C7Δ PrE

Category	Gene	GenBank ID	Description	ACF
Transcription Factors	ARHE	NM_00518	Ras homolog gene	3.67
	MAFG	NM_00239	v-maf oncogene homolog G	3.27
	SON	NM_05818	Similarities with MYC MOS	−2.29
	HRASLS3	NM_00706	HRAS-like suppressor 3	−2.29
	TCF7	NM_00320	Transcription factor 7	
	TCF12	NM_00320	Transcription factor 12	−4.67
	VAV3	NM_00611	vav 3 oncogene	−1.36
	NFE2L2	NM_00616	Transcription factor	−2.53
	FOSL2	NM_00525	Dimerizes with JUN forming the transcription of factor complex AP-1	−1.65
	Notch3	NM_00871	Transcription factor	−3.64
	RABA1	NM_00416	Member RAS oncogene family	−1.78
Growth factors	INSL4	NM_00219	Member of the insulin superfamily	
	VEGF	NM_00337	Vascular endothelial growth factor	
Kinases	MKNK2	NM_01757	MAP kinase interacting serine/threonine kinase 2	−2.32
	SCAP1	NM_00372	Belongs to the src family kinases	−4.69
Adaptor molecules	NCK1	NM_00615	Adaptor protein involved in transducing signals from receptor tyrosine kinases to downstream recipients such as RAS	−1.67
	SP110	NM_08042	May have a role in the regulation of gene transcription	−2.28
	ABR	NM_02196	These proteins might interact with members of the Rho family	−2.68
	RNF4	NM_00293	RING finger protein, enhances AR-dependent transcription	−3.49
Apoptosis	BCL2A1	NM_00404	BCL2-related protein A1	−1.56
	PDCD4	NM_14534	Thought to play a role in apoptosis	−1.53
	CASP3	NM_00434	Caspase 3 apoptosis-related protease	
Extracellular matrix	ADAM15	NM_00381	A disintegrin and metalloproteinase domain 15 (metargidin)	−1.34
	TIMP1	NM_00325	Tissue inhibitor of MMP1	2.26
	MMP14	NM_00499	Matrix metalloproteinase activates MMP2 protein may be involved in tumor invasion	−1.71
	TIMP2		Tissue inhibitor of MMP 2	−2.71
Cell cycle	S100A10	NM_00296	Calcium-binding, involved in the regulation of cell cycle progression and differentiation	−2.23
	CDK4	NM_00007	Cyclin-dependent kinase 4	−1.75
Proliferation/ Differentiation	DUSP6	NM_00194	Gene product inactivates ERK2,	−1.95
	MAPRE2	NM_01426	Homology with APC suggests involvement in tumorigenesis and proliferative control of normal cells	−1.39
	SHC1	NM_18300	Couples activated growth factor receptors to a signaling pathway	−1.5
Proteases	Kallikrein 10	NM_00277	Serine proteases having diverse physiological functions	−1.72
	KLK5	NM_01242	Kallikrein 5	−1.59
	SPUVE	NM_00717	Protease, serine, 23	
	SLP1	NM_00306	Secreted serine protease inhibitor protects epithelial tissues	−5.04
	CSTA	NM_00521	Encodes a stefin that functions as a cysteine protease inhibotor	−4.65
Cytoskeleton/Motility	DSTN	NM_00687	Actin depolymerizing factor	−1.7
	CLDN1	NM_12110	Integral membrane protein component of tight junctions	−2.45
	CLDN4	NM_00130	Integral membrane protein, which belongs to the Claudine family	−1.33

(*Continued*)

TABLE I. (*Continued*)

Category	Gene	GenBank ID	Description	ACF
	THYB4	NM_02110	Actin sequestering protein, regulates actin polymerization, proliferation migration, and differentiation	−5.1
	LAMC2	NM_00556	Extracellular marrix glycrprotein, implicated in adhesion megration, differentiation, and metastasis	−1.5
	WIRE	NM_13326	Has a role in the WASP-mediated organization of the actin	−4.15
	KRT13	NM_15349	Keratin 13	−4.51
Neuronal	NDN	NM_00248	Mouse studies suggest a role in growth suppression in postmitotic neurons	−1.84
	SST Somatostatin	NM_00104	A regulator of endocrine and nervous system function	−1.97
Metastasis	p8	NM_01238	p8 protein (candidate of metastasis)	−1.94

of the EGFP expressing retrovirus induces the cancer phenotype. The tumors formed in this model retain some key characteristics of human prostate cancer, notably the expression of AR and PSA, and the ability to metastasize.

The c-MYC overexpression combined with a large percentage of infected cells produces a cancer phenotype within our xenograft model that is aggressive and progressive. The cells were obtained from tissue derived from aging males and may already have accumulated genetic hits that, of themselves, are insufficient to alter histology. The levels of c-MYC expressed by a CMV-driven retroviral delivery system would certainly constitute a very large additional molecular hit. The resulting tumors resemble a poorly differentiated advanced carcinoma, however, the growth rate is accelerated in comparison with the human disease. Myc expression can be a pivot point in the cellular decision-making process that determines if a cell will undergo proliferation or apoptosis [50–55]. Myc overexpression within the primary huPrE appears to be exhibiting a proliferative effect demonstrated by the extremely large number of Ki67 positive cells present within the renal capsule graft and the metastatic lesions. The lack of expression of the basal cell markers keratin 14 and p63 indicate that the c-Myc tumor, like human prostate adenocarcinoma, loses basal cells during tumor formation.

Similar c-MYC-based retroviral rodent models created by Thompson and co-workers [25–27,56–59] in prostate and by Edwards [60] in the breast lacked the aggressiveness of our model unless activated ras was also present. Less than 0.1% of epithelial cells carried the retrovirally introduced genes in the mouse TR's while our grafts contained 10%–50% infected cells thus altering the environment considerably as normal cells

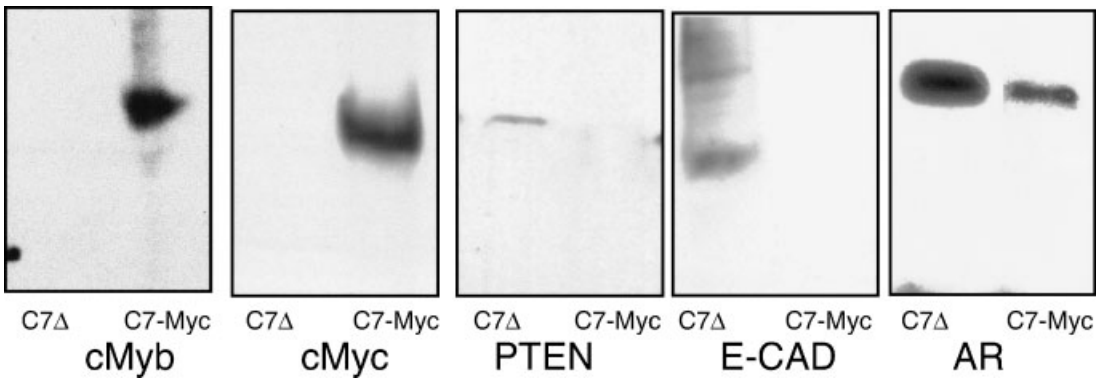

Fig. 5. Western blot analysis of C7-Myc and C7Δ infected cells. Western blot of human prostatic epithelial cells infected with C7-Myc or C7Δ (empty vector). All lanes contain 100 of protein except PTEN (250 μg). EGFP (Top left) is detected only in C7-Myc infected cells, C7Δ infected cells made up approximately 1% of the culture and while fluorescent cells were visible no signal was detected by western analysis. E-cadherin 120 kDa (top middle), Androgen receptor 130 kDa (Top right), cMyb 75 kDa (bottom left) c-MYC 67 kDa (bottom middle) PTEN 60 kDa (bottom right).

have the potential to inhibit the growth of transformed cells [61]. Microarray data do not indicate increased levels of ras mRNA within our C7-Myc tumors. Mouse strain backgrounds modify the effects of the oncogenes myc and ras [27] within the retrovirally infected TR's. By virtue of using human tissue, the present study examines an outbred epithelial cell population.

More recent transgenic mouse studies have demonstrated that the degree of response to c-MYC overexpression in mouse prostatic epithelium is dose related, with increased expression giving rise to more severe phenotypes [20,22]. All three described prostate-specific c-MYC-overexpressing mice develop mPIN. Mice expressing c-MYC using the Probasin promoter progress to invasive cancer in a time frame that is determined by the relative strength of the promoter construct used (ARR_2PB or sPB) [20]. Low levels of c-MYC expression are thought to cause prostatic dysplasia in the prostates of rats treated in the neonatal period with DES [62]. Progression beyond PIN is not observed within the lifetime of the C(3)Myc mouse. As serial recombination experiments using the C(3)-Myc mouse or the DES treated prostates have not been performed it is not known if these PIN-like lesions would progress over time as is thought to happen in humans. Our model possibly shows such an accelerated progression because the epithelium is already primed by both age related genetic changes and environmental/physiological events within the diseased prostate combined with expression of c-MYC from an extremely strong constitutive promoter.

Human prostatic epithelium expresses prostate specific antigen (PSA), in vivo this weak protease belongs to the large family of Kallikreins, and is not, despite the name, totally specific for the prostate. However, PSA is the main basis of the blood tests used to detect and monitor prostate cancer. PSA is androgen-regulated in normal and low-grade prostate cancers, however, as cancers progress to an androgen-independent state, PSA levels climb marking disease progression. Primary cultures of benign prostate cells initially express PSA as do the established cell line LNCaP [63]. However, it is commonly observed that cells in culture rapidly lose expression of steroid receptors, including AR, and consequently lose expression of steroid regulated gene products such as PSA. Tissue recombinants composed of normal prostatic epithelium and rUGM express both AR and PSA [47], as would be expected, since these genes are both regulated by the context in which the cell is growing. More remarkably Myc overexpressing cells express PSA and maintain their androgen receptor expression in culture. Tumors derived from these cells continue to express PSA and AR in vivo adding an important element to the relevance of this model.

Sawyers and co-workers [20] have identified a molecular signature that identifies both the c-MYC overexpressing prostate tumors present in their transgenic mouse model and a subset of human prostate tumors that overexpress Myc. Our cDNA analysis identified several targets that were subsequently analyzed by Western blotting, as our cDNA array differed from that used by the Sawyers group we were unable to compare their molecular signature with the one we obtained. We were however able to use the microarray data to identify proteins previously shown to be involved in tumorigenesis which were regulated in this model. Western blot analysis was used to confirm microarray data on the loss of PTEN and E-cadherin in the c-MYC expressing cells. Both of these proteins are implicated as playing a tumor suppressive role in cancer development and show a marked decrease in expression compared to control cells. Decreased or absent E-cadherin expression is a frequent occurrence in human prostate cancer [64] and this is recapitulated within our myc overexpressing tumor. The undetectable levels (by Western blotting) of E-cadherin present in our myc tumor cells in culture may represent a general loss of adhesion, which would in part explain the low adhesion of the cells both to the tissue culture plastic and other cells resulting in loss of the cobblestone morphology and lack of strong junctions between cells. Immunohistochemistry on the tumor tissue failed to pick up E-cadherin staining on the cell membranes within the tumor (data not shown).

PTEN is a tumor suppressor gene situated at 10q23, a deletion hot spot in prostate cancer [65]. PTEN Knockout mice are embryonic lethal [66] but tissue specific homozygotes (0% gene dose in prostate 100% in most other tissues) and the newer hypomorphic mice (25%–35% gene dose) [67–70] display mPIN that progresses to invasive carcinoma over time. Heterozygote PTEN deletion results in mPIN but requires the presence of a second genetic lesion to progress to an invasive cancer phenotype [71,72]. PTEN encodes a lipid phosphatase that inhibits the PI3 kinase/AKT pathway. The AKT pathway is a pivotal point in the control of cellular homeostasis. Many pathways including TGFβ, IGF, EGF and Ras interact with AKT. The activation of AKT appears to indirectly promote androgen-independent survival of prostate cancer cells, but the mechanism is as yet undetermined [73,74]. PTEN and AKT are upstream of c-MYC; PTEN loss causes upregulation of AKT that in turn upregulates c-MYC. The role of AKT on AR and subsequent repercussions on c-MYC are unknown but the importance of AKT and by extension PTEN in androgen independent growth of prostate cancer correlates with the role of c-MYC.

Microarray data verified by Western blot analysis demonstrated upregulation of the cMyb oncogene in

the C7-Myc model. Myb is usually regarded as a proto-oncogene within the hematopoietic line where it functions as a cell cycle promoter. c-Myb inhibits expression of $p15^{ink4b}$ while transactivating c-MYC, Bcl-2, COX2, IGF-I, and IGF-IR [75–77]. While c-Myb has primarily been studied in the hematopoietic lineage it is also expressed in breast, the gastrointestinal lineage [78], and prostate [79–81], it is upregulated in cancers and some premalignant lesions of these tissues [79,80,82–85]. The upregulation of cMyb in the C7-Myc model may further enhance the transforming ability of c-MYC by stimulating pathways that are not stimulated by Myc.

This work demonstrates the application of retroviral infection strategy followed by tissue recombination to examine the contribution of individual gene products to carcinogenesis. The approach can be used on any of the regulated products within the 8q24 amplicon, or those identified in the cDNA microarray analysis, both alone and in combination to determine their contribution to the final graft phenotype. This in vivo model of prostate cancer based upon human prostatic epithelium has many interesting and potentially useful features. However, the rapid progression and extremely high proliferative rate limits the ability to examine early tumorigenic events. The model retains many characteristics of human prostate cancer including continued expression of AR and PSA. The model also demonstrates downregulation of two tumor suppressors (PTEN and E-cadherin), which are suppressed in human prostate cancer and shows upregulation of Myb, which is known to be upregulated in the human disease. Metastasis is also an important component of the in vivo model. Cell cultures derived from both the initial viral infections and from the tumors retain many of these important characteristics and represent a potentially useful resource to examine prostate cancer biology. We are working to modify the model using a series of weaker constitutive, conditional, and regulatible promoters that will better allow us to follow stages of progression.

ACKNOWLEDGMENTS

Preliminary feasibility studies were supported by a grant to S.W.H and Y.F.L from the University of California, San Francisco Prostate Cancer Center. This work was supported by a postdoctoral fellowship grant DAMD 17-01-1-0037 to KW from the Department of Defense Prostate Cancer Research Program by NIH grant CA96403 and support from the Joe C. Davis Foundation to S.W.H. All microarray experiments were performed in the Vanderbilt Microarray Shared Resource. All DNA sequencing took place in the Vanderbilt DNA Sequencing Facility. Both core resources are supported in part by the Vanderbilt Ingram Cancer Center (P30 CA68485) and the Vanderbilt Diabetes Research and Training Center (P60 DK20593). SWH and KW wish to express their personal gratitude to Dr. Peter Carroll of UCSF for his unhesitating and selfless support.

REFERENCES

1. Quinn M, Babb P. Patterns and trends in prostate cancer incidence, survival, prevalence and mortality. Part I: International comparisons. BJU Int 2002;90(2):162–173.
2. Hsing AW, Tsao L, Devesa SS. International trends and patterns of prostate cancer incidence and mortality. Int J Cancer 2000; 85(1):60–67.
3. Chiarodo A. National Cancer Institute roundtable on prostate cancer: Future research directions. Cancer Res 1991;51(9):2498–2505.
4. Carroll PR. Trends in prostate cancer mortality among black men and white men in the United States. In: Chu KC, Tarone RE, Freeman HP, editors. Center to reduce cancer health disparities. Bethesda, MD: National Cancer Institute, Cancer 2003;97:1507–1516 (Urol Oncol 2003;21(6):483–484).
5. Lau YF, Lau HW, Komuves LG. Expression pattern of a gonadoblastoma candidate gene suggests a role of the Y chromosome in prostate cancer. Cytogenet Genome Res 2003;101(3–4):250–260.
6. DeMarzo AM, Nelson WG, Isaacs WB, Epstein JI. Pathological and molecular aspects of prostate cancer. Lancet 2003;361(9361): 955–964.
7. Malynn BA, de Alboran IM, O'Hagan RC, Bronson R, Davidson L, DePinho RA, Alt FW. N-myc can functionally replace c-myc in murine development, cellular growth, and differentiation. Genes Dev 2000;14(11):1390–1399.
8. Davis AC, Wims M, Spotts GD, Hann SR, Bradley A. A null c-myc mutation causes lethality before 10.5 days of gestation in homozygotes and reduced fertility in heterozygous female mice. Genes Dev 1993;7(4):671–682.
9. Davis A, Bradley A. Mutation of N-myc in mice: What does the phenotype tell us? Bioessays 1993;15(4):273–275.
10. Blackwood EM, Eisenman RN. Max: A helix-loop-helix zipper protein that forms a sequence-specific DNA-binding complex with Myc. Science 1991;251(4998):1211–1217.
11. Hurlin PJ, Queva C, Koskinen PJ, Steingrimsson E, Ayer DE, Copeland NG, Jenkins NA, Eisenman RN. Mad3 and Mad4: Novel Max-interacting transcriptional repressors that suppress c-myc dependent transformation and are expressed during neural and epidermal differentiation. Embo J 1995;14(22):5646–5659.
12. Bowen H, Biggs TE, Phillips E, Baker ST, Perry VH, Mann DA, Barton CH. c-Myc represses and Miz-1 activates the murine natural resistance-associated protein 1 promoter. J Biol Chem 2002;277(38):34997–35006.
13. Gartel AL, Shchors K. Mechanisms of c-myc-mediated transcriptional repression of growth arrest genes. Exp Cell Res 2003; 283(1):17–21.
14. Peukert K, Staller P, Schneider A, Carmichael G, Hanel F, Eilers M. An alternative pathway for gene regulation by Myc. Embo J 1997;16(18):5672–5686.
15. Beier R, Burgin A, Kiermaier A, Fero M, Karsunky H, Saffrich R, Moroy T, Ansorge W, Roberts J, Eilers M. Induction of cyclin E-cdk2 kinase activity, E2F-dependent transcription and cell

growth by Myc are genetically separable events. Embo J 2000; 19(21):5813–5823.

16. Coller HA, Grandori C, Tamayo P, Colbert T, Lander ES, Eisenman RN, Golub TR. Expression analysis with oligonucleotide microarrays reveals that MYC regulates genes involved in growth, cell cycle, signaling, and adhesion. Proc Natl Acad Sci USA 2000;97(7):3260–3265.
17. Bouchard C, Thieke K, Maier A, Saffrich R, Hanley-Hyde J, Ansorge W, Reed S, Sicinski P, Bartek J, Eilers M. Direct induction of cyclin D2 by Myc contributes to cell cycle progression and sequestration of p27. Embo J 1999;18(19):5321–5333.
18. Herold S, Wanzel M, Beuger V, Frohme C, Beul D, Hillukkala T, Syvaoja J, Saluz HP, Haenel F, Eilers M. Negative regulation of the mammalian UV response by Myc through association with Miz-1. Mol Cell 2002;10(3):509–521.
19. Staller P, Peukert K, Kiermaier A, Seoane J, Lukas J, Karsunky H, Moroy T, Bartek J, Massague J, Hanel F, Eilers M. Repression of p15INK4b expression by Myc through association with Miz-1. Nat Cell Biol 2001;3(4):392–399.
20. Ellwood-Yen K, Graeber TG, Wongvipat J, Iruela-Arispe ML, Zhang J, Matusik R, Thomas GV, Sawyers CL. Myc-driven murine prostate cancer shares molecular features with human prostate tumors. Cancer Cell 2003;4(3):223–238.
21. Nesbit CE, Tersak JM, Prochownik EV. MYC oncogenes and human neoplastic disease. Oncogene 1999;18(19):3004–3016.
22. Zhang X, Lee C, Ng PY, Rubin M, Shabsigh A, Buttyan R. Prostatic neoplasia in transgenic mice with prostate-directed overexpression of the c-myc oncoprotein. Prostate 2000;43(4): 278–285.
23. Pelengaris S, Littlewood T, Khan M, Elia G, Evan G. Reversible activation of c-Myc in skin: Induction of a complex neoplastic phenotype by a single oncogenic lesion. Mol Cell 1999;3(5): 565–577.
24. Jensen NA, Pedersen KM, Lihme F, Rask L, Nielsen JV, Rasmussen TE, Mitchelmore C. Astroglial c-Myc overexpression predisposes mice to primary malignant gliomas. J Biol Chem 2003;278(10):8300–8308.
25. Thompson TC, Park SH, Timme TL, Ren C, Eastham JA, Donehower LA, Bradley A, Kadmon D, Yang G. Loss of p53 function leads to metastasis in ras+myc-initiated mouse prostate cancer. Oncogene 1995;10(5):869–879.
26. Thompson TC, Southgate J, Kitchener G, Land H. Multistage carcinogenesis induced by ras and myc oncogenes in a reconstituted organ. Cell 1989;56(6):917–930.
27. Thompson TC, Timme TL, Kadmon D, Park SH, Egawa S, Yoshida K. Genetic predisposition and mesenchymal–epithelial interactions in ras+myc-induced carcinogenesis in reconstituted mouse prostate. Mol Carcinog 1993;7(3):165–179.
28. Fleming WH, Hamel A, MacDonald R, Ramsey E, Pettigrew NM, Johnston B, Dodd JG, Matusik RJ. Expression of the c-myc protooncogene in human prostatic carcinoma and benign prostatic hyperplasia. Cancer Res 1986;46(3):1535–1538.
29. Jain M, Arvanitis C, Chu K, Dewey W, Leonhardt E, Trinh M, Sundberg CD, Bishop JM, Felsher DW. Sustained loss of a neoplastic phenotype by brief inactivation of MYC. Science 2002; 297(5578):102–104.
30. Karlsson A, Giuriato S, Tang F, Fung-Weier J, Levan G, Felsher DW. Genomically complex lymphomas undergo sustained tumor regression upon MYC inactivation unless they acquire novel chromosomal translocations. Blood 2003;101(7): 2797–2803.
31. Elo JP, Visakorpi T. Molecular genetics of prostate cancer. Ann Med 2001;33(2):130–141.
32. Tsuchiya N, Kondo Y, Takahashi A, Pawar H, Qian J, Sato K, Lieber MM, Jenkins RB. Mapping and gene expression profile of the minimally overrepresented 8q24 region in prostate cancer. Am J Pathol 2002;160(5):1799–1806.
33. Porkka KP, Tammela TL, Vessella RL, Visakorpi T. RAD21 and KIAA0196 at 8q24 are amplified and overexpressed in prostate cancer. Genes Chromosomes Cancer 2004;39(1): 1–10.
34. Reiter RE, Sato I, Thomas G, Qian J, Gu Z, Watabe T, Loda M, Jenkins RB. Coamplification of prostate stem cell antigen (PSCA) and MYC in locally advanced prostate cancer. Genes Chromosomes Cancer 2000;27(1):95–103.
35. El Gedaily A, Bubendorf L, Willi N, Fu W, Richter J, Moch H, Mihatsch MJ, Sauter G, Gasser TC. Discovery of new DNA amplification loci in prostate cancer by comparative genomic hybridization. Prostate 2001;46(3):184–190.
36. Bubendorf L, Kononen J, Koivisto P, Schraml P, Moch H, Gasser TC, Willi N, Mihatsch MJ, Sauter G, Kallioniemi OP. Survey of gene amplifications during prostate cancer progression by high-throughout fluorescence in situ hybridization on tissue microarrays. Cancer Res 1999;59(4):803–806.
37. Qian J, Jenkins RB, Bostwick DG. Detection of chromosomal anomalies and c-myc gene amplification in the cribriform pattern of prostatic intraepithelial neoplasia and carcinoma by fluorescence in situ hybridization. Mod Pathol 1997;10(11):1113–1119.
38. Chaib H, Cockrell EK, Rubin MA, Macoska JA. Profiling and verification of gene expression patterns in normal and malignant human prostate tissues by cDNA microarray analysis. Neoplasia 2001;3(1):43–52.
39. Buttyan R, Sawczuk IS, Benson MC, Siegal JD, Olsson CA. Enhanced expression of the c-myc protooncogene in high-grade human prostate cancers. Prostate 1987;11(4):327–337.
40. Hayward SW, Haughney PC, Lopes ES, Danielpour D, Cunha GR. The rat prostatic epithelial cell line NRP-152 can differentiate in vivo in response to its stromal environment. Prostate 1999; 39(3):205–212.
41. Wang YZ, Sudilovsky D, Zhang B, Haughney PC, Rosen MA, Wu DS, Cunha TJ, Dahiya R, Cunha GR, Hayward SW. A human prostatic epithelial model of hormonal carcinogenesis. Cancer Res 2001;61:6064–6072.
42. Hallowes RC, Bone EJ, Jones W. A new dimension in the culture of human breast. In: Richards RJ, Rajan KT, editors. Tissue culture in medical research. Vol 2. Oxford: Pergamon Press; 1980. pp 213–220.
43. Hayward SW. A simple method for freezing and storing viable tissue fragments. In Vitro Cell Dev Biol Anim 1998;34(1): 28–29.
44. Taylor-Papadimitriou J, Stampfer M, Bartek J, Lewis A, Boshell M, Lane EB, Leigh IM. Keratin expression in human mammary epithelial cells cultured from normal and malignant tissue: Relation to in vivo phenotypes and influence of medium. J Cell Sci 1989;94:403–413.
45. Perkins W, Campbell I, Leigh IM, MacKie RM. Keratin expression in normal skin and epidermal neoplasms demonstrated by a panel of monoclonal antibodies. J Cutan Pathol 1992; 19(6):476–482.
46. Cunha GR, Vanderslice KD. Identification in histological sections of species origin of cells from mouse, rat and human. Stain Technol 1984;59(1):7–12.

47. Hayward SW, Haughney PC, Rosen MA, Greulich KM, Weier HU, Dahiya R, Cunha GR. Interactions between adult human prostatic epithelium and rat urogenital sinus mesenchyme in a tissue recombination model. Differentiation 1998;63(3):131–140.
48. Snibson KJ, Woodcock D, Orian JM, Brandon MR, Adams TE. Methylation and expression of a metallothionein promoter ovine growth hormone fusion gene (MToGH1) in transgenic mice. Transgenic Res 1995;4(2):114–122.
49. Smith MR, Biggar S, Hussain M. Prostate-specific antigen messenger RNA is expressed in non-prostate cells: Implications for detection of micrometastases. Cancer Res 1995;55(12):2640–2644.
50. Pelengaris S, Khan M, Evan GI. Suppression of Myc-induced apoptosis in beta cells exposes multiple oncogenic properties of Myc and triggers carcinogenic progression. Cell 2002;109(3):321–334.
51. Prendergast GC. Mechanisms of apoptosis by c-Myc. Oncogene 1999;18(19):2967–2987.
52. Prendergast GC. Myc and Myb: Are the veils beginning to lift? Oncogene 1999;18(19):2914–2915.
53. Dang CV, Resar LM, Emison E, Kim S, Li Q, Prescott JE, Wonsey D, Zeller K. Function of the c-Myc oncogenic transcription factor. Exp Cell Res 1999;253(1):63–77.
54. Dang CV. c-Myc target genes involved in cell growth, apoptosis, and metabolism. Mol Cell Biol 1999;19(1):1–11.
55. Amati B, Alevizopoulos K, Vlach J. Myc and the cell cycle. Front Biosci 1998;3:D250–D268.
56. Thompson TC. Growth factors and oncogenes in prostate cancer. Cancer Cells 1990;2(11):345–354.
57. Thompson TC, Egawa S, Kadmon D, Miller GJ, Timme TL, Scardino PT, Park SH. Androgen sensitivity and gene expression in ras + myc-induced mouse prostate carcinomas. J Steroid Biochem Mol Biol 1992;43(1–3):79–85.
58. Thompson TC, Kadmon D, Timme TL, Merz VW, Egawa S, Krebs T, Scardino PT, Park SH. Experimental oncogene induced prostate cancer. Cancer Surv 1991;11:55–71.
59. Lehr JE, Pienta KJ, Yamazaki K, Pilat MJ. A model to study c-myc and v-H-ras induced prostate cancer progression in the Copenhagen rat. Cell Mol Biol (Noisy-le-grand) 1998;44(6):949–959.
60. Edwards PA, Ward JL, Bradbury JM. Alteration of morphogenesis by the v-myc oncogene in transplants of mammary gland. Oncogene 1988;2(4):407–412.
61. Mehta PP, Bertram JS, Loewenstein WR. Growth inhibition of transformed cells correlates with their junctional communication with normal cells. Cell 1986;44(1):187–196.
62. Pylkkanen L, Makela S, Valve E, Harkonen P, Toikkanen S, Santti R. Prostatic dysplasia associated with increased expression of c-myc in neonatally estrogenized mice. J Urol 1993;149(6):1593–1601.
63. Denmeade SR, Sokoll LJ, Dalrymple S, Rosen DM, Gady AM, Bruzek D, Ricklis RM, Isaacs JT. Dissociation between androgen responsiveness for malignant growth vs. expression of prostate specific differentiation markers PSA, hK2, and PSMA in human prostate cancer models. Prostate 2003;54(4):249–257.
64. Umbas R, Schalken JA, Aalders TW, Carter BS, Karthaus HF, Schaafsma HE, Debruyne FM, Isaacs WB. Expression of the cellular adhesion molecule E-cadherin is reduced or absent in high-grade prostate cancer. Cancer Res 1992;52(18):5104–5109.
65. Verma RS, Manikal M, Conte RA, Godec CJ. Chromosomal basis of adenocarcinoma of the prostate. Cancer Invest 1999;17(6):441–447.
66. Di Cristofano A, Pesce B, Cordon-Cardo C, Pandolfi PP. Pten is essential for embryonic development and tumour suppression. Nat Genet 1998;19(4):348–355.
67. Backman SA, Ghazarian D, So K, Sanchez O, Wagner KU, Hennighausen L, Suzuki A, Tsao MS, Chapman WB, Stambolic V, Mak TW. Early onset of neoplasia in the prostate and skin of mice with tissue-specific deletion of Pten. Proc Natl Acad Sci USA 2004;101(6):1725–1730.
68. Dose of PTEN Gene Drives Progression of Prostate Cancer. PLoS Biol 2003;1(3):E70.
69. Trotman LC, Niki M, Dotan ZA, Koutcher JA, Cristofano AD, Xiao A, Khoo AS, Roy-Burman P, Greenberg NM, Dyke TV, Cordon-Cardo C, Pandolfi P. Pten Dose Dictates Cancer Progression in the Prostate. PLoS Biol 2003;1(3):E59.
70. Wang S, Gao J, Lei Q, Rozengurt N, Pritchard C, Jiao J, Thomas GV, Li G, Roy-Burman P, Nelson PS, Liu X, Wu H. Prostate-specific deletion of the murine Pten tumor suppressor gene leads to metastatic prostate cancer. Cancer Cell 2003;4(3):209–221.
71. Di Cristofano A, De Acetis M, Koff A, Cordon-Cardo C, Pandolfi PP. Pten and p27KIP1 cooperate in prostate cancer tumor suppression in the mouse. Nat Genet 2001;27(2):222–224.
72. Abate-Shen C, Banach-Petrosky WA, Sun X, Economides KD, Desai N, Gregg JP, Borowsky AD, Cardiff RD, Shen MM. Nkx3.1; Pten mutant mice develop invasive prostate adenocarcinoma and lymph node metastases. Cancer Res 2003;63(14):3886–3890.
73. Nan B, Snabboon T, Unni E, Yuan XJ, Whang YE, Marcelli M. The PTEN tumor suppressor is a negative modulator of androgen receptor transcriptional activity. J Mol Endocrinol 2003;31(1):169–183.
74. Ghosh PM, Malik S, Bedolla R, Kreisberg JI. Akt in prostate cancer: Possible role in androgen-independence. Curr Drug Metab 2003;4(6):487–496.
75. Wolff L, Schmidt M, Koller R, Haviernik P, Watson R, Bies J, Maciag K. Three genes with different functions in transformation are regulated by c-Myb in myeloid cells. Blood Cells Mol Dis 2001;27(2):483–488.
76. Ramsay RG, Friend A, Vizantios Y, Freeman R, Sicurella C, Hammett F, Armes J, Venter D. Cyclooxygenase-2, a colorectal cancer nonsteroidal anti-inflammatory drug target, is regulated by c-MYB. Cancer Res 2000;60(7):1805–1809.
77. Baserga R, Hongo A, Rubini M, Prisco M, Valentinis B. The IGF-I receptor in cell growth, transformation and apoptosis. Biochim Biophys Acta 1997;1332(3):F105–F126.
78. Zorbas M, Sicurella C, Bertoncello I, Venter D, Ellis S, Mucenski ML, Ramsay RG. c-Myb is critical for murine colon development. Oncogene 1999;18(42):5821–5830.
79. Rijnders AW, van der Korput JA, van Steenbrugge GJ, Romijn JC, Trapman J. Expression of cellular oncogenes in human prostatic carcinoma cell lines. Biochem Biophys Res Commun 1985;132(2):548–554.
80. Edwards J, Krishna NS, Witton CJ, Bartlett JM. Gene amplifications associated with the development of hormone-resistant prostate cancer. Clin Cancer Res 2003;9(14):5271–5281.
81. Katz AE, Benson MC, Wise GJ, Olsson CA, Bandyk MG, Sawczuk IS, Tomashefsky P, Buttyan R. Gene activity during the early phase of androgen-stimulated rat prostate regrowth. Cancer Res 1989;49(21):5889–5894.
82. Guerin M, Sheng ZM, Andrieu N, Riou G. Strong association between c-myb and oestrogen-receptor expression in human breast cancer. Oncogene 1990;5(1):131–135.

83. Guerin M, Barrois M, Riou G. [The expression of c-myb is strongly associated with the presence of estrogen and progesterone receptors in breast cancer]. C R Acad Sci III 1988;307(20): 855–861.

84. Ramsay RG, Thompson MA, Hayman JA, Reid G, Gonda TJ, Whitehead RH. Myb expression is higher in malignant human colonic carcinoma and premalignant adenomatous polyps than in normal mucosa. Cell Growth Differ 1992;3(10): 723–730.

85. Thompson MA, Flegg R, Westin EH, Ramsay RG. Microsatellite deletions in the c-myb transcriptional attenuator region associated with over-expression in colon tumour cell lines. Oncogene 1997;14(14):1715–1723.

genesis 42:263–275 (2005)

ARTICLE

A Cre Gene Directed by a Human TSPY Promoter Is Specific for Germ Cells and Neurons

Tatsuo Kido and Yun-Fai Chris Lau*

Division of Cell and Developmental Genetics, Department of Medicine, VA Medical Center, University of California, San Francisco, San Francisco, California

Received 15 December 2004; Accepted 23 May 2005

Summary: The testis-specific protein Y-encoded (TSPY) gene is a candidate for the gonadoblastoma locus on the Y chromosome and is expressed in normal testicular germ cells and gonadoblastoma cells of XY sex-reversed females. Although TSPY expression has been demonstrated in gonadoblastoma tissues, it is uncertain if such expression is involved in a causative or consequential event of the oncogenic process. We postulate that if TSPY is involved in gonadoblastoma development, its promoter should be functional in the female gonad before and/or at early stages of tumorigenesis. To test this hypothesis, we generated several lines of transgenic mice harboring a Cre-recombinase transgene directed by a 2.4-kb hTSPY promoter. These mice were crossed with the Z/EG reporter line that expresses EGFP only after a Cre-mediated recombination. Our results showed that hTSPY-Cre;Z/EG double transgenic mice expressed EGFP specifically in the germ cells of both male and female gonads. Further, neurons of the central and peripheral nervous systems also expressed EGFP as early as E12.5 embryonic stage. EGFP was particularly observed in the trigeminal nerve, trigeminal ganglion, dorsal root of the ganglia, and in postnatal and adult brains. These observations support the hypothesis that TSPY plays an active role in gonadoblastoma. The tissue-specific expression of the hTSPY-Cre transgene should also be useful in studies utilizing Cre-mediated gene activation/inactivation strategies in gamatogenesis and/or neurogenesis. genesis 42:263–275, 2005.

Key words: TSPY promoter; gonadoblastoma; germ cell; neurons; Cre recombinase; transgenic mice

INTRODUCTION

The human testis-specific protein Y-encoded (hTSPY) gene was initially identified as a testis-specific gene repeated tandemly >35 times on the short arm of the human Y chromosome (Arnemann *et al.*, 1987; Zhang *et al.*, 1992; Skaletsky *et al.*, 2003). hTSPY is expressed normally in the germ cells of both adult and fetal testes (Zhang *et al.*, 1992; Schnieders *et al.*, 1996; Honecker *et al.*, 2004). It has been postulated to serve a vital function(s) in male germ cell formation and early spermatogenesis (Schnieders *et al.*, 1996; Lau, 1999). Further, TSPY expression has also been observed in germ cells of gonadoblastoma, various forms of testicular tumors, and epithelial cells of prostate cancer (Schnieders *et al.*, 1996; Lau *et al.*, 2000, 2003; Lau and Zhang, 2000). The human TSPY shares significant homology with the SET oncoprotein and is a founding member of the TSPY/SET/NAP-1 protein family (von Lindern *et al.*, 1992; Vogel *et al.*, 1998; Ozbun *et al.*, 2001). Members of this gene family encode proteins that harbor a conserved NAP/SET domain (Ishimi and Kikuchi, 1991) and have been demonstrated to play various roles in cell cycle regulation or cell differentiation (Chai *et al.*, 2001; Seo *et al.*, 2001; Canela *et al.*, 2003). Hence, hTSPY has been hypothesized to regulate the spermatogenic cells in entering male meiosis or in mediating the meiotic divisions (Schnieders *et al.*, 1996; Lau, 1999).

The human TSPY gene cluster has been mapped to the critical region on the Y chromosome harboring the gonadoblastoma locus (GBY), the only oncogenic or tumor-promoting locus currently identified on this male-specific chromosome (Page, 1987; Salo *et al.*, 1995; Tsuchiya *et al.*, 1995). Gonadoblastoma develops most frequently in the dysgenic gonads of XY sex-reversed females and those of girls harboring a mixture of XX/XO and XY gonadal cells. Gonadoblastoma shares significant similarities with the testicular carcinoma-in-situ (CIS) and both have been considered as precursors for the more aggressive germ cell tumors (Jorgensen *et al.*, 1997; Rajpert-De-Meyts *et al.*, 2003). Although the disease mechanism(s) is still uncertain, the aberrant expression of a Y

* Correspondence to: Chris Lau, Ph.D., Division of Cell and Developmental Genetics, Department of Medicine, VA Medical Center, 111C5, University of California, San Francisco, 4150 Clement Street, San Francisco, CA 94121.
E-mail: clau@itsa.ucsf.edu

Contract grant sponsor: Department of Defense Prostate Cancer Research Program; Contract grant number: DAMD-17-03-1-0081 (to Y-F. C.L.); Contract grant sponsor: National Institutes of Health; Contract grant number: 1RO1HD038117.
Published online in
Wiley InterScience (www.interscience.wiley.com).
DOI: 10.1002/gene.20147

chromosome gene(s) in a female gonadal environment has been hypothesized to play an important role in predisposing the dysgenic gonads to tumorigenesis (Page, 1987). TSPY is a strong candidate for GBY locus based on several lines of indirect evidence, including its mapping to the GBY critical region, abundant expression in gonadoblastoma tissues, and significant homology to a family of cell cycle regulatory proteins. However, it is uncertain whether the TSPY expression in gonadoblastoma is a causative event or a consequence of the oncogenic process. Hence, in order to further substantiate its role in gonadoblastoma, we need to demonstrate that its promoter is active in normal or pretumorigenic female gonads. To achieve this goal, we developed a transgenic strategy to investigate the hTSPY promoter activity. We generated several lines of transgenic mice harboring a Cre recombinase gene directed by the promoter of hTSPY gene and evaluated the functionality of the human TSPY promoter by either reverse transcription–polymerase chain reaction (RT-PCR) analysis of the Cre transgene or crossing them with the Z/EG reporter line that expresses EGFP only after a Cre-mediated recombination (Novak *et al.*, 2000). Since EGFP expression can be directly observed as green fluorescence, it provides a convenient means in indirectly detecting the human TSPY promoter activity in tissues and cells of transgenic embryos and adult mice. Our study demonstrated that the hTSPY-Cre transgene was expressed in germ cell lineage in embryos and adult mice of both sexes. In particular, EGFP transgene was activated in adult hTSPY-Cre;Z/EG mice mediated by the hTSPY-Cre gene in the germ cells of both male and female animals, confirming that human TSPY promoter is active in testicular and ovarian germ cells. Significantly, we also detected high levels of EGFP expression in neurons of the central nervous system (CNS) and peripheral nervous system of adult mice. This hTSPY promoter-directed transgene activation could also be observed in selected neurons of fetal brains of mouse embryos as early as E12.5 stage. These latter observations raise the possibility that if similar embryonic expression can be demonstrated in humans, hTSPY might play additional roles in neuronal development in embryos and nervous functions in adults.

RESULTS

Previous studies have demonstrated that a 1.35-kb promoter of the TSPY gene is capable and sufficient in directing a transgene expression in the spermatogonia-derived cell line, GC-1spg (Tascou *et al.*, 2000) and that transgenic mice harboring a human TSPY gene integrated in their Y chromosome show a transgene expression pattern similar to that of humans (Schubert *et al.*, 2003). In the latter study, the transgene harbors a 2.9-kb promoter sequence of the human TSPY gene that is integrated into the Y chromosome of the host. While this transgenic line closely resembles the human TSPY gene in terms of its chromosomal location and expression pattern, it cannot be used in the evaluation of the transgene

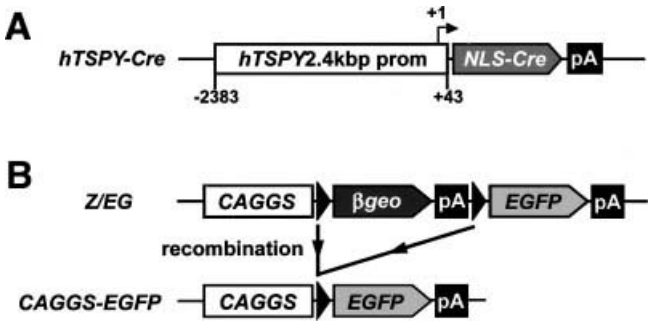

FIG. 1. The Cre-LoxP transgene activation system. **A:** The hTSPY-Cre gene contains a 2.4-kb promoter of the human TSPY gene (white box), Cre recombinase cDNA with a nuclear localization signal (gray arrow), and an SV40 polyadenylation signal (black box). +1 indicates the transcription start site. **B:** The Z/EG responder construct (Novak *et al.*, 2000) consists of two expression cassettes, βgeo and EGFP, directed by a strong CAGGS promoter. Two LoxP sites flank the βgeo gene that is normally expressed in transgenic mice harboring only Z/EG. In hTSPY-Cre;Z/EG double transgenic mice the hTSPY promoter directs the expression of Cre recombinase which subsequently cleaves the sequence flanked by the LoxP sites, thereby repositioning the EGFP gene under the direct regulation of the ubiquitous CAGGS promoter. Hence, EGFP expression is indirectly linked to the hTSPY promoter activity.

expression in the female environment. Based on these results, we selected a 2.4-kb promoter in the present study to identify cells capable of expressing the hTSPY gene in the mouse using the Cre-LoxP gene activation scheme (Novak *et al.*, 2000). Preliminary characterization of this 2.4-kb promoter suggested that it was capable of directing the expression of a reporter gene in the spermatogonia or spermatocytes-derived cell lines, GC-1spg and GC-2spd, respectively, as previously described (Tascou *et al.*, 2000). An expression cassette in which this 2.4 kb promoter of the human TSPY gene was constructed to direct the expression of a Cre recombinase gene (Fig. 1A). Two transgenic founder animals designated #25 (male) and #33 (female) were obtained with this construct using a standard microinjection procedure. The #33 founder when bred with nontransgenic mouse produced offspring with two different copy numbers of the transgene, suggesting the possibility of two integration sites for this founder. Indeed, two sublines from founder #33 were derived, resulting in line 33A (42 copies) and line 33B (6 copies), respectively (Fig. 2A). All transgenes seemed to have integrated into the autosomes of the founding animals, since we did not observe any sex-linked inheritance of the respective transgenes. To determine the expression of the Cre transgene, the animals from lines 25, 33A, and 33B were analyzed by the RT-PCR technique. Line 25 did not show any detectable signal of Cre transgene expression in any tissue (data not shown). However, lines 33A and 33B showed expression of the hTSPY-Cre transgene primarily in the cerebral cortex, cerebellum, and gonads of male and female animals (Fig. 2B,C). These expression patterns are similar to that of a transgenic line harboring a human TSPY transgene on the Y chromosome of the host (Schubert *et al.*, 2003).

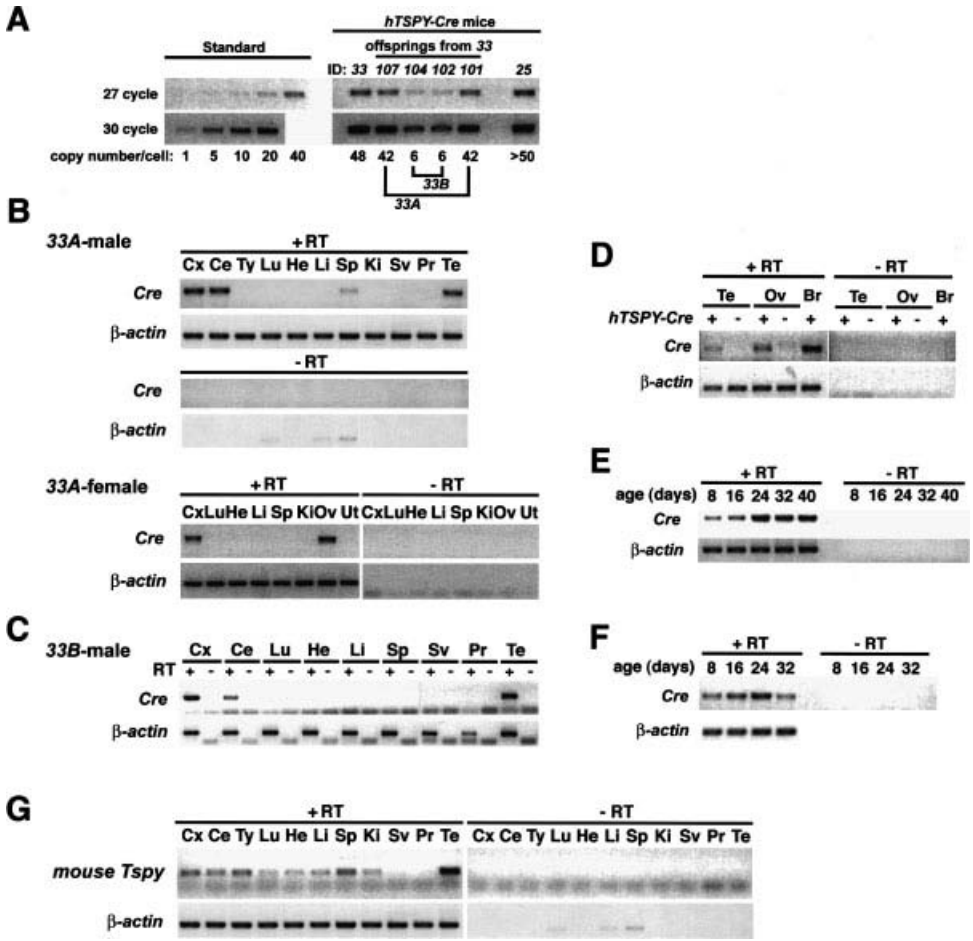

FIG. 2. Estimation of transgene copy numbers and expression analysis by RT-PCR analyses. **A:** Estimation of copy number of hTSPY-Cre transgene in transgenic mice by semiquantitative PCR of tail DNAs. Founder animal 33 had two integration sites that were segregated into two sublines: line 33A (42 copies) and line 33B (6 copies). ID: identity number for individual mouse. **B:** Cre expression patterns in adult hTSPY-Cre transgenic mice from lines 33A (**B**) and 33B (**C**). In both lines 33A and 33B, Cre mRNA was detected only in cerebral cortex, cerebellum, and gonads. Cx, cerebral cortex; Ce, cerebellum; Ty, thymus; Lu, lung; He, heart; Li, liver; Sp, spleen; Ki, kidney; Sv, seminal vesicle; Pr, prostate; Te, testis; Ov, ovary; Ut, uterus. **D:** hTSPY promoter-directed Cre transcripts in the gonads and brains of newborn transgenic mice. Cre transcript was detected in gonads and brains of newborn pups of both sexes. Te, testis; Ov, ovary ; Br, brain. **E:** Cre transcripts in testes of mice at various postnatal ages (days 8–40). **F:** Cre expression in ovary at various postnatal ages (days 8–32). **G:** Expression pattern of the mouse endogenous Tspy. The mouse Tspy transcript was preferentially expressed in testis and at low levels in a wide range of tissues, including the brain. β-Actin was used as a control. +RT indicates the results with reverse transcription reaction; −RT, without reverse transcription reaction. Signals are represented by negative printing of ethidium bromide staining of the RT-PCR products fractionated by agarose gel electrophoresis.

The expression of hTSPY-Cre transgene in the mouse brain was somewhat unexpected. To determine if the expression pattern of the transgene resembled the endogenous mouse Tspy gene, we extended our investigation to the Tspy genes in mouse. The mouse harbors an apparently noncoding Tspy gene on its Y chromosome, due to the presence of several in-frame stop codons (Mazeyrat and Mitchell, 1998). The mouse Tspy transcripts were detected most prominently in the testis and at low levels among other tissues, including the brain (Fig. 2G, mouse Tspy). Hence, the mouse Tspy gene behaves similarly to the hTSPY-Cre transgene in male mice (Fig. 2B,C).

We adopted the Cre-LoxP gene activation system to visualize the hTSPY promoter activity (Fig. 1A,B). In this scheme, animals from the hTSPY-Cre lines were crossed with those harboring the reporter gene, Z/EG, to generate double transgenic mice harboring both transgenes. The hTSPY promoter directed the expression of the Cre recombinase that cleaved the sequence, βgeo gene (i.e. a fusion gene coding for both the β-galactosidase and neo resistant marker), between the loxP sites in the Z/EG transgene, thereby repositioning the EGFP gene directly under the strong CAGGS promoter (Novak *et al.*, 2000). The CAGGS promoter was initially derived from the CAGG (or CAG) promoter (Niwa *et al.*, 1991) consisting of the CMV enhancer and the chicken β-actin promoter, being capable of mediating a high level of expression for the recombined EGFP gene. Hence, EGFP expression indirectly represents the hTSPY promoter activities in these double-transgenic mice. Using this strategy, we

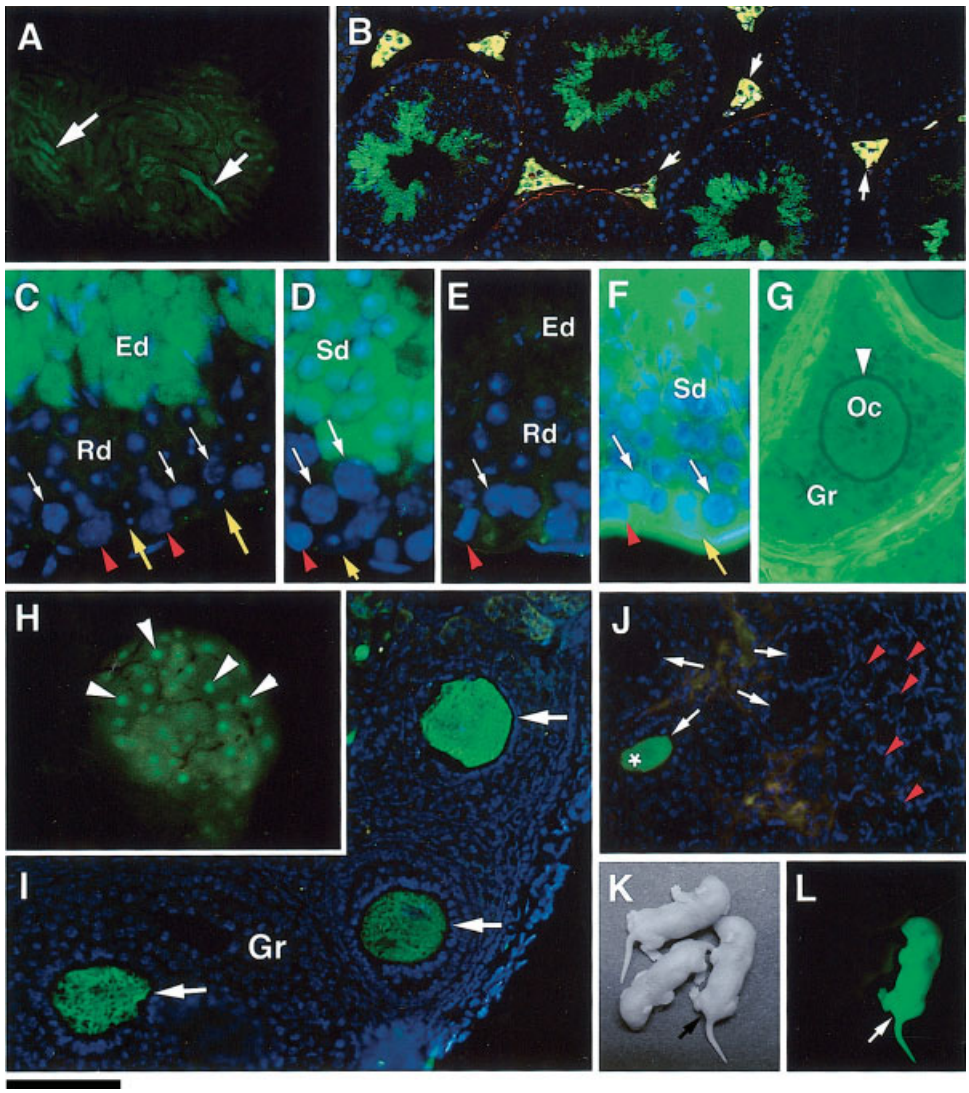

FIG. 3. Expression of EGFP in gonads of hTSPY-Cre;Z/EG double-transgenic mice. **A:** EGFP expression could be observed directly in dissected hTSPY-Cre;Z/EG adult testis (arrows). **B–D:** EGFP expression in male germ cells of testis in hTSPY-Cre;Z/EG mice generated by crossing 33A (**C**) and 33B (**D**) with the Z/EG line. DNA was counterstained by DAPI (blue). Interstitial tissues including the Leydig cells showed yellow fluorescence that was not part of the EGFP signal (arrows in **B**). **E:** No EGFP expression was observed in the testis of a single transgenic Z/EG mouse. Orange arrowheads indicate spermatogonia; yellow arrows, Sertoli cells; white arrows, spermatocytes; Rd, round spermatids; Ed, elongated spermatids. **F,G:** Testis (**F**) and ovary (**G**) sections of F2 animals showing ubiquitous expression of the fully recombined CAGGS-EGFP reporter, respectively. **H:** Direct observation of EGFP fluorescence from a dissected ovary from an 8-day-old hTSPY-Cre; Z/EG mouse. EGFP positive oocytes were identifiable (arrowheads). **I,J:** EGFP expression in maturing oocytes (arrows) of adult (**I**) and 8-day old (**J**) ovaries of hTSPY-Cre;Z/EG mice. DNA was counterstained by DAPI (blue). Granulosa cells (Gr) were EGFP negative. Arrowheads (in **J**) indicate oocytes in primary follicles; white arrows indicate oocytes in late primary and early secondary follicles; asterisk, an EGFP-positive oocyte. **K,L:** Pups from a hTSPY-Cre;Z/EG female mouse mated with a nontransgenic male mouse. Pups harboring the recombined CAGGS-EGFP transgene could be identified by their EGFP fluorescence (**K**, room light, and **L**, blue excitation light). Scale bar = 115 μm in **B**; 34 μm in **C–E**; 100 μm in **I**; 83 μm in **G**.

tested both lines 33A and 33B and showed that both were capable of inducing similar Cre-mediated recombination and activation of the EGFP transgene in the hTSPY-Cre;Z/EG double transgenic mice. Since line 33A harbored a higher number of transgene and the intensity of its expression was also higher than that of line 33B, line 33A was primarily used in the analyses described below.

The expression of the EGFP reporter was readily observed directly in dissected adult testis of hTSPY-Cre;Z/EG double transgenic mice (Fig. 3A). Immunofluorescence analysis showed that EGFP was primarily detected in round and elongating spermatids (Fig. 3B–D) in double-transgenic mice derived from crossing of the Z/EG animals with those of Line 33A (Fig. 3C) and Line 33B (Fig. 3D). However, somatic cells, spermatogonia, and spermatocytes did not show EGFP expression (arrows in Fig. 3C,D), suggesting that the Cre-mediated recombination might have occurred around the second

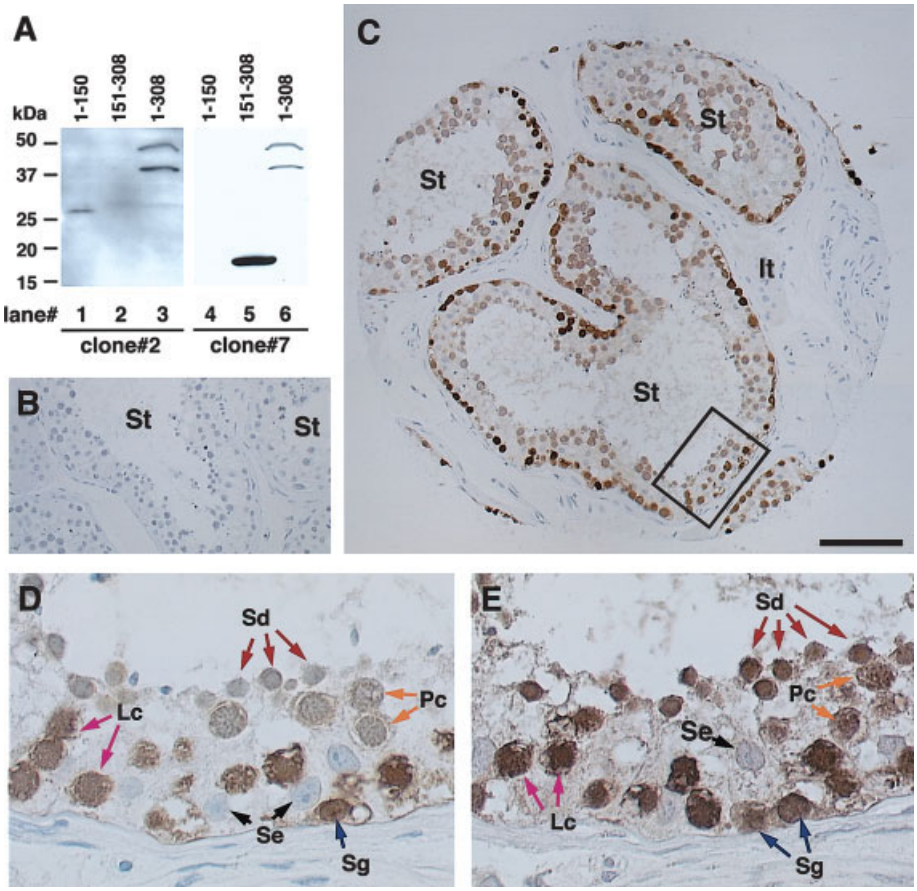

FIG. 4. TSPY expression in normal human testis. **A:** Western-blotting of protein extracts of COS7 cells transfected modular genes coding for different domains of TSPY. Antibodies from hybridoma clone #2 and clone #7 showed specificities for N-terminal (residue 1–150, lanes 1, 4) and C-terminal (residue 151–308, lanes 2, 5) halves of the human TSPY, respectively. The phosphorylated full-length (residues 1–308, lanes 3, 6) TSPY is ~38-kDa in the testis (Schnieders *et al.*, 1996) was detected by both monoclonal antibodies. The larger 48-kDa band in lanes 3 and 6 could be result(s) of additional posttranslational modification of the protein by the COS7 cells. **B–E:** Images of normal human testis immunostained by mouse pre-immune serum (**B**), and clone #2 (**C,D**), and clone #7 (**E**) antibodies, respectively. **D,E:** Magnified images of the boxed area in **C**, stained by clone #2 (**D**) and clone #7 (**E**), respectively. Most germ cells from spermatogonia to spermatids were immunoreactive to both clone #2 and clone #7 (Sg, Lc, Pc and Sd in **D,E**), while the somatic cells including Sertoli cells and Leydig cells were negative. However, clone #7 stained both the spermatogonial cells and the spermatids with equal intensity, while clone #2 showed a preferential staining of the spermatogonial cells. St, seminal tubules; It, interstitial cells; Se, Sertoli cells; Sg, spermatogonia; Lc, leptotene spermatocytes; Pc, pachytene spermatocytes; Sd, spermatids. Scale bar = 100 μm in **B,C**.

meiotic division. This observation is somewhat different from the previously reported human situation in which TSPY is specifically expressed in spermatogonia (Schnieders *et al.*, 1996). It is conceivable that the recombination in these hTSPY-Cre;Z/EG mice might have occurred at earlier stages, e.g., spermatogonia and/or spermatocytes, but the levels of recombination were insufficient to activate the EGFP gene and/or CAGGS promoter could become most active in later stages, thereby delaying the expression of the EGFP reporter at the round and elongated spermatids. Alternatively, TSPY could be expressed in other germ cells, such as the spermatids, in addition to the spermatogonia, but the available TSPY antibodies are incapable of detecting its expression in later stages of spermatogenesis.

To resolve these two possibilities, we reexamined the expression of TSPY in normal human testis using immunohistochemistry with two monoclonal antibodies generated against a full-length recombinant human TSPY protein. The antibodies from two hybridoma lines, designated as clone #2 and clone #7, recognized the N-terminal (residue #1–150) and C-terminal (residue #151–308) halves of the human TSPY protein respectively (Fig. 4A). Clone #7 stained positively for most germ cells, but preferentially for the spermatogonia and round spermatids (Fig. 4E). However, clone #2 stained preferentially the spermatogonial cells (Fig. 4C,D). The somatic cells, including Sertoli and Leydig cells, were negative for both antibodies. These findings, specifically the expression of TSPY protein in the germ cells at late stages of spermatogenesis, differ from previous reports of TSPY expression in the spermatogonial cells of the human testis (Schnieders *et al.*, 1996). The differential detection of TSPY proteins by these two N- and C-terminus-specific

monoclonal antibodies is an interesting observation. Recent studies demonstrated that several minor TSPY transcripts (designated Exon1A, 1B, and 1C) could be derived from alternative splicing of cryptic splice sites located at the first exon, resulting in in-frame deletions of 87, 104, and 139 amino acids from the N-terminal half of the TSPY protein (Lau *et al.*, 2003). Since clone #2 is specific for the N-terminus, variant proteins lacking this domain, as encoded by Exon1A–1C transcripts, will not be recognized by this monoclonal antibody. On the other hand, clone #7 is specific for the C-terminal half of the protein, present in all TSPY isoforms, and is capable of detecting most TSPY proteins. The present results suggest that the abbreviated forms of the TSPY protein could be preferentially expressed in round spermatids, while both the full-length and the abbreviated forms could be expressed in the spermatogenic cells. These findings suggest that TSPY expression in different stages of the spermatogenic cells in the human testis may be more complex than what was originally observed.

The Cre transcript levels were also evaluated in the testes of single hTSPY-Cre transgenic mice from newborn (day 1) to 40 days after birth by semiquantitative RT-PCR. Our results showed that the Cre recombinase transcripts were present in newborn male testis, ovary, and brain (Fig. 2D), but not in nontransgenic littermates. The level of Cre transcripts increased in the testis and became most abundant at day 24, when meiotic II division was initially observed and round spermatids appeared (Fig. 2E, Cre). Our results, together with recent observations of TSPY expression in prespermatogonial cells in both fetal and postnatal human testes (Honecker *et al.*, 2004), suggest that the human TSPY promoter is active in most gonocytes and prespermatogonia at fetal and postnatal testes and early and late stages of spermatogenesis in adult testis.

The ovarian expression of the Cre transgene could be detected with RT-PCR as early as newborn (Fig. 2D) and throughout the postnatal stages (Fig. 2F). When these hTSPY-Cre transgenic mice were crossed with the Z/EG reporter line, EGFP could be observed directly at the follicles in ovaries of 8-day-old double-transgenic mice (Fig. 3H, white arrowheads). EGFP was primarily located in the oocytes in the late primary follicles (Fig. 3J, white arrows) and those of maturing secondary follicles of adult females (Fig. 3I, white arrows). However, EGFP was not observed in the granulosa cells (Fig. 3I, Gr) nor the early primary follicles (Fig. 3J, orange arrowheads) in these hTSPY-Cre;Z/EG mice. The expression of EGFP in either the oocytes or sperm of these hTSPY-Cre;Z/EG mice did not seem to affect their fertility nor reproductive functions. The recombined CAGGS-EGFP gene could be transmitted to the offspring when these double-transgenic mice were mated with nontransgenic partners. Since recombined EGFP transgene was under the direction of the CAGGS promoter, it is expressed ubiquitously among many tissues of positive pups of the F2 generations (Fig. 3K,L). Although the Cre transgene could also be expressed in early primary oocytes and spermatogonia and spermatocytes, since its transcript could be detected in the ovaries and testes of newborn and prepuberty animals, respectively, by RT-PCR (Fig. 2D,E), the expression of EGFP reporter in the double transgenic mice is probably a true indication of the actual activities of the Cre recombinase directed by the human TSPY promoter. Analysis the F2 animals harboring the recombined CAGGS-EGFP transgene showed that EGFP was expressed almost ubiquitously in most cells in both the testis and the ovary (Fig. 3F,G, respectively), hence the differential expression of EGFP cannot be attributed to any differences in CAGGS promoter activities in the respective cell types in the hTSPY-Cre;Z/EG double transgenic mice. These results support the postulation that the 2.4-kb human TSPY promoter is functional in germ cells of postnatal testis and ovary, and is most active in germ cells at late meiotic stages.

Detection of Cre transcripts in brains of hTSPY-Cre mice was an interesting observation (Fig. 2B,C). Although TSPY transcripts have been reported in human brain EST databases (GenBank access. nos. BI828033, BX281192) and in transgenic mice harboring a human TSPY transgene on their Y chromosome (Schubert *et al.*, 2003), the expression of TSPY in the brain has not been characterized in detail. The availability of the hTSPY-Cre transgenic mouse offers an opportunity to evaluate the behavior of the human TSPY promoter in directing expression of the EGFP reporter gene in the brain. The frontal view of the whole brain from hTSPY-Cre;Z/EG transgenic mice showed a general green fluorescence

FIGURE 5. EGFP expression mediated by hTSPY-Cre recombination in adult brain. **A–D:** Frontal (**A,C**) brain and brain stem views (**B,D**) of double-transgenic and single transgenic mice respectively were observed under the regular room light (left panels) and EGFP excitation light (right panels). Only brains of double-transgenic mice showed EGFP expression. Yellow arrowhead, the trigeminal nerve; orange arrows, anterior lobes of pituitary gland in **B,D**. **E:** A section of the cerebral cortex; no cell was double-stained by anti-GFP (green) and anti-GFAP (red), indicating that these two proteins did not express in the same cells. **F–H:** Sections of the dorsal cortex of the inferior colliculus (DCIC), the molecular layer (MOL), and the granule layers (GRN) of the cerebellum, showing EGFP (**F**) and NeuN (**G**) expression. **H:** Merged image of **F** and **G**, showing a colocalization (orange color) of both EGFP and NeuN in the same cells. White arrows point to Purkinje cells that are negative for NeuN antibody. **I–N:** Sections of the hippocampus showing EGFP (**I**) and NeuN (**J**) expression, respectively. The boxed areas in **I** and **J** are magnified in **K** and **L**, respectively. **M,N:** DNA (blue) staining and merged images of the boxed areas, respectively. Samples presented in **F–N** were derived from a female hTSPY-Cre;Z/EG double transgenic mouse. **O–R:** hTSPY-Cre33B;Z/EG also showed EGFP expression in neuron-specific manner. EGFP expression (**O,Q**) and merged image with NeuN expression (**P,R**) in cerebellum (**O,P**) and pyramid cell layer of hippocampus (**Q,R**), respectively. Arrows indicate Purkinje cell (**F,H,O,P**). Only NeuN-positive neurons, except Purkinje's cells (arrows in **G,P**), expressed the EGFP reporter and were observed as yellow/orange in the merged images (**H,N,P,R**). All figures, except **O–R**, were obtained from hTSPY-Cre33A;Z/EG double transgenic mice, while **O–R** were derived from hTSPY-Cre33B;Z/EG mice. CA1-CA3, fields of the hippocampus; DG, dentate gyrus; cortex, cerebral cortex; Or, oriens layer of hippocampus; Py, pyramidal cell layer of hippocampus; Rad, stratum radiatum of hippocampus. Scale bar = 50 μm in **E,Q,R**; 100 μm in **F–H** and **O,P;** 126 μm in **K–N**.

(Fig. 5A). At the brain stem, green fluorescence was observed in the optic cord and trigeminal nerve (Fig. 5B, yellow arrowhead), but not in anterior pituitary gland (Fig. 5B, orange arrowhead). Single transgenic mice harboring only the Z/EG transgene did not show any green fluorescence at the same brain structures (Fig. 5C,D).

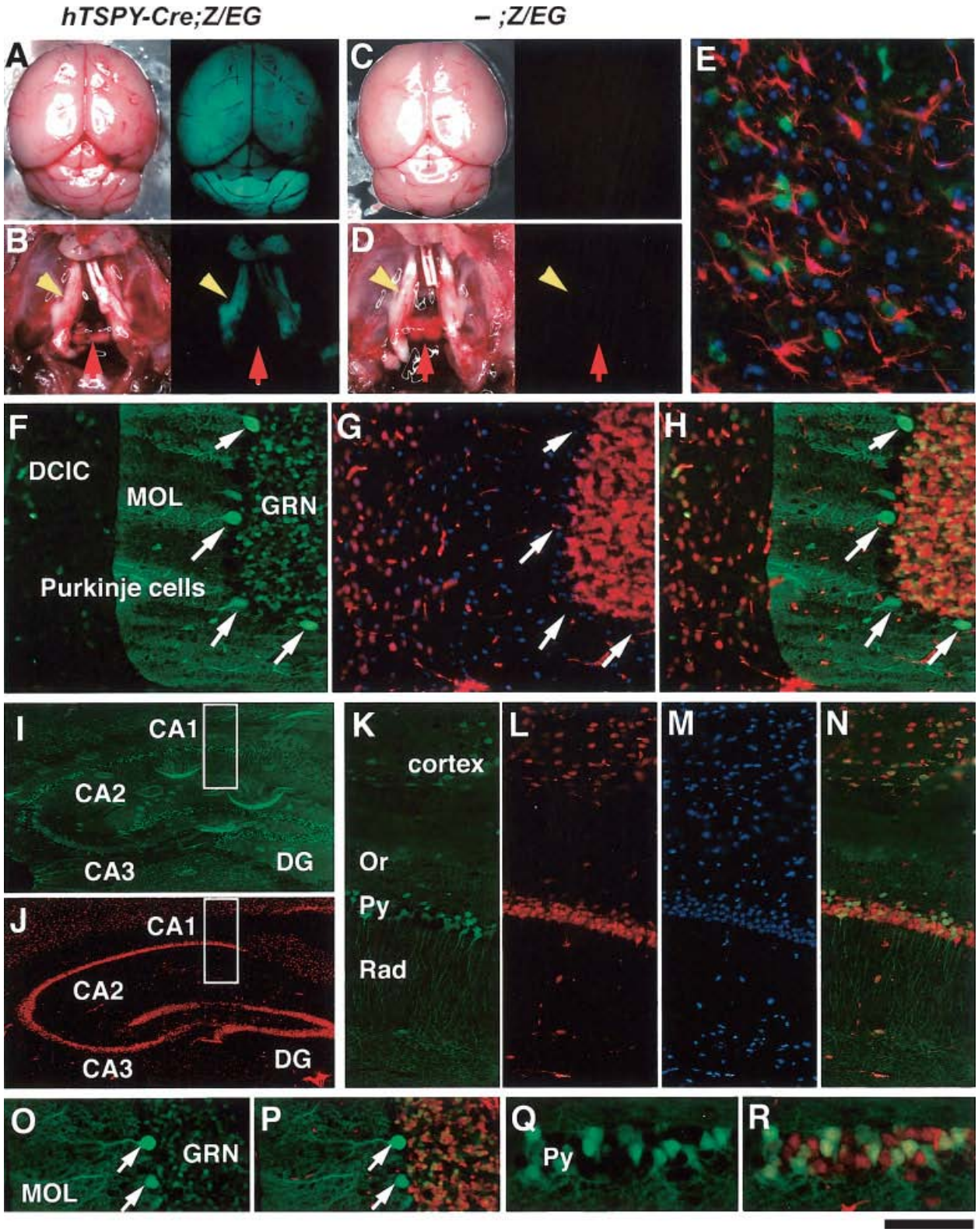

FIG. 5

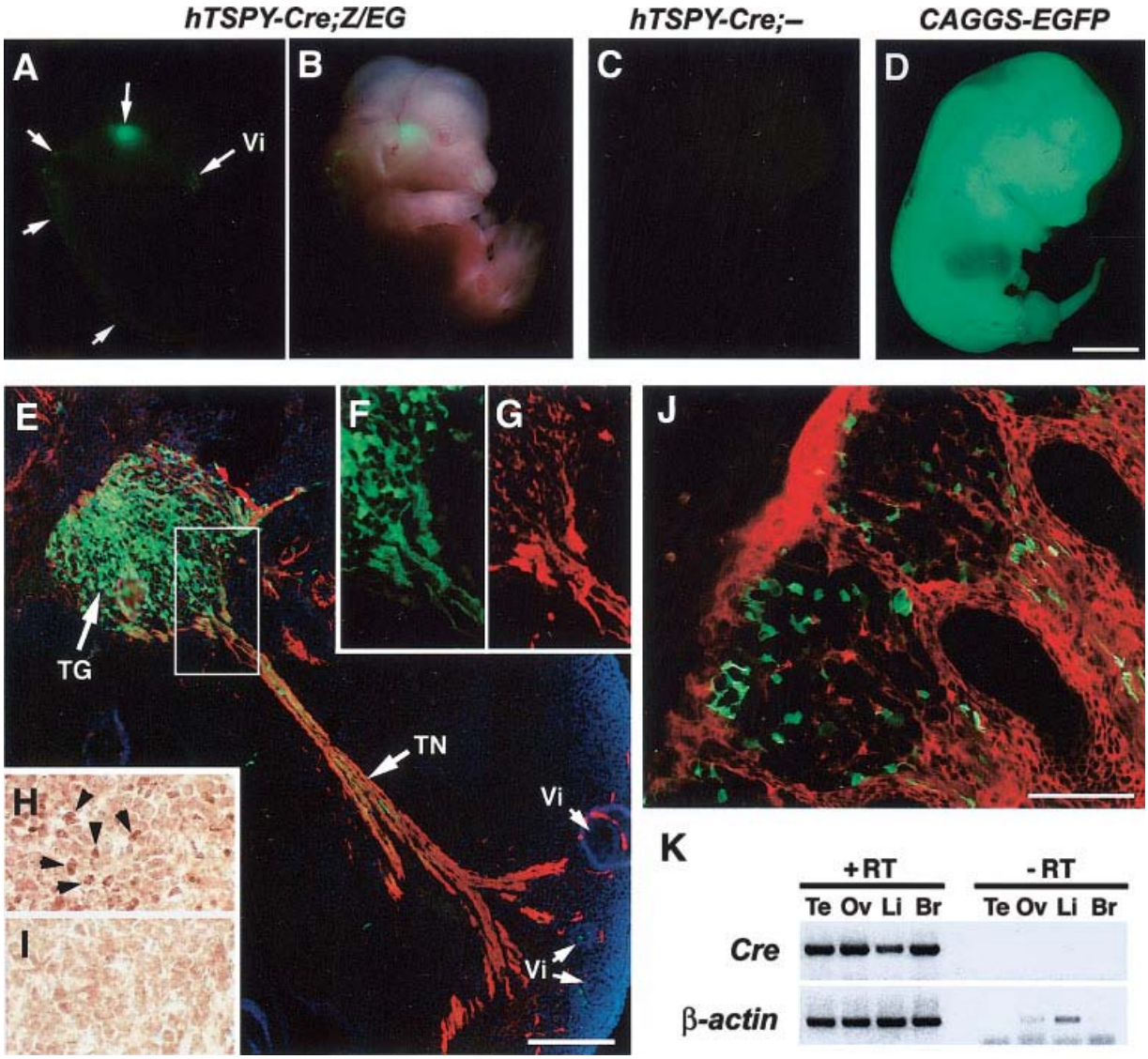

FIG. 6. EGFP and Cre transgene expression in E12.5 hTSPY-Cre;Z/EG embryos. **A–D:** Embryos observed under EGFP excitation light. **A,B:** A hTSPY-Cre;Z/EG embryo. **B:** Merged image of that in **A** and one under room light. Green fluorescence was observed only around the nerve systems (arrows). Vi indicates follicles of vibrissa. **C:** A single hTSPY-Cre transgenic embryo showing no green fluorescence. **D:** An F2 embryo harboring a fully recombined CAGGS-EGFP expressed EGFP ubiquitously. **E–G:** Immunofluorescence of section at the head area (similar to that in **A**) of a female hTSPY-Cre;Z/EG embryo. **E:** Merged image of EGFP (green), neurofilament-M (red), and DNA (blue). **F,G:** Individual images of EGFP (**F**) and neurofilament-M (**G**) of boxed area in **E**. **H,I:** Cre expression in trigeminal ganglion detected by anti-Cre antibody staining. Cre expressing cells were detected only in hTSPY-Cre;Z/EG embryo (**H**, arrowheads), but not in –;Z/EG embryo (**I**). **J:** Section of DRG from a male hTSPY-Cre;Z/EG embryo immunostained by anti-EGFP (green) and anti-β-galactosidase (red). Cells that had undergone a Cre-mediated recombination showed EGFP expression, i.e., in the sensory neurons, and those that did not go through such a recombination showed β-galactosidase expression. **K:** hTSPY promoter activities in hTSPY-Cre tissues of E12.5 embryos detected by RT-PCR method. Cre expression was found in gonads, liver, and brain. Abbreviations are the same as in Figure 2. Scale bars = 2 mm in **A–D;** 200 μm in **E;** 100 μm in **J**.

To characterize the hTSPY promoter activity in the brain, we analyzed the EGFP expression in conjunction with immunofluorescence staining against the neuronal-specific nuclear protein (NeuN) and astrocyte-specific glial fibrillary acidic protein (GFAP) (Debus *et al.*, 1983; Mullen *et al.*, 1992). The cerebellum and the dorsal cortex of the inferior colliculus (DCIC) contained only NeuN-positive cells, while Purkinje cells were positive for only EGFP (Fig. 5F–H). The ratio of EGFP-positive cells to all NeuN-positive cells was slightly different among the hTSPY-Cre;Z/EG mice; however, there was no significant difference between male and female animals (data not shown). Similar results were observed in the cerebral cortex and the hippocampus (Fig. 5I–N) of the double-transgenic mice, while EGFP did not show any colocalization with GFAP-positive cells (Fig. 5E). As shown in hTSPY-

Cre33A;Z/EG mice, the hTSPY-Cre33B;Z/EG mice also showed EGFP expression in a neuron-specific manner (e.g., Fig. 5O–R). These results suggest that the hTSPY promoter is specific for neurons, but not astrocytes, in the brain.

Sexual dimorphism has been postulated to play a role in brain development during embryogenesis (MacLusky and Naftolin, 1981; Arnold and Burgoyne, 2004; De Vries, 2004). The availability of the hTSPY-Cre and Z/EG mice provided an opportunity to determine the promoter activities of a human Y chromosome gene during mouse embryogenesis. Embryos at or immediately after sex determination, i.e., at stages E12.5–13.5, were used in the present studies. At this time gonadal sex has already been decided by the action of the Sry gene while the sexual hormonal environments are still not fully developed (MacLusky and Naftolin, 1981; Arnold and Burgoyne, 2004; De Vries, 2004). RT-PCR analysis of total RNAs derived from testis, male liver and brain, and ovary of E12.5 hTSPY-Cre embryos showed detectable Cre transcripts (Fig. 6K). At E12.5, green fluorescence was visible directly at the head and vertebral column of both male and female double-transgenic hTSPY-Cre;Z/EG embryos (Fig. 6A,B, white arrows) while it was absent in single transgenic hTSPY-Cre embryos (Fig. 6C). Immunofluorescence staining of tissue sections from these embryos showed that EGFP was expressed principally in the trigeminal ganglion (TG) and partially in the trigeminal nerve (TN) of the primitive brain (Fig. 6E), which were also positive for neurofilament M (Fig. 6E–G). Immunostaining of similar sections showed that they were also positive for the Cre protein (Fig. 6H). These results suggest that the human TSPY promoter is most active in embryonic neurons at these developmental stages of embryogenesis.

Although Cre recombinase transcripts were detected in various embryonic tissues at this developmental stage, EGFP, indicative of an efficient recombination, was not easily observed among these tissues, including both the testis and ovary. To evaluate the recombination status of the Z/EG transgene in the double-transgenic embryos, we analyzed the expression of both EGFP and βgeo genes in these tissues, detected by antibodies against EGFP and β-galactosidase, respectively. Our results demonstrate that neurons in the dorsal root ganglion (DRG) underwent successful recombination and showed high EGFP expression (Fig. 6A, white arrows, and 6J), while the EGFP reporter transgene in most surrounding nonneuronal cells did not undergo any recombination and remained β-galactosidase-positive. Morphologically, many of these EGFP-positive cells seemed to be sensory neurons of the peripheral nervous system. The fetal gonads, however, showed little or no EGFP immunofluorescence and most cells were still positive for β-galactosidase (data not shown). These results suggest that insufficient Cre recombinase was available for an efficient recombination in the fetal gonads, and perhaps other tissues (e.g., liver), despite the presence of the Cre transcripts (Fig. 6K).

DISCUSSION

The GBY locus has been hypothesized to harbor a gene(s) that serves a vital function in the testis; however, when present in a female gonad it exerts an oncogenic function leading to gonadoblastoma development (Page, 1987; Lau, 1999; Tsuchiya *et al.*, 1995). For the past several years the human TSPY gene has been considered a strong candidate for the GBY locus, based on its mapping to the GBY critical region on the human Y chromosome and expression in tumor germ cells of gonadoblastoma samples and in male-specific cancers, testicular seminoma, and prostate cancer (Lau, 1999; Lau *et al.*, 2000, 2003). Although TSPY encodes a protein(s) harboring an NAP/SET domain capable of binding to type B cyclins (Kellogg *et al.*, 1995), the exact mechanism of its postulated oncogenic or tumor-promoting properties has not been resolved. Significantly, it is uncertain whether its expression in gonadoblastoma tissue represents a causative or consequential event. If it plays an oncogenic or tumor-promoting role, we surmise that it should be expressed in female germ cells, prior to or at the early stages of gonadoblastoma development. The present study demonstrates that the 2.4-kb human TSPY promoter, when integrated into the autosomes of transgenic mice, is capable of directing the expression of a modular Cre gene in the female germ cell lineage. Its expression increases significantly in the late primary and secondary oocytes of the ovaries, thereby efficiently activating the EGFP reporter in the Cre-LoxP system used in this study. Hence, it is possible that TSPY could be similarly active in the germ cell lineage of XY sex-reversed females before or at the early stages of the oncogenic process, thereby supporting the hypothesis that TSPY plays a causative or predisposing role in gonadoblastoma development in these patients.

TSPY expression has been observed in the gonocytes and prespermatogonia in human fetal and postnatal testes (Honecker *et al.*, 2004) and spermatogonia and spermatocytes in adult testis (Schnieders *et al.*, 1996). Similar expression in adult testis has been reported in transgenic mice harboring an 8.2-kb genomic fragment encompassing the entire human TSPY gene on the mouse Y chromosome (Schubert *et al.*, 2003). However, our results clearly demonstrate that the human TSPY promoter is active in both early and late stages of spermatogenesis in the mouse. Reexamination of TSPY expression pattern in adult human testis using a panel of domain-specific monoclonal antibodies suggests a bimodal expression pattern of TSPY isoforms initially in early spermatogonia and spermatocytes and then in late spermatids (Fig. 4). We surmise that the discrepancy in detecting TSPY protein in various stages of spermatogenesis between the laboratories could be attributed to the differences in the specificities of the antibodies used in the respective studies. Unfortunately, the single-copy Tspy gene on the mouse Y chromosome harbors several in-frame stop codons in its coding sequence and does not encode any functional protein and, therefore, could

not be used in expression studies of the endogenous Tspy protein in the present study (Mazeyrat and Mitchell, 1998). The rat, however, possesses a functional Tspy gene on its Y chromosome. Using a rat Tspy-specific polyclonal antibody, we were able to detect the rat Tspy protein in the spermatids of adult rat testis (Kido and Lau, unpubl. data). This latter observation suggests that the Tspy gene might be active in the spermatids of the rodents. If the regulatory mechanism in the rat is preserved in the mouse, our results suggest that the 2.4-kb human promoter is properly regulated in the spermatids of transgenic mice.

Studies on TSPY expression, initially postulated to be testis-specific, in the brain are somewhat limited, despite the fact that transcripts of the human TSPY transgene could be detected by the Northern hybridization technique (Schubert *et al.*, 2003) and TSPY ESTs have also been reported in databases of brain cDNA libraries (GenBank access. nos. BI828033 and BX281192). The expression of the human TSPY promoter directed Cre recombinase gene, and that of the EGFP reporter gene, in the neurons of both central and peripheral nervous systems of transgenic mice is a significant finding. Using the Cre-LoxP gene activation system, we are able to demonstrate the specific cell types in the central and peripheral nervous systems where the TSPY promoter is active. In particular, the neuron-specific expression of the EGFP reporter in the trigeminal ganglia, trigeminal nerve, and dorsal root ganglia of E12–13 mouse embryos suggests that the human TSPY gene promoter is active at the time or immediately after sex determination in these embryos.

Currently, it is uncertain which cis-elements are involved in germ cell and neuron-specific expression of the human TSPY promoter. The human TSPY gene contains various CpG islands within its promoter and first exon sequences. In fact, these CpG islands were used as functional landmarks in identifying the TSPY functional gene from a human Y chromosome cosmid library (Zhang *et al.*, 1992). Several germ cell-specific genes have been demonstrated to harbor CpG islands that are regulated through various methylation, demethylation process(es), and recruitment of transcription factors (De Smet *et al.*, 1999; Iannello *et al.*, 2000; Hisano *et al.*, 2003). The human TSPY promoter harbors a 5′-GGGTGGG-3′ motif at 108 bp upstream of its transcription start site. This element has also been detected on the promoters of some testis-specific genes, including proacrosin, protamine 1 and 2, and Hsp70-3, and hence could potentially play a key role in determining the germ cell-specific expression of the TSPY gene (Friedrich *et al.*, 1998; Steger, 1999). Currently, we are uncertain if any enhancer element for spermatogonial cells is present in the 2.4-kb TSPY promoter. Since animals from the transgenic line harboring the 8.5-kb (including a 2.9-kb promoter) TSPY transgene (Schubert *et al.*, 2003) express their transgene in spermatogonial cells, as detected by immunostaining with a TSPY antibody generated by these investigators, one might argue that any spermatogonial enhancer elements could likely be present within the 500-nucleotide sequence between −2.9 kb to −2.4 kb of the human TSPY promoter.

Alternatively, the difference in expression between the two studies could reflect the effects of meiotic sex chromosome inactivation (MSCI). During early meiotic prophase, the X and Y chromosomes are subjected to chromosome-wide silencing and for many genes it persists until the end of spermatogenesis. By contrast, the autosomes escape this silencing mechanism (Tuner *et al.*, 2005). Thus, the TSPY transgene that integrated on the Y chromosome of the host (Schubert *et al.*, 2003) will be subjected to MSCI and therefore be silent in late spermatogenesis, while those integrated on the autosomes (such as the hTSPY-Cre transgenes in the present study) will escape MSCI and will therefore be expressed at late spermatogenic stages.

The neuron-expression of the TSPY promoter is somewhat unclear. The Olf-1 transcription factor has been postulated to regulate the olfactory receptor gene expression in adult and during neuronal development, by binding to the Olf-1 binding motif, 5′-TCCYYRRGGAG-3′, present in its target genes (Wang and Reed, 1993). The human TSPY promoter harbors such a motif at 533 bp upstream of its transcription initiation site. This element could be responsible for the hTSPY-Cre activation of the EGFP reporter in the trigeminal ganglia, trigeminal nerve, and sensory neurons of E12.5 embryos and in the brains of adult mice. Although TSPY has been hypothesized to be critical in germ cell development and male meiosis, its roles in neural development and brain function is clearly understood. However, a recent study of the sudden infant death with dysgenesis of the testis syndrome (SIDDT) detected a mutation of the TSPY-like 1 gene (TSPYL1), an autosomal analog of the TSPY gene (Puffenberger *et al.*, 2004). The mutated TSPYL1 gene encodes a protein with a deleted TSPY/NAP/SET domain, conserved among members of this gene family. This finding and those of the present study suggest that TSPYL1 and TSPY may play a role(s) in neuronal development and/or functioning of the nervous system, in addition to its function as a germ cell factor in the testis. The hTSPY-Cre lines should be useful for studies requiring germ cell and neuron-specific gene activation or gene deletion with the Cre-LoxP system in transgenic mice.

MATERIALS AND METHODS

Animals

The Z/EG reporter mouse (Novak *et al.*, 2000) was obtained from the Jackson Laboratory (Bar Harbor, ME; stock number 003920). FVB mice (Charles River Laboratories, Wilmington, MA) were used in maintaining the animals. Mice older than 6 weeks were analyzed as adults. All transgenic mice used in this study were heterozygous for the respective transgene. The Institutional Animal Care and Use Committee of the VA Medical Center approved all experimental procedures in accordance with the NIH *Guide for Care and Use of Laboratory Animals*.

Construction of the phTSPY-Cre Plasmid and Generation of Transgenic Mice

The 2.4k-bp promoter region (−2383 to +43 from the transcription start site) of human TSPY gene was excised by SphI from the plasmid, pTSPY12.5 (Zhang *et al.*, 1992), and subcloned as a blunt-end fragment into the XhoI site of pGL2-basic plasmid (Promega, Madison, WI), resulting in the plasmid pGL2-hTSPY2.4. The CMV promoter in the expression plasmid pCS2plus (Rupp *et al.*, 1994; Turner and Weintraub, 1994) was replaced by the hTSPY2.4 promoter, resulting in an expression vector, phTSPY2.4, consisting of a hTSPY2.4 promoter, multiple cloning site, and polyadenylation site from SV40. The Cre gene was excised from pCAGGS-NLS-Cre-PGKPuro/cg (a gift of C. Lobe, Sunnybrook and Women's College Health Science Center, Toronto) by PstI and BglII, and inserted into the HindIII site of phTSPY2.4. The resultant phTSPY-Cre plasmid was linearized by ScaI and gel-purified by binding to glass beads (BIO 101, La Jolla, CA). The fragment was microinjected into the pronuclei of one-cell embryos of B6CBAF1 and processed for transgenic mouse construction using standard procedures by the Stanford Transgenic Mouse Core Laboratory. All offspring were analyzed by PCR on genomic DNA from tail biopsies with Cre primers (Cre-2F: 5′-TGC ATT ACC GGT CGA TGC AA-3′, Cre-3R: 5′-AGC TAC ACC AGA GAC GGA AA-3′) and EGFP primers (EGFP-F: 5′-GCA AGC TGA CCC TGA AGT TCA TC-3′, EGFP-B: 5′-AAC TCC AGC AGG ACC ATG TGA TCG-3′). A semiquantitative PCR procedure was used to estimate the transgene copy numbers with 0.1 μg of genomic DNA from tail biopsies at 27 and 30 cycles, using phTSPY-Cre plasmid as a reference.

Semiquantitative RT-PCR

Total RNA was isolated from various tissues by the TORIZOL reagents (Invitrogen, Carlsbad, CA) or RNA easy mini kit (Qiagen, Valencia, CA) according to protocols supplied by the respective vendors for adult stages and newborn stages, respectively. After treatment by RQ1-DNase (Promega) to remove any contaminated DNA, 0.36 μg of total RNA (final 21 μl reaction) was reverse-transcribed with the SuperScript reverse transcriptase kit 2 (Invitrogen). One μl of reverse-transcribed product was subjected to PCR using the touchdown procedure: 1 × 95°C, 5 min; 2 × (95°C, 1 min; 68°C, 1 min; 72°C, 1 min), 2 × (95°C, 1 min; 66°C, 1 min; 72°C, 1 min), 2 × (95°C, 1 min; 64°C, 1 min; 72°C, 1 min), 2 × (95°C, 1 min; 62°C, 1 min; 72°C, 1 min), 32–40 × (95°C, 1 min; 60°C, 1 min; 72°C, 1 min), and 72°C, 7 min. The PCR products were analyzed by electrophoresis in a 1.2% agarose gel and visualized by ethidium bromide staining. The following primers were used for semiquantitative RT-PCR: mouse Tspy (5′-CCT GAC TCC ACC TGG ACT GCT TAT AT-3′, 5′-TCA TCT TGG TTG CTG ATG ATG GAC GA-3′); β-actin (5′-TCA CCC ACA CTG TGC CCA TCT ACG A-3′, 5′-CCA CGT CAC ACT TCA TGA TGG A-3′), and Cre primers, as described above.

Histology and Immunohistochemistry

Whole embryos or dissected tissue were initially observed under the Leica MZ-FLIII fluorescence stereomicroscope and recorded with a DC300F digital imaging system. They were then fixed overnight in 10% formaldehyde-PBS (phosphate-buffered saline), pH 7.2 (Fisher Scientific, Hampton, NH) at 4°C. The tissues were incubated progressively through 10–30% sucrose in 2% DMSO / 100 mM PB (pH 7.2) for 12 h at each step at 4°C. They were then incubated in Tissue Freezing Medium (Triangle Biomedical Sciences, Durham, NC) at 4°C for 1 h prior to being embedded in the Tissue Freezing Medium over liquid nitrogen. Ten-μm cryosections were cut with a cryostat, air-dried for 30 min, and then washed 3 times in PBS for 5 min each. The sections were blocked with 3% bovine serum albumin (BSA) in PBS and then reacted with the primary antibodies at appropriate dilutions. After overnight incubation at 4°C, the slides were washed in PBS and then incubated with the appropriate secondary antibody for 3 h at 37°C. DNA was stained by the DAPI dyne in the mounting buffer (Vector Laboratories, Burlingame, CA). Fluorescent staining was examined with a Zeiss Axiophoto fluorescence microscope and recorded by a LEI-750 digital imaging system. Alexa488 conjugated rabbit anti-GFP antibody (1:400) and Alexa568 conjugated donkey antimouse IgG antibody (1:600) were obtained from Molecular Probes (Eugene, OR). Mouse anti-neurofilament M antibody (1:500), mouse anti-glial fibrillary acidic protein (GFAP) antibody (1:500), and mouse anti-neuronal nuclei (NeuN) antibody (1:150) were obtained from Chemicon International (Temecula, CA). Mouse anti-β-galactosidase antibody (1:100) was obtained from AbCam (Cambridge, UK).

For the immunohistological analysis of Cre expression, cryosections were air-dried and treated with a 3% H_2O_2 solution for 10 min. The sections were blocked with 10% normal goat serum in PBS and incubated with a rabbit anti-Cre antibody (1:1,000, Novagen, San Diego, CA) overnight at 4°C. The primary antibody was visualized by reacting with biotinylated antirabbit IgG antibody (1:600, Upstate Biochemicals, Lake Placid, NY) and horseradish peroxidase conjugated avidin (Vector Laboratories), using diaminobenzine as substrate. Nuclei were visualized by counterstaining with hematoxylin. The immunostained sections were examined and recorded with a Zeiss Axiophot microscope as before.

Analysis of TSPY Expression in Normal Human Testis

Antihuman TSPY mouse monoclonal antibodies were produced with the hybridoma technology against the full-length recombinant human TSPY by a commercial vendor (Vancouver Biotechnology, Vancouver, BC). The locations of epitopes were assigned by Western blotting of protein extracts from COS7 cells transfected with expression vectors consisting of pCS2plus (Rupp *et al.*, 1994; Turner and Weintraub, 1994) and cDNA fragments coding for 1–150 aa, 151–308 aa, or 1–308 aa of the

human TSPY (Zhang *et al.*, 1992). Western blotting was performed as described previously (Oh *et al.*, 2005).

Human testis sections were purchased from Ambion (LandMark Normal Tissue MicroArray, Austin, TX). The donors' age ranged from 63–78 years old. Sections were dewaxed and rehydrated through descending grades of alcohol to distilled water. The sections were treated with an antigen retrieval procedure in 100 mM Tris-HCl (pH 10) at 95°C for 30 min, incubated in 3% hydrogen peroxide, and washed in PBS. Nonspecific protein binding was blocked by pretreatment with 3% BSA in PBS. Sections were then incubated overnight in a humid chamber at 4°C with the respective TSPY monoclonal antibody (1:500 for clone #2, 1:3,000 for clone #7). The primary antibody was visualized as described above. The human study was performed under an exempt protocol approved by the Institutional Committee on Human Research, VA Medical Center, San Francisco.

ACKNOWLEDGMENTS

We thank Dr. Corrine Lobe of the Sunnybrook and Women's College Health Science Center, Toronto, for providing the plasmid pCAGGS-NLS-Cre-PGKPuro/cg, Dr. Yunmin Li for technical assistance, and Drs. Shane Oram and Lynn Pulliam for critical reading of the manuscript. Y-F. C. Lau is a Research Career Scientist of the Department of Veterans Affairs.

LITERATURE CITED

Arnemann J, Epplen JT, Cooke HJ, Sauermann U, Engel W, Schmidtke J. 1987. A human Y-chromosomal DNA sequence expressed in testicular tissue. Nucleic Acids Res 15:8713–8724.

Arnold AP, Burgoyne PS. 2004. Are XX and XY brain cells intrinsically different? Trends Endocrinol Metab 15:6–11.

Canela N, Rodriguez-Vilarrupla A, Estanyol JM, Diaz C, Pujol MJ, Agell N, Bachs O. 2003. The SET protein regulates G2/M transition by modulating cyclin B-cyclin-dependent kinase 1 activity. J Biol Chem 278:1158–1164.

Chai Z, Sarcevic B, Mawson A, Toh BH. 2001. SET-related cell division autoantigen-1 (CDA1) arrests cell growth. J Biol Chem 276:33665–33674.

De Smet C, Lurquin C, Lethe B, Martelange V, Boon T. 1999. DNA methylation is the primary silencing mechanism for a set of germ line- and tumor-specific genes with a CpG-rich promoter. Mol Cell Biol 19:7327–7335.

De Vries GJ. 2004. Minireview: Sex differences in adult and developing brains: compensation, compensation, compensation. Endocrinology 145:1063–1068.

Debus E, Weber K, Osborn M. 1983. Monoclonal antibodies specific for glial fibrillary acidic (GFA) protein and for each of the neurofilament triplet polypeptides. Differentiation 25:193–203.

Friedrich H, Walter L, Gunther E. 1998. Analysis of the 5′-flanking regions of the MHC-linked Hsp70-2 and Hsp70-3 genes of the rat. Biochim Biophys Acta 1395:57–61.

Hisano M, Ohta H, Nishimune Y, Nozaki M. 2003. Methylation of CpG dinucleotides in the open reading frame of a testicular germ cell-specific intronless gene, Tact1/Actl7b, represses its expression in somatic cells. Nucleic Acids Res 31:4797–4804.

Honecker F, Stoop H, De Krijger RR, Chris Lau YF, Bokemeyer C, Looijenga LH. 2004. Pathobiological implications of the expression of markers of testicular carcinoma in situ by fetal germ cells. J Pathol 203:849–857.

Iannello RC, Gould JA, Young JC, Giudice A, Medcalf R, Kola I. 2000. Methylation-dependent silencing of the testis-specific Pdha-2 basal promoter occurs through selective targeting of an activating transcription factor/cAMP-responsive element-binding site. J Biol Chem 275:19603–19608.

Ishimi Y, Kikuchi A. 1991. Identification and molecular cloning of yeast homolog of nucleosome assembly protein I which facilitates nucleosome assembly in vitro. J Biol Chem 266:7025–7029.

Jorgensen N, Muller J, Jaubert F, Clausen OP, Skakkebaek NE. 1997. Heterogeneity of gonadoblastoma germ cells: similarities with immature germ cells, spermatogonia and testicular carcinoma in situ cells. Histopathology 30:177–186.

Kellogg DR, Kikuchi A, Fujii-Nakata T, Turck CW, Murray AW. 1995. Members of the NAP/SET family of proteins interact specifically with B-type cyclins. J Cell Biol 130:661–673.

Lau YF. 1999. Gonadoblastoma, testicular and prostate cancers, and the TSPY gene. Am J Hum Genet 64:921–927.

Lau YF, Zhang J. 2000. Expression analysis of thirty one Y chromosome genes in human prostate cancer. Mol Carcinog 27:308–321.

Lau Y, Chou P, Iezzoni J, Alonzo J, Komuves L. 2000. Expression of a candidate gene for the gonadoblastoma locus in gonadoblastoma and testicular seminoma. Cytogenet Cell Genet 91:160–164.

Lau YF, Lau HW, Komuves LG. 2003. Expression pattern of a gonadoblastoma candidate gene suggests a role of the Y chromosome in prostate cancer. Cytogenet Genome Res 101:250–260.

MacLusky NJ, Naftolin F. 1981. Sexual differentiation of the central nervous system. Science 211:1294–1302.

Mazeyrat S, Mitchell MJ. 1998. Rodent Y chromosome TSPY gene is functional in rat and non-functional in mouse. Hum Mol Genet 7:557–562.

Mullen RJ, Buck CR, Smith AM. 1992. NeuN, a neuronal specific nuclear protein in vertebrates. Development 116:201–211.

Niwa H, Yamamura K, Miyazaki J. 1991. Efficient selection for high-expression transfectants with a novel eukaryotic vector. Gene 108:193–199.

Novak A, Guo C, Yang W, Nagy A, Lobe CG. 2000. Z/EG, a double reporter mouse line that expresses enhanced green fluorescent protein upon Cre-mediated excision. genesis 28:147–155.

Oh HJ, Li Y, Lau YF. 2005. Sry associates with the heterochromatin protein 1 complex by interacting with a KRAB domain protein. Biol Reprod 72:407–415.

Ozbun LL, You L, Kiang S, Angdisen J, Martinez A, Jakowlew SB. 2001. Identification of differentially expressed nucleolar TGF-beta1 target (DENTT) in human lung cancer cells that is a new member of the TSPY/SET/NAP-1 superfamily. Genomics 73:179–193.

Page DC. 1987. Hypothesis: a Y-chromosomal gene causes gonadoblastoma in dysgenetic gonads. Development 101(Suppl):151–155.

Puffenberger EG, Hu-Lince D, Parod JM, Craig DW, Dobrin SE, Conway AR, Donarum EA, Strauss KA, Dunckley T, Cardenas JF, Melmed KR, Wright CA, Liang W, Stafford P, Flynn CR, Morton DH, Stephan DA. 2004. Mapping of sudden infant death with dysgenesis of the testes syndrome (SIDDT) by a SNP genome scan and identification of TSPYL loss of function. Proc Natl Acad Sci U S A 101:11689–11694.

Rajpert-De-Meyts E, Bartkova J, Samson M, Hoei-Hansen CE, Frydelund-Larsen L, Bartek J, Skakkebaek NE. 2003. The emerging phenotype of the testicular carcinoma in situ germ cell. APMIS 111:267–278; discussion 278–279.

Rupp RA, Snider L, Weintraub H. 1994. Xenopus embryos regulate the nuclear localization of XMyoD. Genes Dev 8:1311–1323.

Salo P, Kaariainen H, Petrovic V, Peltomaki P, Page DC, de la Chapelle A. 1995. Molecular mapping of the putative gonadoblastoma locus on the Y chromosome. Genes Chromsomes Cancer 14:210–214.

Schnieders F, Dork T, Arnemann J, Vogel T, Werner M, Schmidtke J. 1996. Testis-specific protein, Y-encoded (TSPY) expression in testicular tissues. Hum Mol Genet 5:1801–1807.

Schubert S, Skawran B, Dechend F, Nayernia K, Meinhardt A, Nanda I, Schmid M, Engel W, Schmidtke J. 2003. Generation and characterization of a transgenic mouse with a functional human TSPY. Biol Reprod 69:968–975.

Seo SB, McNamara P, Heo S, Turner A, Lane WS, Chakravarti D. 2001. Regulation of histone acetylation and transcription by INHAT, a human cellular complex containing the set oncoprotein. Cell 104:119–130.

Skaletsky H, Kuroda-Kawaguchi T, Minx PJ, Cordum HS, Hillier L, Brown LG, Repping S, Pyntikova T, Ali J, Bieri T, Chinwalla A, Delehaunty A, Delehaunty K, Du H, Fewell G, Fulton L, Fulton R, Graves T, Hou SF, Latrielle P, Leonard S, Mardis E, Maupin R, McPherson J, Miner T, Nash W, Nguyen C, Ozersky P, Pepin K, Rock S, Rohlfing T, Scott K, Schultz B, Strong C, Tin-Wollam A, Yang SP, Waterston RH, Wilson RK, Rozen S, Page DC. 2003. The male-specific region of the human Y chromosome is a mosaic of discrete sequence classes. Nature 423:825–837.

Steger K. 1999. Transcriptional and translational regulation of gene expression in haploid spermatids. Anat Embryol (Berl) 199:471–487.

Tascou S, Nayernia K, Samani A, Schmidtke J, Vogel T, Engel W, Burfeind P. 2000. Immortalization of murine male germ cells at a discrete stage of differentiation by a novel directed promoter-based selection strategy. Biol Reprod 63:1555–1561.

Tsuchiya K, Reijo R, Page DC, Disteche CM. 1995. Gonadoblastoma: molecular definition of the susceptibility region on the Y chromosome. Am J Hum Genet 57:1400–1407.

Turner DL, Weintraub H. 1994. Expression of achaete-scute homolog 3 in Xenopus embryos converts ectodermal cells to a neural fate. Genes Dev 8:1434–1447.

Turner JM, Mahadevaiah SK, Fernandez-Capetillo O, Nussenzweig A, Xu X, Deng CX, Burgoyne PS. 2005. Silencing of unsynapsed meiotic chromosomes in the mouse. Nat Genet 37:41–47.

Vogel T, Dittrich O, Mehraein Y, Dechend F, Schnieders F, Schmidtke J. 1998. Murine and human TSPYL genes: novel members of the TSPY-SET-NAP1L1 family. Cytogenet Cell Genet 81:265–270.

von Lindern M, van Baal S, Wiegant J, Raap A, Hagemeijer A, Grosveld G. 1992. Can, a putative oncogene associated with myeloid leukemogenesis, may be activated by fusion of its 3′ half to different genes: characterization of the set gene. Mol Cell Biol 12:3346–3355.

Wang MM, Reed RR. 1993. Molecular cloning of the olfactory neuronal transcription factor Olf-1 by genetic selection in yeast. Nature 364:121–126.

Zhang JS, Yang-Feng TL, Muller U, Mohandas TK, de Jong PJ, Lau YF. 1992. Molecular isolation and characterization of an expressed gene from the human Y chromosome. Hum Mol Genet 1:717–726.

Human Pathology (2005) **36**, 512–521

ELSEVIER

Human PATHOLOGY

www.elsevier.com/locate/humpath

Identification of germ cells at risk for neoplastic transformation in gonadoblastoma☆ An immunohistochemical study for OCT3/4 and TSPY

Anne-Marie F. Kersemaekers PhD[a,1], Friedemann Honecker MD[a,b,1,2], Hans Stoop BSc[a], Martine Cools MD[a], Michel Molier BSc[a,2], Katja Wolffenbuttel MD[c], Carsten Bokemeyer MD[b], Yunmin Li PhD[d], Yun-Fai Chris Lau PhD[d], J. Wolter Oosterhuis MD, PhD[a], Leendert H.J. Looijenga PhD[a,*]

[a]*Department of Pathology, Josephine Nefkens Institute, Daniel den Hoed Cancer Center, Erasmus MC-University Medical Center Rotterdam, PO Box 1738, 3000 DR Rotterdam, The Netherlands*
[b]*Department of Hematology/Oncology, University of Tübingen, 72076 Tübingen, Germany*
[c]*Department of Pediatric Urology, Sophia Children's Hospital, Erasmus MC-University Medical Center Rotterdam, 3015 GJ Rotterdam, The Netherlands*
[d]*Division of Cell and Developmental Genetics, Department of Medicine, VA Medical Center, University of California, San Francisco, CA 94121, USA*

Received 1 February 2005; accepted 15 February 2005

Keywords:
Gonadoblastoma;
Dysgerminoma;
CIS;
OCT3/4;
TSPY;
Progression;
Malignant transformation;
Clonal selection

Summary Carcinoma in situ (CIS) is the precursor of malignant testicular germ cell tumors (GCTs) of adolescents and young adults, being the neoplastic counterpart of primordial germ cells/gonocytes. Carcinoma in situ cells will develop into invasive seminoma/nonseminoma. Gonadoblastoma (GB) is the precursor of invasive GCTs in dysgenetic gonads, predominantly dysgerminoma (DG). In this process, part of the Y chromosome (GBY region) is involved, for which *TSPY* is a candidate gene. A detailed immunohistochemical survey was performed for the known diagnostic markers, germ cell/placental alkaline phosphatase (PLAP), c-KIT, and OCT3/4, as well as testis-specific protein on the Y chromosome (TSPY) on a series of GBs, and adjacent invasive DGs. All 5 patients were XY individuals (4 females and 1 male). In contrast to c-KIT, PLAP was positive in all cases. The immature germ cells of GBs were positive for OCT3/4, whereas the mature germ cells were negative for this

☆ This study was financially supported by the Dutch Cancer Society, grant number 2002 2682 (AMK, HS, JWO, LHJL), and the Deutsche Krebshilfe, Dr Mildred Scheel Stiftung (F.H.), and the European Society for Pediatric Endocrinology, ESPE sponsored by Novo Nordisk A/S (MC).

Abbreviations: GB, Gonadoblastoma; CIS, Carcinoma in situ; CH, Choriocarcinoma; DG, Dysgerminoma; EC, Embryonal carcinoma; (T)GCT, (testicular) germ cell tumor; H&E, Hematoxylin and eosin; OCT3/4, Octamer binding transcription factor involved in regulation of pluripotency, also referred to as POU domain class 5 transcription factor 1 (POU5F1); PLAP, Germ cell/placental alkaline phosphatase; TE, Teratoma; TSPY, Testis-specific protein on the Y chromosome. This gene maps to the gonadoblastoma region on the Y chromosome (GBY); WHO, World Health Organization; YST, Yolk sac tumor.

* Corresponding author.
E-mail address: l.looijenga@erasmusmc.nl (L.H.J. Looijenga).

[1] Both authors contributed equally to the work.

[2] Current address: Department of Oncology and Hematology, University Hospital Hamburg Eppendorf, Martinstr. 52, 20246 Hamburg, Germany.

0046-8177/$ – see front matter
doi:10.1016/j.humpath.2005.02.016

marker, but positive for TSPY. In every GB, a minor population of germ cells positive for both markers could be identified, similar to most CIS cells and early invasive DG. On progression to an invasive tumor, TSPY can be lost, a process that is also detectable in invasive testicular GCTs compared to CIS. These results indicate that GB is a heterogeneous mix of germ cells, in which the OCT3/4-positive cells have the potential to undergo progression to an invasive tumor. These early invasive stages are initially also positive for TSPY (like CIS), supporting a positive selection mechanism. Therefore, OCT3/4 in combination with TSPY is valuable to identify malignant germ cells in dysgenetic gonads. This could allow better prediction of the risk of progression to a GCT. In addition, the data support the model that GB represents the earliest accessible developmental stage of malignant GCTs.

1. Introduction

Human germ cell tumors (GCTs) represent a unique and complex group of neoplasms. Recently, we proposed a classification system on the basis of various parameters, including age at clinical presentation, anatomical site of the tumor, sex of the patient, histology, and chromosomal constitution (see Refs [1,2] for review). This classification has been acknowledged by the World Health Organization [3]. The group of tumors referred to as type II GCTs are the seminomas and the nonseminomas of the testis and mediastinum, known as (non)dysgerminomas of the ovary and dysgenetic gonad, and (non)germinomas of the brain. Various risk factors for these types of GCTs have been identified, in particular, related to those of the gonads, including cryptorchidism and gonadal dysgenesis [4-6]. The precursor of testicular seminomas and nonseminomas is well established and known as carcinoma in situ (CIS) [7], also referred to as intratubular germ cell neoplasia unclassified. The precursor lesion of the tumors of the dysgenetic gonad is called gonadoblastoma (GB) [4]. Like CIS, it shows the potential to progress to an invasive GCT, mainly dysgerminoma (DG), and less frequently to other tumor components, as embryonal carcinoma (EC), teratoma (TE), yolk sac tumor (YST), and choriocarcinoma (CH). Being a rare condition, GB has not been studied extensively, even though it might increase our understanding of the different pathogenetic steps involved in the development of malig-

Table 1 Clinical data and summary of immunohistochemical results of PLAP, c-KIT, OCT3/4, and TSPY staining experiments of germ cells in GB, DG, and TGCTs of adolescents and adults

Organ	Sex	Case	Age (y)	Histology	PLAP	c-KIT	OCT3/4	TSPY
Dysgenetic gonad	F	1	18	GB	+−	−	++	+
				Early invasive DG	+	−	++	+
	F	2[a]	20	GB	+−	+	++	+
				Early invasive DG	+	+	++	+
	F	3	14	GB	+−	+	++	+
				Early invasive DG	+	+	++	+
	M	4	21	GB	+−	−	++	+
				Early invasive DG	+	−	++	+
				Progressed DG	+−/−	−	++	+/−
	F	5	16	GB	+−	−	++	+
Testis	M	n = 31	>16	CIS	++	+/−	++	++(−)
		n = 21	>16	Seminoma	++	+/−	++	+−
			>16	Nonseminoma:				
		n = 18		EC	−+	−+	+	−
		n = 9		TE	−	−	−	−
		n = 7		YST	−	−	−	−
		n = 4		CH	−	−	−	−

The organ, phenotype of the patient (all patients with a dysgenetic gonad had a 46,XY karyotype), age of the patient at time of tissue sampling (years), histology of the tumor, and staining results of immunohistochemistry at different stages of progression (GB, early invasive DG, progressed DG), EC, TE, YST, and CH are indicated. Immunohistochemistry for c-KIT was not always positive in GB; all cases consistently showed expression of TSPY, OCT3/4, and PLAP. Expression of the latter 2 was mainly found in immature germ cells (indicated by +/−). Staining results were the same on both sides (data not shown). − indicates negative; +/−, heterogeneity of staining; +, moderate; ++, strong intensity of a homogenous staining.

[a] Case 2 presented with bilateral gonadoblastoma.

nant GCTs. Both the comparatively young age at presentation [4] and the genomic constitution [8] suggest that GB could be the earliest accessible stage in the development of a malignant GCT.

There are strong indications that both GB and CIS are the result of a disturbance in germ cell maturation. This model is supported by epidemiological and morphological observations, as well as the presence of a number of immunohistochemical markers like germ cell/placental alkaline phosphatase (PLAP) and the protooncogene receptor c-KIT in CIS and GB [9-11]. Besides c-KIT and PLAP, GBs were recently found to express *TSPY* (testis-specific protein on the Y chromosome) in a limited number of cases [12,13]. This is of particular interest, because development of GBs has been linked to the presence of a specific part of the Y chromosome, namely the GBY (GB on the

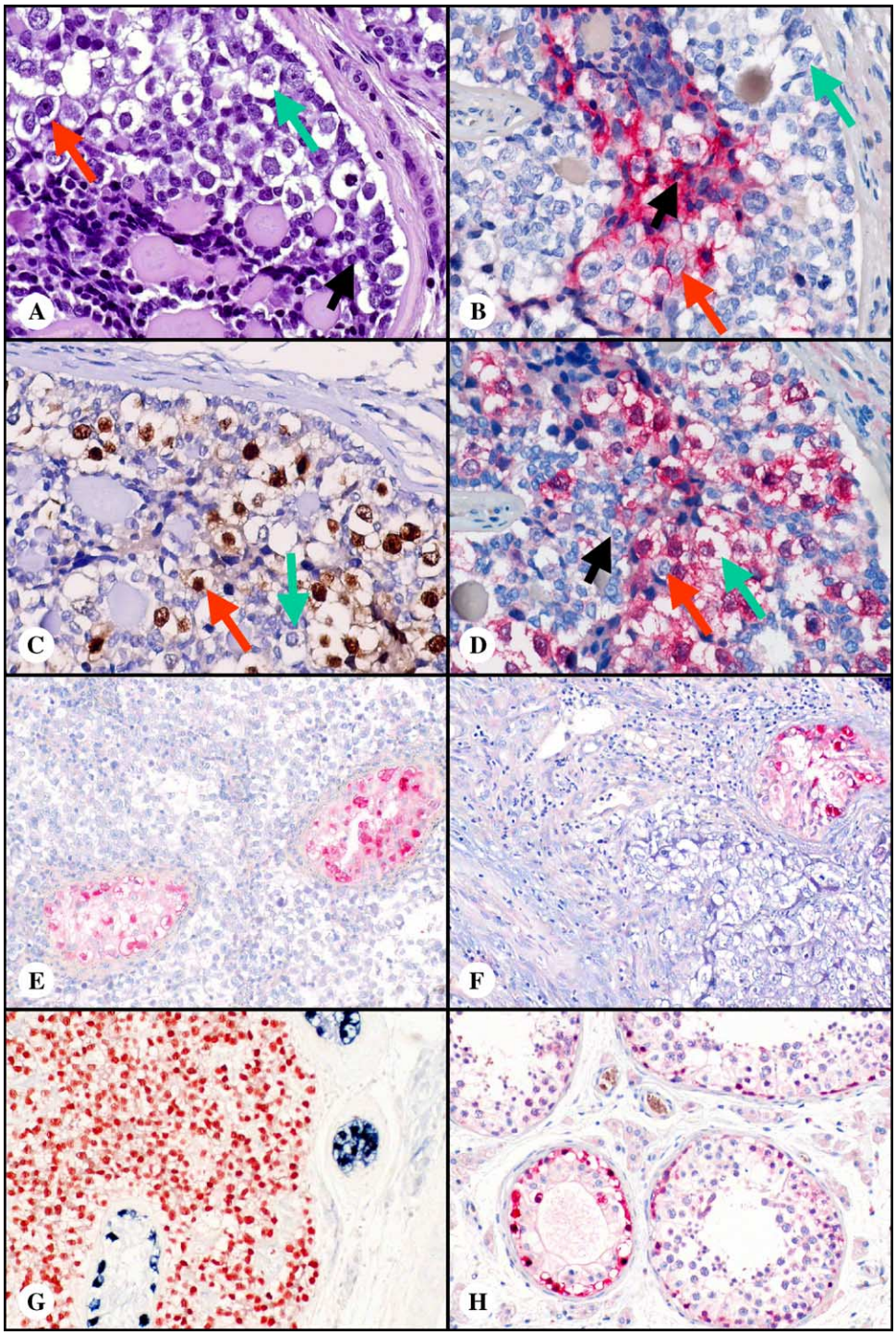

Y chromosome) region [14-16]. A candidate gene in this region is *TSPY*. Although its function is still unclear, a role in the proliferation of germ cells has been suggested [13].

The model that CIS originates from an early germ cell, either a primordial germ cell or a gonocyte, is strongly supported by our recent finding that the octamer binding transcription factor POU5F1, also known as OCT3/4, is specifically found in CIS, seminoma, and EC [17]. OCT3/4 is a known marker for pluripotency. Its presence mimics the expression pattern during embryogenesis, where this factor is restricted to embryonic stem cells and early germ cells (as discussed in Ref [17]). We recently found that OCT3/4 is down-regulated during germ cell maturation both in male and female gonadogenesis [18,19]. In a large series investigating various malignancies, one case of GB was positive for OCT3/4, as were all cases with testicular CIS [17]. Recently, this was confirmed in larger series [20-25].

Presence of c-KIT, PLAP, OCT3/4, and TSPY proteins has not been investigated systematically in a single study in multiple GBs. To further investigate the pathogenesis of GB, and to shed light on its pathogenetic relationship with testicular CIS, we performed a detailed investigation of these markers in a series of 6 GBs and adjacent invasive tumor components. The findings were compared to those obtained in testicular CIS and adjacent invasive GCTs. Our results confirm that GB is a mixture of germ cells at different stages of maturation, which can be identified by morphology as well as the presence of various markers. A process of selection of immature germ cells leads to the precursor cells of invasive GCTs. This is demonstrated by the consistent and homogenous staining pattern for both OCT3/4 and TSPY in these cells, as well as in early invasive tumor cells and CIS. Upon further progression, eventually resulting in an invasive tumor, TSPY can be lost, whereas OCT3/4 remains positive. These observations are in line with the model that GB is an intermediate between normal immature germ cells and CIS of the testis.

2. Materials and methods

2.1. Material

Use of tissues for scientific reasons has been approved by an institutional review board (MEC 02.981). The samples were used according to the "Code for Proper Secondary Use of Human Tissue in the Netherlands," developed by the Dutch Federation of Medical Scientific Societies (FMWV) (version 2002).

Six dysgenetic gonads (including one individual with bilateral dysgenetic gonads) containing GB with or without an invasive tumor component were collected in the south-western part of the Netherlands in collaboration with pediatric surgeons, urologists, and pathologists (Table 1). Furthermore, 21 seminomas and 38 nonseminomas of different, sometimes mixed, histologies (18 EC, 7 YSTs, 9 TEs, 4 CHs) of the adult testis were included, also, 31 cases of CIS adjacent to invasive testicular germ cell tumors (TGCTs) were retrieved from our archive. In addition, intratubular seminoma and nonseminoma could be identified in a number of cases. Two testicular CIS cases without the presence of an invasive tumor were also included. Two normal testes from fetuses of 16 and 21 weeks gestational age were obtained after spontaneous miscarriages. The postmortem examinations were carried out in our department. Tissues were routinely formalin fixed and paraffin embedded. Diagnosis of GB and invasive tumor parts was made according to the World Health Organization classification by a pathologist experienced in GCT pathology (JWO).

On the basis of morphology, the germ cells present in GBs were classified as immature or mature. The immature cells are characterized by their smaller size and a higher nuclear to cytoplasmic ratio. These cells are similar to normal gonocytes/oogonia. The mature germ cells, which are larger with a clear cytoplasm and which has a lower nuclear to cytoplasmic ratio, are similar to oocytes/prespermatogonia.

Fig. 1 Representative examples of histology and immunohistochemistry of a GB included in this study (A-D, case 4, Table 1). Parallel sections were used, allowing direct comparison of the different staining results. A, Hematoxylin and eosin staining. Note the presence of supportive cells, Sertoli/granulosa cells (indicated by a black arrow) as well as germ cells, with various stages of maturation; immature germ cells are small and show a high nuclear/cytoplasmic ratio (indicated throughout this figure with a red arrow), whereas mature germ cells show the opposite characteristics (indicated throughout this figure with a green arrow). B, PLAP staining: the red cytoplasmic signal in predominantly the immature germ cells, as well as in some stromal cells. C, OCT3/4 staining. Note the positive brown staining predominantly in the immature and not the mature germ cells. None of the other cell types shows a positive staining. D, TSPY staining: the red nuclear and cytoplasmic signal, predominantly in the mature compared to immature germ cells. In addition, supportive cells can be positive. All images are at a magnification factor of ×400. Representative example of immunohistochemistry for TSPY on a tissue section of (E) seminiferous tubules with CIS and invasive testicular seminoma and (F) seminiferous tubule with CIS and invasive EC. Note that the CIS cells are specifically stained, and note the absence of TSPY in the invasive tumor cells. G, Double staining for OCT3/4 (red) and TSPY (blue) in an invasive seminoma (same case as shown in E). Note the double-positive CIS cells and the loss of TSPY, but only of OCT3/4 in the invasive cells, that is, TSPY is lost upon invasive growth. Coexpression can result in a dark almost black signal. H, Representative example of immunohistochemistry for TSPY on a tissue section of testicular parenchyma, containing both seminiferous tubules with normal spermatogenesis (right part of the image) and CIS (left lower part of the image). Carcinoma in situ cells stain stronger than spermatogonia (hematoxylin and eosin, original magnification ×200).

2.2. Immunohistochemistry

Staining was performed as described before [26]. For immunohistochemistry, 3-μm-thick paraffin-embedded tissue sections were incubated with the primary antibodies overnight at 4°C: PLAP (1:200, Cell Marque, Hot Springs, Ark), c-KIT (1:500, Dako-Cytomation, Glostrup, Denmark), and TSPY (1:3000, provided by C. Lau). Ki-67 (1:100, Dako-Cytomation) were incubated for 1 hour and OCT3/4 (1:1000, Santa Cruz Bio-technology, Santa Cruz, Calif) for 2 hours at room temperature. All slides of the single-staining experiments were counterstained with hematoxylin. Alkaline phosphatase staining with new fuchsin was used for the detection of PLAP, c-KIT, and TSPY, resulting in a red signal of cytoplasmic, membranous, and cytoplasmic/nuclear localization, respectively. Diaminobenzidine was used as chromogen in the peroxidase staining for the detection of OCT3/4, resulting in a brown nuclear signal.

Double-staining experiments were performed using a combination of the same detection methods but with

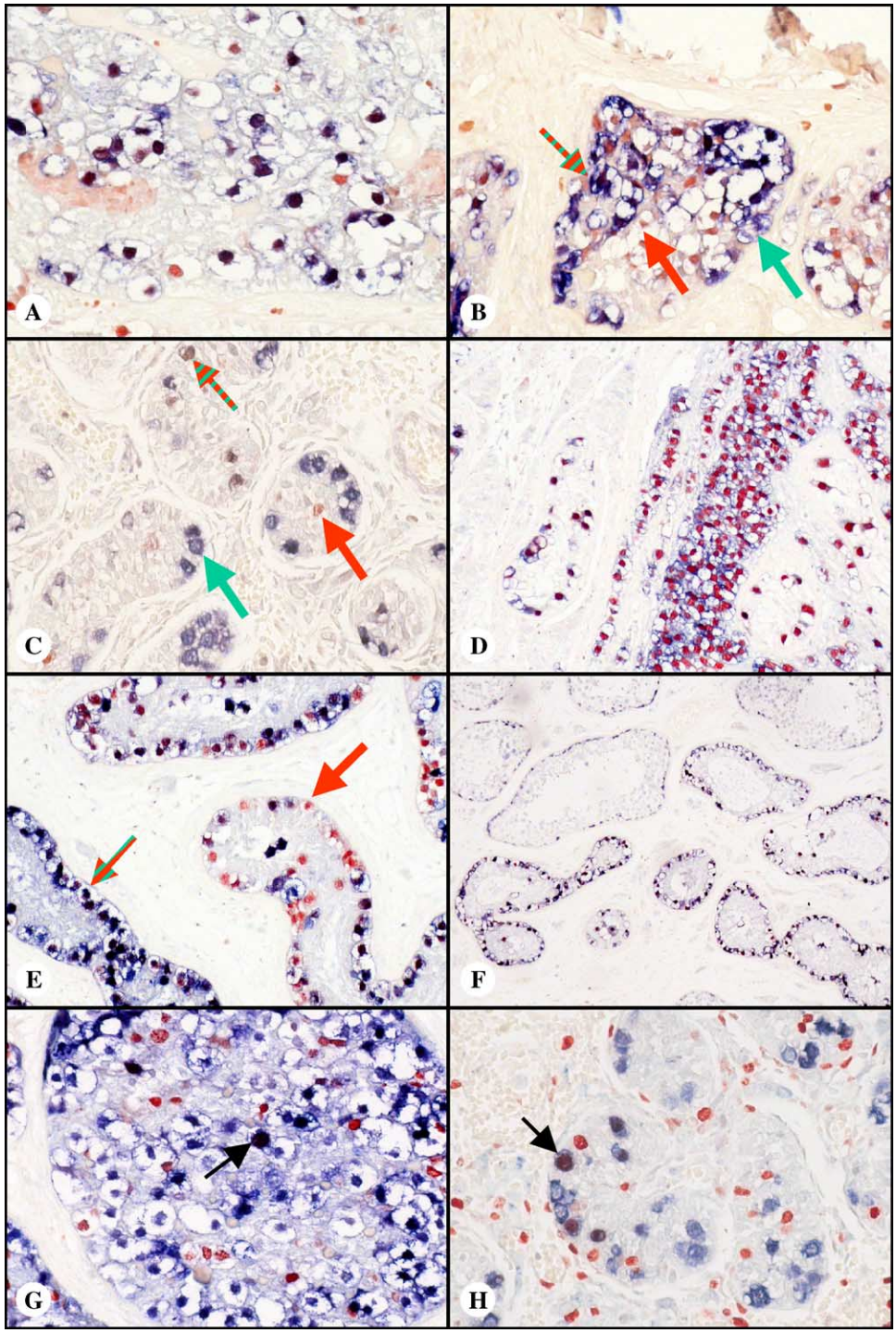

different visualization methods: Fast Blue/Naphthol ASMX phosphate (F3378 and N500; Sigma, Steinheim, Germany) for a blue staining (TSPY) and 3-amino-9-ethyl-carbazole (A.5754 and D4254; Sigma)/H_2O_2 for a red staining (OCT3/4; Ki-67), without counterstaining. To reduce background signal, endogenous peroxidase activity and endogenous biotin were blocked using 3% H_2O_2 (for 5 minutes) and a blocking kit for endogenous biotin (Vector Laboratories, Burlingame, Calif).

2.3. Fluorescence in situ hybridization

Fluorescence in situ hybridization (FISH) was performed as previously described [27] on paraffin-embedded tissue sections using probes specific for the centromeric regions of chromosomes X (DXZ1) and Y (DYZ3). Only whole nuclei of intact cells were scored in 2 different tumor areas, both in regions containing GB and DG, if present. The mean number of spots per nucleus is indicated; minimum number of cells assessed was 117.

3. Results

c-KIT and PLAP are established markers suitable for the immunohistochemical detection of CIS cells of the adult testis (for review, see Ref [28]). This also counts for OCT3/4 [17], of which multiple confirmative studies have been reported [20-25], and for TSPY [29], although this is less well established. Here we compare the staining pattern of these markers in CIS with the findings in a series of GBs. In total, 6 GBs were included of 5 independent patients with a 46,XY karyotype (one was bilateral). In 4 cases, an adjacent invasive DG component was available for investigation. Three of the invasive tumors showed an early stage of invasiveness near the GB areas (termed *early invasive dysgerminoma*, Table 1), and 1 case also contained large invasive tumor areas at a distance from the precursor lesion (termed *progressed dysgerminoma*, Table 1). The results of the staining experiments are summarized in the Table 1, and representative examples of staining results are shown in Fig. 1. Double-staining experiments were performed for TSPY and OCT3/4, and TSPY and Ki-67, of which representative examples are shown in Figs. 1G and 2. To assess the presence of chromosome X and Y, FISH analysis was performed using centromere probes for these chromosomes.

Morphologically, GB lesions contain various cell types, including somatic cells and germ cells (Fig. 1A). The first show characteristics of Sertoli/granulosa cells (further supported by a weak staining for vimentin using immunohistochemistry, data not shown), whereas the germ cells are a mixture of cells at different stages of maturation. The smaller cells with a high nuclear to cytoplasmic ratio are immature germ cells, resembling gonocytes/oogonia. The bigger cells with a large clear cytoplasm are mature germ cells, which are similar to prespermatogonia/oocytes.

3.1. Results of single-staining experiments

c-KIT was the least consistent marker investigated in the GBs in this study. It showed no staining in the 3 GBs and the 2 matched DGs. In contrast, PLAP was detected in all GBs and adjacent invasive components, with a heterogeneous pattern in the most advanced DG. However, not all germ cells present in GBs were positive for PLAP (Fig. 1B). Although most mature germ cell were negative, the immature germ cells were mainly positive, although stromal cells could show staining. Most of the tumor cells in invasive DG showed a weaker signal intensity or were negative for PLAP (Table 1). This indicates that PLAP is present in GB but weaker to negative in invasive DG. A similar pattern has been observed in testicular CIS and seminoma, in which PLAP is down-regulated upon tumor progression (Table 1).

OCT3/4 was readily detectable as a nuclear staining in all GBs (Fig. 1C), in which the protein was restricted to the immature germ cells, although the more differentiated germ cells were negative. In contrast to the heterogeneity seen in GB, all tumor cells of DGs, both adjacent to and at distance from GB areas, showed a homogenous staining for OCT3/4 (see also Fig. 2). Therefore, a selection of OCT3/4-positive

Fig. 2 Representative examples of double immunohistochemical staining experiments. Shown are TSPY (blue cytoplasmic and nuclear signal) and OCT3/4 (red nuclear signal) in (A) early invasive DG (case 3, Table 1). Similar to seminoma, the vast majority of DG cells show expression of both markers. Original magnification ×400. B, Gonadoblastoma (case 1, Table 1). Note the heterogeneous staining pattern, only a minority of cells shows a positive staining of both factors. The germ cells only positive for OCT3/4 are indicated by a red arrow, and the germ cells only positive for TSPY by a green arrow. The double-positive cells are indicated by a red/green arrow. Original magnification ×400. C, Normal fetal germ cells, gestational age 21 weeks. Note that whereas TSPY is predominantly expressed in prespermatogonia (located on the basal membrane, green arrow), OCT3/4 is seen more frequently in gonocytes in a more central localization of the tubule (red arrow). Only a minority of germ cells is positive for both factors (green/red arrow). Original magnification ×400. D, CIS and early (micro-)invasive seminoma. The CIS and early invasive seminoma cells (left and middle panel of the image) show expression of both markers. Invasive seminoma cells at more distance (right panel of the image) show loss of TSPY but not of OCT3/4. Original magnification ×200. E, CIS adjacent to an invasive tumor. Note the presence of CIS cells with both markers (red/green arrow) as well as CIS cells without TSPY, but staining for OCT3/4 (red arrow). Original magnification ×400. F, CIS before invasiveness. All cells show coexpression of both factors. Original magnification ×100. G, Double-staining for TSPY (blue cytoplasmic and nuclear signal) and Ki-67 (red nuclear signal) in GB (case 5). Mature germ cells are TSPY positive, whereas Ki-67 is mainly positive in immature cells. Only a minority of the cells is positive for both factors, indicated by an arrow. Original magnification ×400. H, Normal fetal germ cells (same case as shown in C). Only a minority of germ cells (around 30%) is positive for both factors (indicated by a black arrow). Original magnification ×400.

cells takes place during development of an invasive tumor from GB. These data are in accordance to observations in CIS and TGCTs (see the following paragraphs and see Ref [17] for discussion).

A heterogeneous staining pattern was found in GB for TSPY. In contrast to OCT3/4, TSPY was detected in both a nuclear localization and in the cytoplasm (Fig. 1D). The protein was not detectable in somatic cells resembling granulosa/Sertoli cells. Tumor cells of early invasive DG closely adjacent to the GB areas consistently showed a strong and homogenous staining for TSPY, similar to the pattern seen for OCT3/4 (see Fig. 2 for examples). TSPY expression could be lost in invasive DG areas at distance from the preinvasive lesion. A similar pattern was also detected in the testis: TSPY was strongly expressed in CIS adjacent to invasive tumors, both seminoma and nonseminoma (see Table 1 and Fig. 1E-G). Intratubular seminoma was consistently positive, whereas invasive seminoma, like DG, can lose expression of TSPY. In contrast, all nonseminomas lack TSPY. Interestingly, even the intratubular EC component is already negative (data not shown). Because FISH analysis revealed that the Y chromosome is not lost in these tumors (data not shown), loss of TSPY protein is not due to gross loss of Y-genetic material on progression.

In normal spermatogenesis, TSPY staining was predominantly seen in spermatogonia and sometimes spermatocytes (see Fig. 1H, right panel). However, the staining intensity of TSPY in CIS was stronger than in spermatogonia (Fig. 1H, left panel).

3.2. Results of double-staining experiments

To further investigate the observed heterogeneity in expression of OCT3/4 and TSPY in GB, CIS and invasive tumor components, double-staining experiments were performed. The results for OCT3/4 and TSPY were in line with the results of single-staining experiments. The early invasive DG components showed a homogenous staining for both OCT3/4 and TSPY, in which most tumor cells were positive for both markers (Fig. 2A). In GB, however, the mature germ cells were positive for TSPY and negative for OCT3/4, whereas immature germ cells were mainly positive for OCT3/4 only (Fig. 2B). Only a subpopulation of germ cells in GB showed coexpression of both markers. To investigate whether coexpression of OCT3/4 and TSPY is a physiological event during normal intrauterine male germ cell development, we stained 2 normal testes of fetuses of 16 and 21 weeks of gestational age. Most of the germ cells were found to be positive for only one factor, either OCT3/4 or TSPY. A minority of OCT3/4-positive germ cells also showed expression of TSPY (Fig. 2C). Interestingly, these cells were located on the basal membrane of the seminiferous tubule. Whereas the overall number of OCT3/4-positive cells decreased from weeks 16 to 21 of gestational age, the fraction of germ cells showing expression of both markers remained unchanged.

These results were compared to the samples of testicular CIS and TGCTs, subjected to the same protocol for double staining. In accordance with the single-staining results, CIS and early invasive seminoma components were homogenously positive for both OCT3/4 and TSPY (Fig. 2D, left and middle panel). A more heterogeneous pattern was seen in later stages of invasiveness of seminomas, where expression of TSPY could be lost, but OCT3/4 remained positive (Fig. 2D, right panel, and Fig. 1G). In all cases of CIS adjacent to an invasive tumor, either seminoma or nonseminoma (which were all negative for TSPY), CIS cells without expression of TSPY but positive for OCT3/4 were found (Fig. 2E). In 2 cases of CIS without invasive tumor, all CIS cells expressed TSPY (Fig. 2F). These data indicate that TSPY is lost upon invasiveness of GCT cells. This step can already occur in the in situ stage (Fig. 2E).

Finally, to assess whether there is a correlation between TSPY expression and proliferation, we performed double-staining analyses for TSPY and Ki-67. In addition to CIS and GB, the 2 normal fetal testes were investigated. Most malignant germ cells (around 90%) of both CIS and intratubular seminoma were positive for both TSPY and Ki-67. Gonadoblastoma with an adjacent invasive tumor component showed a similar pattern as CIS, whereas GB without invasive tumor was much more heterogeneous (case 5, Fig. 2G). In fact, less double-positive cells were identified. In these cases, mature germ cells were mainly TSPY positive, whereas immature cells were mostly positive for Ki-67 only, and coexpression of both markers was rarely seen. This was similar to the pattern seen in fetal testes, where the 2 factors were not frequently coexpressed. Only around 30% (29% at 16 weeks; 32% at 21 weeks gestational age) of germ cells positive for TSPY also showed expression of Ki-67 (see Fig. 2H).

4. Discussion

The term *dysgenetic gonads* is used to describe the phenomenon of a disturbed gonadal sex determination or differentiation. This condition is associated with an increased risk for the development of malignant GCTs. The invasive tumor components, referred to as DGs and non-DGs, resemble those of the adult testis (TGCTs), seminoma, and nonseminoma of various histologies. The precursor lesion is known as GB [4]. Histologically, GBs consist of aggregates of germ cells and sex cord elements, including immature Sertoli and granulosa cells. Some of the germ cells show similarities to CIS, the known precursor of TGCTs [10]. Both CIS and GB are thought to be the result of a maturation arrest of early germ cells, possibly due to a disrupted gonadal environment or unknown pathogenetic hits. Because CIS is highly similar to the invasive TGCTs (ie, seminoma), and is suggested to be “only one step behind in the karyotypic evolution” [30,31], it might not be the best target for the identification of the earliest steps in the

development of TGCTs. This could, however, be the case for GB [8]. We undertook the present study to further understand the biology of this condition, and to compare similarities and differences between GB and CIS.

Immunohistochemical analysis of both known (PLAP, c-KIT) and recent markers of early male germ cells (OCT3/4, TSPY) was performed in GBs and adjacent DGs. Gonadoblastomas have previously been reported to be positive for PLAP and c-KIT [9-11]. Our results are mainly in line with these findings. PLAP can be present in GBs and is weakly but homogenously positive in the invasive component. However, c-KIT was not always detected. We therefore conclude that c-KIT is not a reliable marker for the detection of GB. A heterogeneous staining pattern was found for both OCT3/4 and TSPY in all GBs investigated. Early invasive DG cells closely adjacent to the GB component were positive for both OCT3/4 and TSPY. A similar pattern was found in most CIS cells and could be confirmed by double-staining experiments. TSPY has previously been reported in a few cases of GB [12,13], although, to our knowledge, the presence of TSPY in early invasive DGs and the loss of expression on tumor progression are novel. These findings support a model in which progression from early GB to invasive growth is associated with expression of both TSPY and OCT3/4 in immature germ cells (see Fig. 3 for a schematic representation). A similar pattern is present in CIS and early stages of seminoma. This indicates that TSPY might be involved in the initial selection of tumorigenic

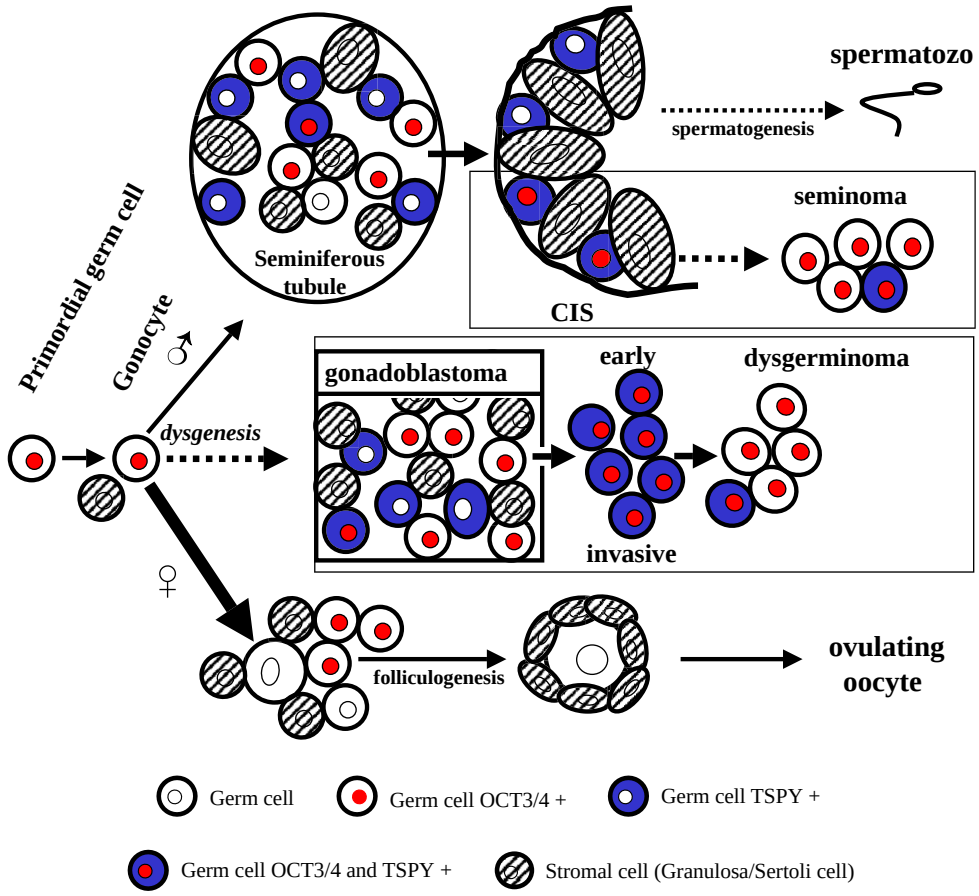

Fig. 3 Schematic representation of normal and neoplastic germ cell development. The earliest stage of maturation (starting with a primordial germ cell) is indicated on the left side of the illustration and the most mature (differentiated) stage at the right. Maturation of germ cells is graphically depicted by increasing size of cells and nuclei. Normal male development (top row) and female development (bottom row) lead to functional gametes (spermatozoa and ovulating oocyte, respectively). Note that in the absence of determining factors for male development, female differentiation occurs—a mechanism known as "default pathway" (see arrow sizes leading from gonocytes to normal male or female development). Red nuclei indicates germ cells positive for OCT3/4; cytoplasmic blue cells, germ cells positive for TSPY. The colors are consistent with the detection methods in the double staining as shown in Figs. 1 and 2. During normal male fetal germ cell development (and in GB), only a minority of cells show coexpression of OCT3/4 and TSPY (depicted by a red nucleus and a blue cytoplasm). A disturbed process of germ cell maturation can result in invasive GCTs (boxed areas, middle panel). Gonadoblastoma contains germ cells at different stages of development in a disturbed stromal environment, classifiable both morphologically and with regard to the presence of the immunohistochemical markers OCT3/4 and TSPY (middle panel). In contrast, CIS (upper boxed panel) and early invasive DG are much more homogeneous, both morphologically and with regard to the expression of OCT3/4 and TSPY. This suggests a process of selection and clonal expansion and supports the model that GB is an earlier stage in the process of GCT formation than CIS.

cells, possibly by playing a role in cell cycle regulation or cell division [13]. We therefore assessed the fraction of cells that were positive for both TSPY and Ki-67, a marker for proliferation. Interestingly, coexpression was found in the vast majority of CIS and early invasive seminoma cells, as well as in GB with an adjacent invasive tumor. This underlines the strong proliferative activity of both lesions. Whereas the proliferative activity of CIS has been reported before [32], little is known about proliferation in GB. TSPY and Ki-67 were less frequently coexpressed in one GB case that had not yet developed into an invasive tumor (case 5, Table 1). In our view, this could indicate that this specific GB case had not yet progressed to the next pathogenetic step, that is, the expansion of one premalignant clone. In fact, it could pathogenetically be one step behind CIS, which is the obvious result of a clonal process. Whatever the role of TSPY in preinvasive lesions, proliferation in the invasive GCTs is no longer dependent on TSPY, as is demonstrated by the loss of TSPY on tumor progression.

Like TSPY, OCT3/4 has been shown to be present in GBs [17,18]. In the present series, OCT3/4 was readily detectable in all GBs in the nuclei of cells showing morphological features of immature germ cells. Furthermore, as OCT3/4 remained positive throughout all stages of tumor development from GB to DG, it can serve as a marker to identify cells showing a high risk for malignant transformation. However, it is important to notice that the coexpression of OCT3/4 and TSPY does not per se confer neoplastic properties to germ cells. This is illustrated by the fact that normal male fetal germ cells of the second trimester can coexpress both TSPY and OCT3/4, although only in a minority of all cells.

Results of the double-staining experiments support the notion that GB consists of a heterogeneous group of mature and immature germ cells, of which the immature cells show the phenotype similar to premalignant cells, in line with earlier findings [10]. Interestingly, we recently observed that mature germ cells in GB resemble more the male germ cell lineage than the female [33]. The higher incidence of these tumors in males compared to females confirms the finding of a crucial role of part of the Y chromosome in the development of this tumor [14]. Our results are compatible with the model that after a process of selection and consecutive clonal expansion, immature germ cells in GB expressing OCT3/4, PLAP, and TSPY progress to the next pathogenetic step, eventually leading to invasive growth. Whether the presence of TSPY is needed to maintain the germ line commitment of these cells at an early stage, or confers a growth advantage during the critical step to invasiveness, remains to be elucidated.

In conclusion, our results show that GB consists of a heterogeneous population of germ cells. Both in DG in ovaries and in seminoma, its counterpart in the adult testis, the step to an invasive GCT seems to involve selection and clonal expansion of an immature germ cell, positive for OCT3/4 and TSPY. At later stages of invasiveness, TSPY can be lost, whereas OCT3/4 always remains present in tumor cells exhibiting germ line characteristics, that is, DG or seminoma. Our analysis places GB at a very early stage of GCT development, making it an interesting entity to elucidate changes involved in the early pathogenesis of this disease in the future.

References

[1] Oosterhuis JW, Looijenga LHJ, Van Echten-Arends J, De Jong B. Chromosomal constitution and developmental potential of human germ cell tumors and teratomas. Cancer Genet Cytogenet 1997;95:96-102.

[2] Looijenga LHJ, Oosterhuis JW. Pathobiology of testicular germ cell tumors: views and news. Anal Quant Cytol Histol 2002;24:263-79.

[3] Woodward PJ, Heidenreich A, Looijenga LHJ, et al. World Health Organization classification of tumours. In: Eble JN, Sauter G, Epstein JI, Sesterhenn IA, editors. Pathology and genetics of the urinary system and male genital organs. Lyon: IARC Press; 2004. p. 217-78 [chapter 4].

[4] Scully RE. Gonadoblastoma/a review of 74 cases. Cancer 1970;25:1340-56.

[5] Skakkebæk NE. Testicular dysgenesis syndrome. Horm Res 2003;60(Suppl 3):49.

[6] Skakkebæk NE, Holm M, Hoei-Hansen C, Jørgensen N, Rajpert-De Meyts E. Association between testicular dysgenesis syndrome (TDS) and testicular neoplasia: evidence from 20 adult patients with signs of maldevelopment of the testis. APMIS 2003;111:1-9.

[7] Skakkebæk NE, Berthelsen JG, Giwercman A, Muller J. Carcinoma-in-situ of the testis: possible origin from gonocytes and precursor of all types of germ cell tumours except spermatocytoma. Int J Androl 1987;10:19-28.

[8] Kildal W, Kraggerud SM, Abeler VM, Heim S, Trope CG, Kristensen GB, et al. Genome profiles of bilateral dysgerminomas, a unilateral gonadoblastoma, and a metastasis from a 46, XY phenotypic female. Hum Pathol 2003;34:946-9.

[9] Hustin J, Gillerot Y, Collette J, Franchimont P. Placental alkaline phosphatase in developing normal and abnormal gonads and in germ-cell tumours. Virchows Arch 1990;417:67-72.

[10] Jørgensen N, Muller J, Jaubert F, Clausen OP, Skakkebæk NE. Heterogeneity of gonadoblastoma germ cells: similarities with immature germ cells, spermatogonia and testicular carcinoma in situ cells. Histopathology 1997;30:177-86.

[11] Slowikowska-Hilczer J, Walczak-Jedrzejowska R, Kula K. Immunohistochemical diagnosis of preinvasive germ cell cancer of the testis. Folia Histochem Cytobiol 2001;39:67-72.

[12] Hildenbrand R, Schroder W, Brude E, Schepler A, Konig R, Stutte HJ, et al. Detection of TSPY protein in a unilateral microscopic gonadoblastoma of a Turner mosaic patient with a Y-derived marker chromosome. J Pathol 1999;189:623-6.

[13] Lau Y, Chou P, Iezzoni J, Alonzo J, Komuves L. Expression of a candidate gene for the gonadoblastoma locus in gonadoblastoma and testicular seminoma. Cytogenet Cell Genet 2000;91:160-4.

[14] Page DC. Hypothesis: a Y-chromosomal gene causes gonadoblastoma in dysgenetic gonads. Development 1987;101:151-5.

[15] Rutgers JL. Advances in the pathology of intersex conditions. Hum Pathol 1991;22:884-91.

[16] Salo P, Kaariainen H, Petrovic V, Peltomaki P, Page DC, de la Chapelle A. Molecular mapping of the putative gonadoblastoma locus on the Y chromosome. Genes Chromosomes Cancer 1995;14:210-4.

[17] Looijenga LHJ, Stoop H, De Leeuw PJC, De Gouveia Brazao CA, Gillis AJM, Van Roozendaal KEP, et al. POU5F1 (OCT3/4) identifies cells with pluripotent potential in human germ cell tumors. Cancer Res 2003;63:2244-50.

[18] Honecker F, Stoop H, de Krijger R, Lau C, Bokemeyer C, Looijenga LHJ. Testicular carcinoma in situ markers in foetal germ cells: pathobiological implications. J Pathol 2004;203:849-57.
[19] Stoop H, Honecker F, Cools M, De krijger R, Bokemeyer C, Looijenga LHJ. Differentiation and development of human female germ cells during prenatal gonadogenesis: an immunohistochemical study. Hum Reprod 2005; March 10 (online ahead).
[20] Rajpert-De Meyts E, Hanstein R, Jørgensen N, Græm N, Vogt PH, Skakkebæk NE. Developmental expression of POU5F1 (OCT3/4) in normal and dysgenetic human gonads. Hum Reprod 2004;19(6): 1338-44.
[21] Gidekel S, Pizov G, Bergman Y, Pikarsky E. Oct-3/4 is a dose-dependent oncogenic fate determinant. Cancer Cell 2003;4:361-70.
[22] Cheng L, Thomas A, Roth LM, Zheng W, Michael H, Karim FW. OCT4: a novel biomarker for dysgerminoma of the ovary. Am J Surg Pathol 2004;28:1341-6.
[23] Cheng L. Establishing a germ cell origin for metastatic tumors using OCT4 immunohistochemistry. Cancer 2004;101:2006-10.
[24] Jones TD, Ulbright TM, Eble JN, Baldridge LA, Cheng L. OCT4 staining in testicular tumors: a sensitive and specific marker for seminoma and embryonal carcinoma. Am J Surg Pathol 2004;28: 935-40.
[25] Jones TD, Ulbright TM, Eble JN, Cheng L. OCT4: a sensitive and specific biomarker for intratubular germ cell neoplasia of the testis. Clin Cancer Res 2004;10:8544-7.
[26] Stoop H, Van Gurp RHJ, De Krijger R, Geurts van Kessel A, Koberle B, Oosterhuis JW, et al. Reactivity of germ cell maturation stage-specific markers in spermatocytic seminoma: diagnostic and etiological implications. Lab Invest 2001;81:919-28.
[27] Kersemaekers AMF, Mayer F, Molier M, Van Weeren PC, Oosterhuis JW, Bokemeyer C, et al. Role of P53 and MDM2 in treatment response of human germ cell tumors. J Clin Oncol 2002;20:1551-61.
[28] Rajpert-De Meyts E, Bartkova J, Samson M, Hoei-Hansen CE, Frydelund-Larsen L, Bartek J, et al. The emerging phenotype of the testicular carcinoma in situ germ cell. APMIS 2003;111:267-78.
[29] Schnieders F, Dork T, Arnemann J, Vogel T, Werner M, Schmidtke J. Testis-specific protein, Y-encoded (TSPY) expression in testicular tissues. Hum Mol Genet 1996;5:1801-7.
[30] Looijenga LHJ, Rosenberg C, Van Gurp RJHLM, Geelen E, Van Echten-Arends J, De Jong B, et al. Comparative genomic hybridization of microdissected samples from different stages in the development of a seminoma and nonseminoma. J Pathol 2000;19:187-92.
[31] Rosenberg C, Van Gurp RJHLM, Geelen E, Oosterhuis JW, Looijenga LHJ. Overrepresentation of the short arm of chromosome 12 is related to invasive growth of human testicular seminomas and nonseminomas. Oncogene 2000;19:5858-62.
[32] Datta MW, Renshaw AA, Dutta A, Hoffman MA, Loughlin KR. Evaluation of cyclin expression in testicular germ cell tumors: cyclin E correlates with tumor type, advanced clinical stage, and pulmonary metastasis. Mod Pathol 2000;13:667-72.
[33] Honecker F, Kersemaekers AMF, Molier M, Van Weeren PC, Stoop RR, De Krijger RR, et al. Involvement of E-cadherin and beta-catenin in germ cell tumours and in normal male foetal germ cell development. J Pathol 2004;204:167-74.

Human Pathology (2006) 37, 101–111

Human
PATHOLOGY
www.elsevier.com/locate/humpath

Maturation delay of germ cells in fetuses with trisomy 21 results in increased risk for the development of testicular germ cell tumors☆

Martine Cools MD[a], Friedemann Honecker MD[a,b], Hans Stoop BSc[a], Joris D. Veltman BSc[a], Ronald R. de Krijger MD, PhD[a], Ewout Steyerberg PhD[c], Katja P. Wolffenbuttel MD[d], Carsten Bokemeyer MD, PhD[b], Yun-Fai Chris Lau PhD[e], Stenvert L.S. Drop MD, PhD[f], Leendert H.J. Looijenga PhD[a,*]

[a]*Department of Pathology, Josephine Nefkens Institute, Erasmus MC–University Medical Center, Daniel den Hoed, 3000 DR Rotterdam, The Netherlands*
[b]*Department of Oncology/Hematology, University Medical Center Hamburg-Eppendorf, 20246 Hamburg, Germany*
[c]*Department of Public Health, Center for Clinical Decision Science, Erasmus MC–University Medical Center, 3000 DR Rotterdam, The Netherlands*
[d]*Department of Pediatric Urology, Sophia Children's Hospital, Erasmus MC–University Medical Center, 3000 DR Rotterdam, The Netherlands*
[e]*Division of Cell and Developmental Genetics, Department of Medicine, VA Medical Center, University of California, San Francisco, CA 94121, USA*
[f]*Department of Pediatric Endocrinology, Sophia Children's Hospital, Erasmus MC–University Medical Center, 3000 DR Rotterdam, The Netherlands*

Received 29 March 2005; accepted 24 September 2005

Keywords:
Trisomy 21;
Gonadal development;
Germ cell neoplasia;
OCT3/4;
TSPY

Summary Trisomy 21 is associated with an increased risk for the occurrence of germ cell tumors in males. The development of these tumors is thought to be related to events in fetal life. A delay in the maturation of germ cells is one of the mechanisms that have been proposed for the development of these tumors in high-risk groups such as intersex patients. To investigate whether a delay in germ cell development also occurs in trisomy 21, we examined the gonads of 30 fetuses, neonates, and infants with trisomy 21 (19 males and 11 females) for the expression of several immunohistochemical germ cell markers throughout pregnancy and compared them with a series of 46 age-matched controls. The results of our study reveal a significant delay in germ cell development in fetuses with trisomy 21, especially in males. Prolonged expression of octamer binding transcription factor 3/4, in combination with an increased expression of testis-specific protein, Y-encoded, might have pathogenetic relevance for the development of testicular germ cell tumors in this population.

☆ This study was financially supported by the ESPE Research Fellowship which is sponsored by Novo Nordisk (Copenhagen, Denmark), the Deutsche Krebshilfe (Bonn, Germany), and the Dutch Cancer Society (Amsterdam, The Netherlands).

* Corresponding author.
E-mail address: l.looijenga@erasmusmc.nl (L.H.J. Looijenga).

0046-8177/$ – see front matter © 2006 Elsevier Inc. All rights reserved.
doi:10.1016/j.humpath.2005.09.021

1. Introduction

In addition to a high incidence of leukemias, trisomy 21 (Down syndrome) is associated with an increased risk for gonadal and extragonadal germ cell tumors [1]. The incidence of testicular germ cell tumors (TGCTs) in individuals with trisomy 21 is estimated at 0.5% compared with an expected incidence of 0.087% in the general population [2]. Some studies even mention a 50-fold increase in incidence [3,4]. Seminomas, nonseminomas, and 2 fetal carcinoma in situ (CIS) lesions (the precursor lesion of these tumors, also called *intratubular germ cell neoplasia unclassified*) have been reported, the first occurring most frequently [4-6]. In view of the young age at which these tumors are diagnosed, a genetic background is suspected. Cryptorchidism, which occurs frequently in Down syndrome, is also a risk factor, although TGCTs are mainly found in normally descended testes. Additional contributing factors are excessive follicle-stimulating hormone stimulation due to hypergonadotropic hypogonadism, a possible gene dosage effect of putative oncogenes on chromosome 21, increased sensitivity of trisomic cells to carcinogenic agents, and increased maternal age [2,4,7]. Recently, maturation delay of germ cells and prolonged expression of the stem cell factor receptor c-KIT (gene encoding the stem cell factor receptor that has tyrosine kinase activity) during intrauterine development have been related to the development of CIS in various intersex conditions and chromosomal anomalies by increasing the survival and proliferative chances of the primordial germ cells (PGCs) [8,9].

To investigate if and to what extent intrauterine maturation delay of germ cells is present in trisomy 21, we studied the expression of several immunohistochemical markers for germ cells in the gonads of 30 fetuses, neonates, and infants with trisomy 21, and compared their expression profiles throughout pregnancy and early infancy with a series of 46 normal controls of comparable gestational age (GA) published previously [10,11].

Immunohistochemistry was performed with the antibodies octamer binding transcription factor 3/4 (OCT3/4); c-KIT; placental-like alkaline phosphatase (PLAP); testis-specific protein, Y-encoded (TSPY); VASA; and caspase 3. Octamer binding transcription factor 3/4 involved in the regulation of pluripotency (also referred to as POU domain class

Table 1 Schematic representation of origin and protocols used for the different antibodies

	Origin	Dilution	Pre-treatment	HIAR	Incubation	Secondary antibody	AB-complex	Chromogen
Primary antibody								
VASA	Kindly provided by Dr D. H. Castrillon, Department of Pathology, Brigham and Women's Hospital and Harvard Medical School, Boston, Mass	1:2000	No	Yes	Overnight, 4°C	SWAR-bio	ABC-AP	New fuchsin
PLAP	Cell Marque, Hot Springs, Ark	1:200	No	Yes	Overnight, 4°C	RAM-bio	ABC-AP	New fuchsin
c-KIT	Dako-Cytomation, Glostrup, Denmark	1:500	No	Yes	Overnight, 4°C	SWAR-bio	ABC-AP	New fuchsin
TSPY	Kindly provided by Prof C. Lau, Department of Medicine, VA Medical Center, University of California, San Francisco, Calif	1:3000	No	No	Overnight, 4°C	SWAR-bio	ABC-AP	New fuchsin
OCT3/4	Santa Cruz Bio-technology, Santa Cruz, Calif	1:1000	H_2O_2 for 5 min	Yes	2 h, RT	HAG-bio	ABC-HRP	DAB
Caspase 3	R&D Systems, Minneapolis, Minn	1:8000	H_2O_2 for 5 min	Yes	Overnight, 4°C	SWAR-bio	ABC-HRP	DAB
Secondary antibody								
SWAR	Dako-Cytomation	1:200						
RAM	Dako-Cytomation	1:200						
HAG	Vector Laboratories, Burlingame, Calif	1:200						

Abbreviations: HIAR, heat-induced antigen retrieval [18]; AB-complex, streptavidin-biotin complex; SWAR-bio, swine antirabbit antibody, biotin labeled; ABC-AP, streptavidin-biotin-alkaline phosphatase complex; RAM-bio, rabbit antimouse antibody, biotin labeled; RT, room temperature; HAG-bio, horse antigoat antibody, biotin labeled; ABC-HRP, streptavidin-biotin-horseradish peroxidase complex; DAB, 3,3′-diaminobenzidine-tetrahydrochloride dehydrate.

5 transcription factor 1) is a transcription factor staining pluripotent stem cells and early germ cells. OCT3/4, c-KIT (the stem cell factor receptor), and PLAP are well-established markers for the diagnosis of CIS and invasive TGCT

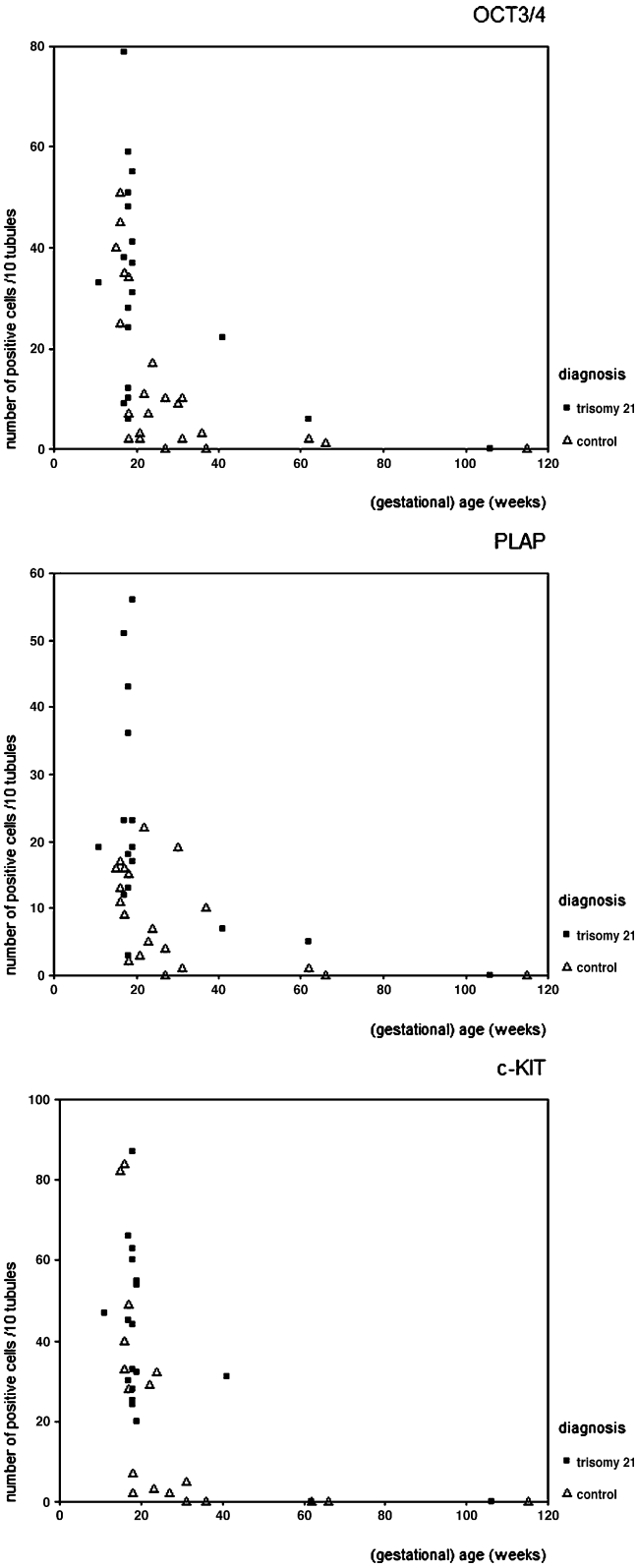

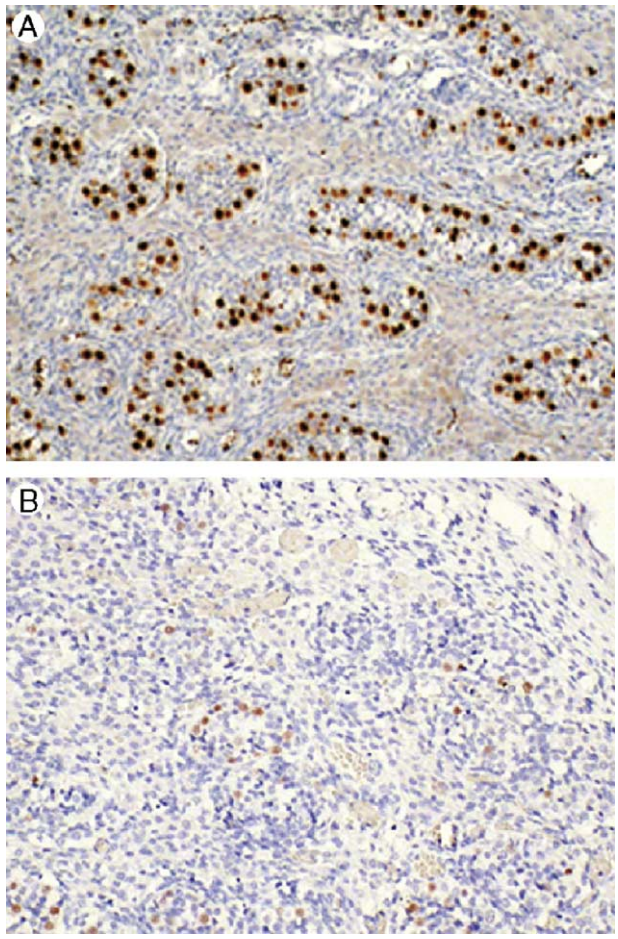

Fig. 2 A, Octamer binding transcription factor 3/4 expression in a male individual with trisomy 21 (18 weeks GA, original magnification ×200). B, Octamer binding transcription factor 3/4 expression in a male control (18 weeks GA, original magnification ×200). The number of OCT3/4-positive cells per tubule cross section is higher in the fetus with trisomy 21 as compared with the age-matched control.

[12-14] and are normally expressed during early fetal life in PGCs/gonocytes, the putative cells of origin of TGCT [10,11]. Testis-specific protein, Y-encoded, encoded by the TSPY gene, is thought to regulate the mitotic proliferation of spermatogonia, just before the onset of meiosis [15]. However, this is most likely not its only function because TSPY is also expressed, mainly in prespermatogonia, during embryonic life, where no meiosis in males occurs [10]. VASA, the human homologue of the mouse *vasa* gene, is a general marker for germ cells [16]. As such, it can be used

Fig. 1 Staining results for OCT3/4 (top), PLAP (middle), and c-KIT (bottom) in male individuals with trisomy 21 (black squares) and controls (triangles). The expression patterns for the 3 markers are similar in trisomy 21 and in controls: the expression is high in the second trimester but decreases sharply thereafter. The number of positive cells is higher in trisomy 21 than in controls at all ages, and the decline in the number of positive cells is slower.

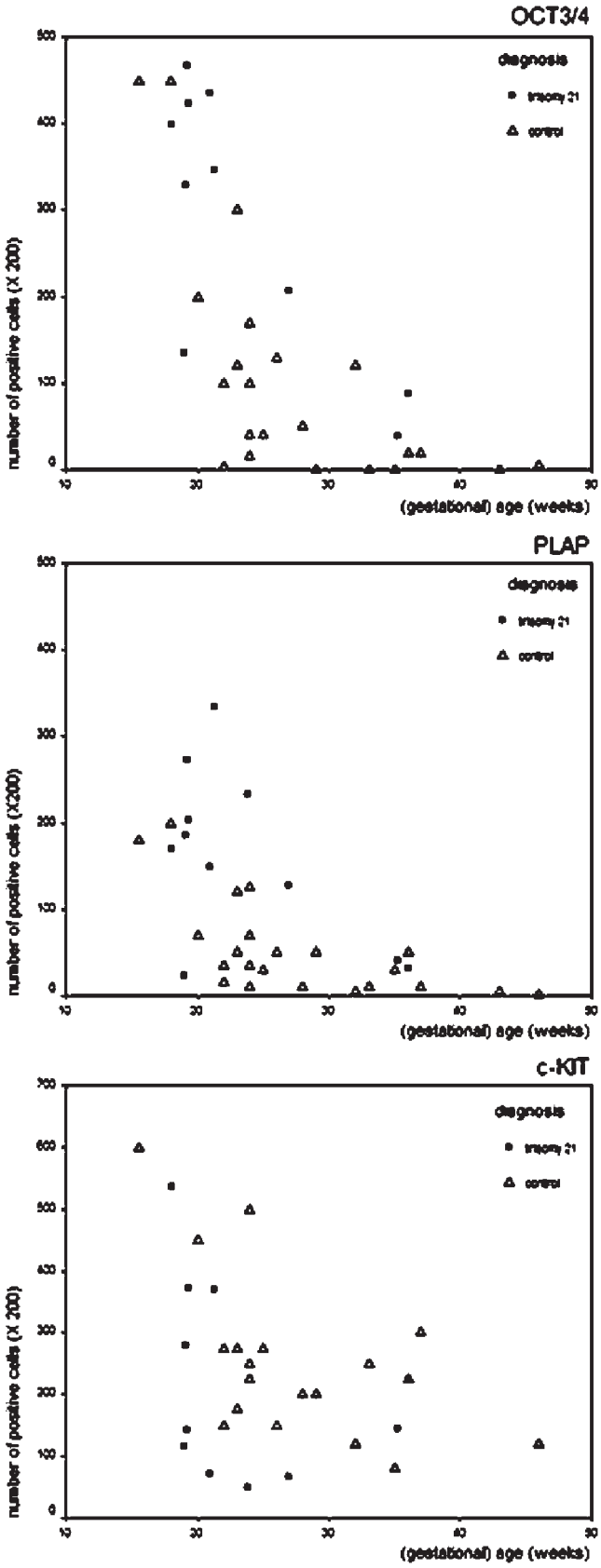

to estimate the total number of germ cells in gonadal tissue samples. In fetal gonadal tissues, VASA was found to be expressed at a constant level from the second trimester of pregnancy onward. VASA stains maturing germ cells (oocytes and prespermatogonia) with a higher intensity than immature germ cells. Therefore, a reverse correlation exists between the staining intensity of VASA and the expression of OCT3/4, the latter staining the immature, pluripotent germ cells (oogonia and gonocytes) [10,11]. Caspase 3 is an early product and further executioner in the apoptotic cascade. Therefore, immunohistochemical detection of activated caspase 3 is a new and reliable method to specifically stain early apoptotic, but not necrotic or autolytic cells [17]. Caspase 3 expression in fetal gonads has not been studied previously.

2. Materials and methods

2.1. Tissue samples

Gonadal tissue of fetuses, neonates, and infants with trisomy 21 was obtained after induced abortion or sudden death (2 due to heart failure, 1 due to meningococcal septicemia, and 1 due to necrotizing enterocolitis). Eleven females with trisomy 21, 18 to 36 weeks GA, and 19 males with trisomy 21, 11 to 19 weeks GA and 1 week to 15 months old, were included. Unsatisfactory preservation of tissue samples, as evaluated by hematoxylin-eosin staining, led to the exclusion of 17 samples. Gonads from 21 females (15-46 weeks GA) and 25 males (15-37 weeks GA and 5-17 months old) without developmental anomalies (referred to as controls) were obtained after spontaneous or induced abortion or cot death. The diagnosis of trisomy 21 was confirmed by amniocentesis and karyotyping in all cases; trisomy 21 mosaicism led to exclusion of 1 additional case. Gestational age of patients and controls was calculated in relation to the mother's last menstrual cycle and was in accordance with the crown-heel length measurements at autopsy.

Use of tissues for scientific reasons was approved by an institutional review board (Medical Ethical Committee 02.981). The samples were used according to the "Code for Proper Secondary Use of Human Tissue in The Nether-

Fig. 3 Staining results for OCT3/4, PLAP, and c-KIT in female individuals with trisomy 21 (black squares) and controls (triangles). The expression patterns are similar for OCT3/4 (top) and PLAP (middle) in trisomy 21 and in controls: high expression early in the second trimester and a sharp decrease thereafter. The number of positive cells is higher in trisomy 21 than in controls at all ages but the decline is sharper, so that around birth, very few positive cells are found in patients as well as in controls. c-KIT expression (bottom) is highest early in the second trimester and decreases afterward, to remain stable at a certain level around birth and during the first weeks thereafter. The number of c-KIT–positive cells does not differ between patients and controls.

lands," as developed by the Netherlands Federation of Medical Scientific Societies (FMWV) (version 2002).

2.2. Immunohistochemical staining

After fixation in 10% formalin, tissue sections of 5 μm thickness were prepared. The antibodies used for immunohistochemistry and a schematic representation of the different protocols for the various antibodies are represented in Table 1. Slides were incubated with the primary and appropriate secondary antibodies in the indicated dilutions. Between the different incubation steps, slides were washed in a phosphate buffered saline (PBS)-Tween 0.01% solution. Staining was performed using 3,3′-diaminobenzidine-tetrahydrochloride dehydrate (DAB)/H_2O_2 or new fuchsin/naphthol ASMX phosphate. Sections were lightly counterstained with hematoxylin. The following positive controls were included: normal adult male gonadal tissue for VASA, and caspase 3 and a seminoma sample for PLAP, c-KIT, TSPY, and OCT3/4.

2.3. Quantification of results

In male gonads, the expression of a marker was assessed by counting the number of positive germ cells in 10 tubular cross sections. In addition, the number of TSPY-positive gonocytes (defined as immature luminal germ cells) per 50 TSPY-positive germ cells (gonocytes + prespermatogonia, defined as maturing germ cells on the basal membrane) was determined.

In females, all germ cells positive for a given marker were counted in 1 representative visual field (original magnification ×200) including comparable surface areas of cortical and medullary tissue of the ovaries. Caspase 3 activity was evaluated separately in oogonia (defined as germ cells not yet engaged in follicle formation) and oocytes (germ cells included in primordial follicles) as follows: caspase 3–positive oogonia were counted in 1 visual field (original magnification ×200) including comparable surface areas of cortical and medullary tissue. Apoptotic oocytes were counted in 1 high-power visual field (original magnification ×400) including only medullary ovarian tissue and expressed as a percentage of the total number of oocytes.

All counts were performed by the same observer (M. C.), who was blinded for GA and origin of the tissue material (patient or control).

Statistical analysis was performed using the SPSS (Chicago, Ill) statistical program (SPSS 11.5 for Windows).

3. Results

3.1. Staining results for OCT3/4, PLAP, and c-KIT in males with trisomy 21 and in male controls

The expression profiles throughout the second and third trimester of pregnancy were similar for the 3 markers in trisomy 21 and in controls: the expression was highest during the first half of the second trimester but decreased sharply thereafter. However, in trisomy 21, the number of positive cells was higher at all GAs and the decrease in the number of positive cells was slower. In controls, around birth, only a few positive cells were encountered, and at 5 months, these markers had virtually disappeared, whereas in trisomy 21, at 5 months, a considerable number of positive cells were still found (Figs. 1 and 2). The prolonged expression of markers in trisomy 21 was more pronounced for OCT3/4 and PLAP as compared with c-KIT. The difference in mean number of positive germ cells per 10 tubule cross sections was statistically significant for the 3 markers (OCT3/4, P = .004; PLAP, P = .003; c-KIT, P = .03).

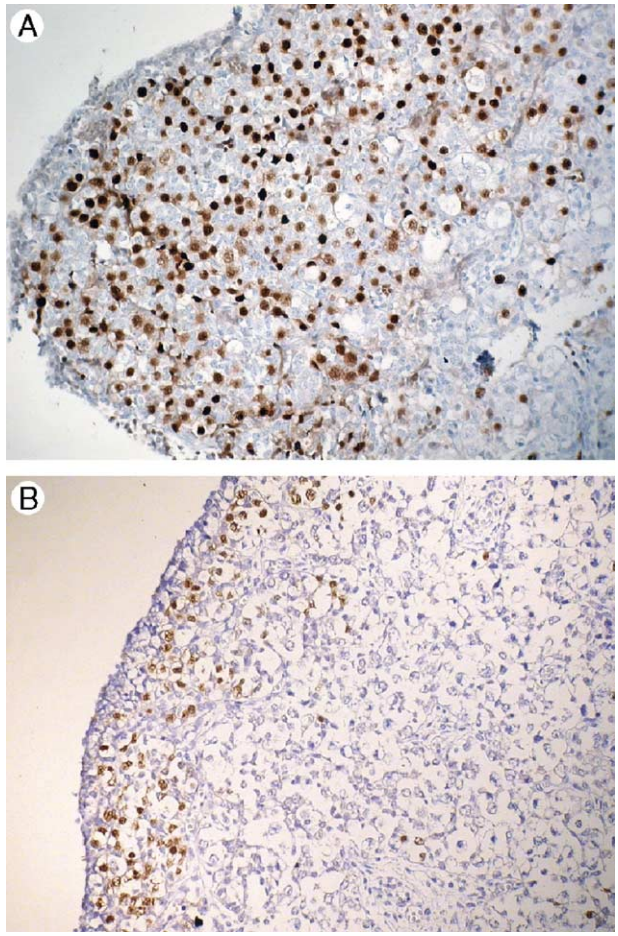

Fig. 4 A, Octamer binding transcription factor 3/4 expression in the ovarian cortex of a female with trisomy 21 (20 weeks GA, original magnification ×200). B, Octamer binding transcription factor 3/4 expression in the ovarian cortex of a control (20 weeks GA, original magnification ×200). Octamer binding transcription factor 3/4 expression in the cortical germ cells of the fetus with trisomy 21 is markedly higher as compared with the age-matched control. Octamer binding transcription factor 3/4–positive cells are only found in the immature oogonia, mainly residing in the cortical region of the ovary (in trisomy 21 and control fetal gonads).

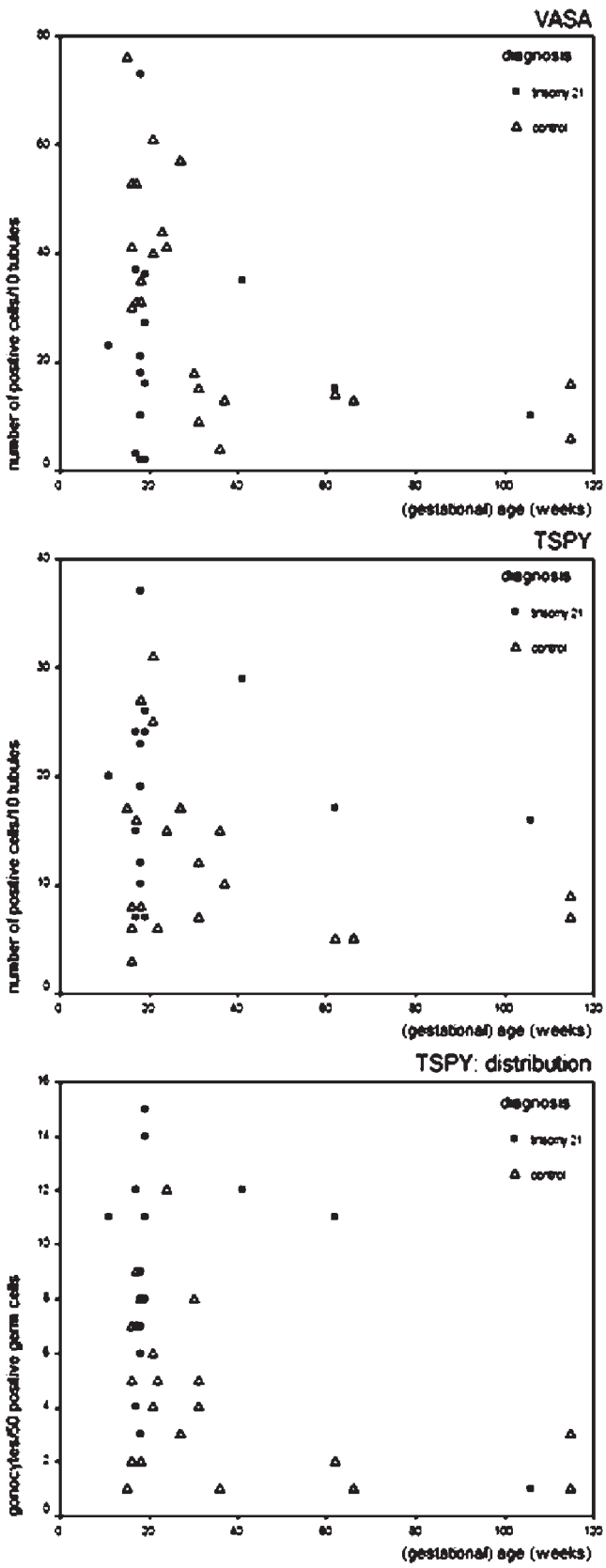

3.2. Staining results for OCT3/4, PLAP, and c-KIT in females with trisomy 21 and in female controls

The expression profiles throughout the second and third trimester of pregnancy were similar in females with trisomy 21 and in controls for OCT3/4 and PLAP. Positive cells were mainly found in the cortical region, where immature oogonia reside, whereas in the medulla, which is rich in maturing oocytes included in primordial follicles, very few positive cells were seen. In both patients and controls, expression of OCT3/4 and PLAP was high early in the second trimester and decreased around 25 weeks GA. Around birth, only a few positive cells were seen. The number of positive cells in trisomy 21 was higher as compared with controls during early pregnancy, but because the decline was sharper in this group than in controls, no maturation delay of germ cells in trisomy 21 was observed anymore around 35 weeks GA (Figs. 3 and 4). The differences in mean number of positive cells per visual field were statistically significant for both OCT3/4 and PLAP (OCT3/4, $P = .005$; PLAP, $P = .003$).

In contrast to OCT3/4 and PLAP, c-KIT was not only expressed in oogonia but also in oocytes. c-KIT expression in females (trisomy 21 cases and controls) was highest early in the second trimester and decreased afterward, but in contrast to the situation in males, it did not disappear but remained stable at a certain level around birth and during the first weeks thereafter (Fig. 3). The number of c-KIT–positive cells did not differ between females with trisomy 21 and controls ($P = .28$).

3.3. Staining results for VASA and TSPY in males with trisomy 21 and in controls

VASA expression in males with trisomy 21 and controls was mostly seen in maturing germ cells on the basal membrane (prespermatogonia), whereas staining in luminal germ cells (the immature gonocytes) was less frequent and showed lower intensity. The expression profiles were similar in trisomy 21 and in controls: VASA was highly expressed around 20 weeks and decreased afterward to reach a stable level around birth and the first months thereafter. The number of positive cells throughout pregnancy was higher in controls, suggesting a higher number of maturing germ

Fig. 5 Staining results for VASA and TSPY in male individuals with trisomy 21 (black squares) and controls (triangles). Top, VASA expression is high around 20 weeks GA, decreases thereafter, and remains at a constant level from birth onward. VASA expression is slightly higher in controls than in males with trisomy 21. Middle, The pattern of TSPY expression is similar to VASA expression but the number of TSPY-positive cells is higher in trisomy 21 than in controls. Bottom, This difference is due to the more frequent positivity for TSPY in gonocytes of patients with trisomy 21 as compared with the control group where TSPY expression is predominantly seen in prespermatogonia.

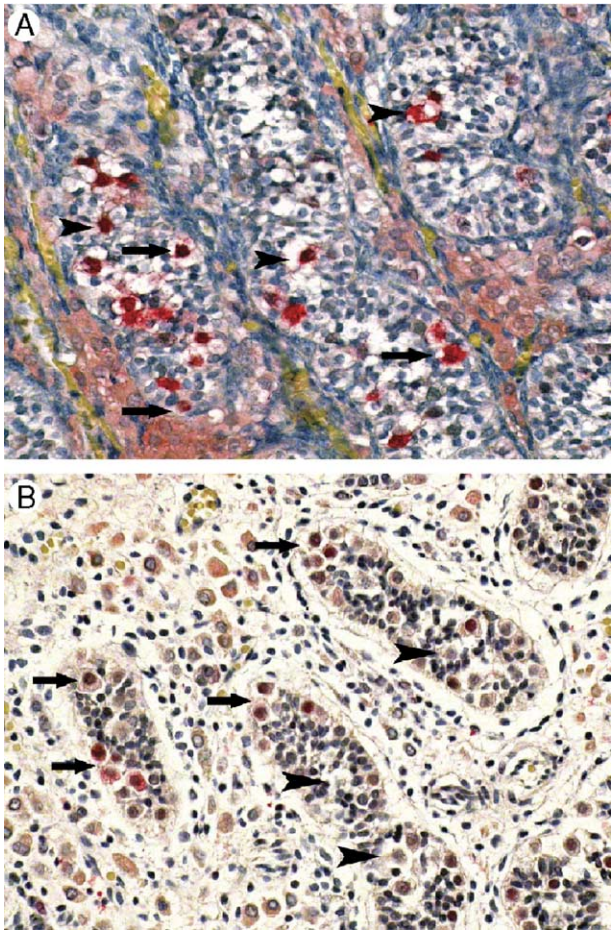

Fig. 6 A, Testis-specific protein, Y-encoded, expression in a male with trisomy 21 (19 weeks GA, original magnification ×400). Testis-specific protein, Y-encoded, expression is frequently seen both in prespermatogonia on the basal membrane (arrows) and in the centrally located gonocytes (arrowheads). The intensity of the TSPY staining is very strong as compared with controls. B, TSPY expression in a male control (18 weeks GA, original magnification ×400). Testis-specific protein, Y-encoded, is mainly seen in prespermatogonia on the basal membrane (arrows); gonocytes are often found to be TSPY-negative (arrowheads).

cells in this group compared with the population with trisomy 21 (Fig. 5). However, this difference did not reach statistical significance (P = .07).

The expression pattern of TSPY throughout pregnancy was similar to the expression pattern of VASA. However, in spite of the lower total germ cell number in trisomy 21, as evaluated by the VASA staining, more TSPY-positive cells were found in this group than in controls (Fig. 5). This difference was statistically significant (P = .02). In the control group, TSPY expression was mainly confined to prespermatogonia, confirming results from our previous study [10]. Yet, in individuals with trisomy 21, TSPY was frequently seen in gonocytes as well as in prespermatogonia. The number of TSPY-positive gonocytes per 50 TSPY-positive germ cells was calculated for males with trisomy 21 and controls (Fig. 5). The difference between the 2 groups was statistically significant (P = .002). Moreover, the staining intensity appeared to be stronger in trisomy 21 than in controls (Fig. 6).

3.4. Staining results for VASA in females with trisomy 21 and controls

The expression profile of VASA throughout pregnancy in females with trisomy 21 and controls was comparable with the profile in males (high expression early in the second trimester and decreasing thereafter to reach a stable level around birth) (Fig. 7). No difference in VASA staining was seen between cortical and medullary regions of the ovary. In contrast to the males, the total number of VASA-positive cells did not differ between females with trisomy 21 and controls (P = .77).

3.5. Staining results for caspase 3 in male and female individuals with trisomy 21 and controls

In males, apoptotic activity, as indicated by a positive staining for caspase 3, was mainly seen in gonocytes and peaked around 20 weeks GA. Around birth, hardly any apoptotic germ cells can be detected (Fig. 8). No difference was found between males with trisomy 21 and controls (P = .17). In females, some apoptotic oogonia were observed before 20 weeks GA. The rate of apoptosis in oogonia remained constant throughout pregnancy, without difference between females with trisomy 21 and controls (P = .40). Apoptotic follicles appeared around 20 weeks

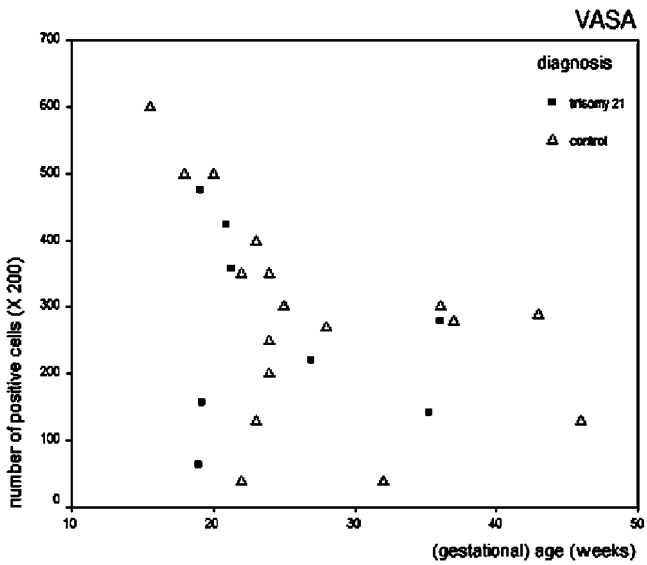

Fig. 7 Staining results for VASA in female individuals with trisomy 21 (black squares) and controls (triangles). VASA expression is high in early pregnancy and starts to decline from the 20th week onward, to remain at a stable level around birth. There is no difference in the number of VASA-positive cells between females with trisomy 21 and controls.

GA; their number showed a slight increase toward the end of pregnancy (Fig. 8). Again, no difference can be detected between females with trisomy 21 and controls (P = .55).

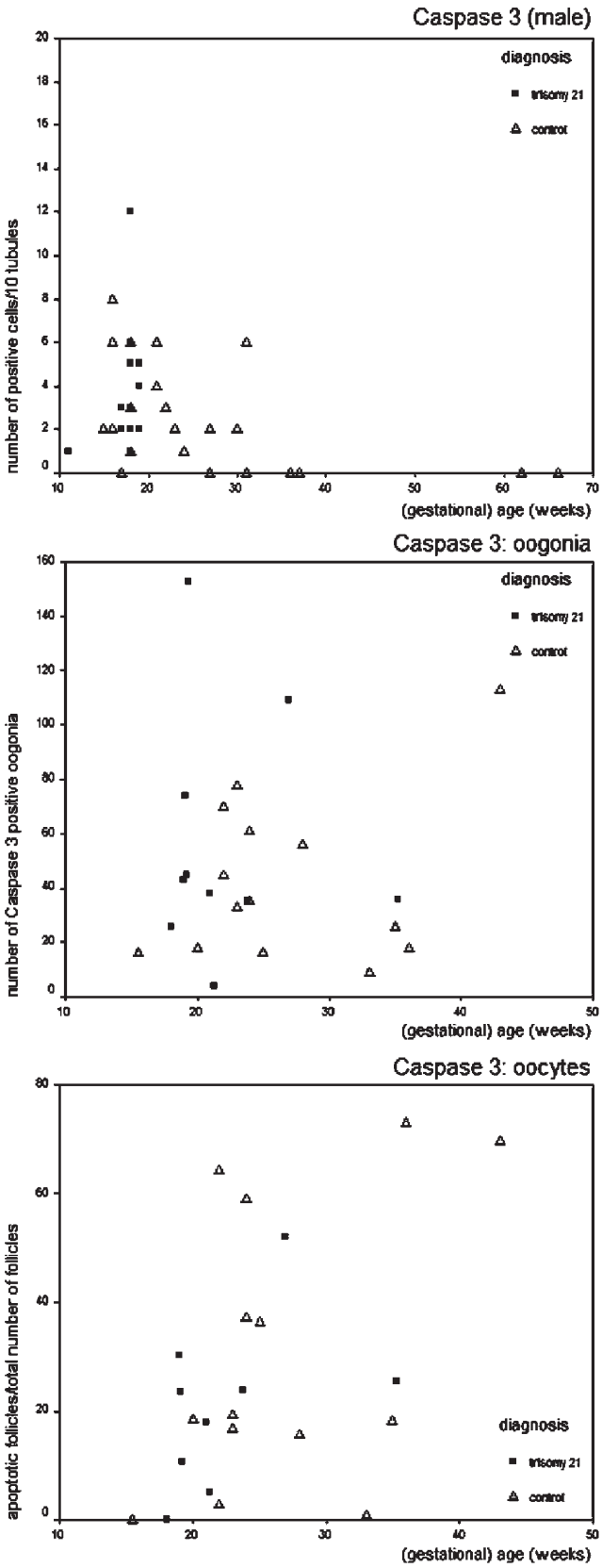

4. Discussion

Boys with trisomy 21 (Down syndrome) have an increased risk for developing a TGCT [1-3]. The earliest steps of tumor formation are believed to occur in fetal life. The current hypothesis is that disturbed migration and maturation of germ cells can result in testicular dysgenesis and finally leads to an increased risk for CIS and invasive neoplasia [8,19]. Prolonged expression of immunohistochemical markers such as OCT3/4, PLAP, and c-KIT in various intersex conditions has been interpreted as a result of maturation delay of germ cells and has been linked to the high incidence of germ cell neoplasia seen in these patients [9,20,21]. To investigate whether germ cell development in trisomy 21 is characterized by maturation delay, we examined the expression profiles of an established set of immunohistochemical markers (see Table 2 for an overview of expression profiles and references) during fetal life and early childhood in individuals with trisomy 21 and compared them with age-matched controls.

The expression profiles of OCT3/4, c-KIT, PLAP, TSPY, and VASA during fetal life have recently been described in detail by our group [10,11]. The same series of fetal gonads served as controls for the present study. In male fetuses with trisomy 21, OCT3/4, PLAP, and c-KIT are expressed longer and at higher levels throughout pregnancy than in controls. For OCT3/4 and PLAP, this differential expression extends well beyond birth. In female fetuses with trisomy 21, OCT3/4 and PLAP are also expressed at a higher level during the first half of the second trimester, but thereafter, their expression decreases more sharply than in controls, so that no differences between female fetuses with trisomy 21 and controls are seen around 35 weeks GA. c-KIT expression did not differ between female individuals with trisomy 21 and controls. Based on these results, it is concluded that germ cell development is delayed in males and females with trisomy 21, but that this delay is more pronounced in the male group.

Fig. 8 Staining results for caspase 3 in male and female individuals with trisomy 21 (black squares) and controls (triangles). Top, In males, apoptotic activity is highest in early pregnancy but decreases afterward and is almost undetectable around birth. There is no difference in apoptotic activity between males with trisomy 21 and controls. Middle, Apoptosis is frequently observed in oogonia throughout pregnancy. There is no difference in the number of apoptotic oogonia in females with trisomy 21 and controls. Bottom, Apoptotic oocytes appear at 20 weeks GA, and their number increases toward the end of pregnancy. There is no difference in the number of apoptotic oocytes in females with trisomy 21 and controls.

Table 2 Immunohistochemical markers used for the diagnosis of CIS and invasive germ cell tumors

	CIS	Seminoma	Nonseminoma	Reference
VASA	+	+	–	[16]
TSPY	++	Variable	–	[15,22]
OCT3/4	++	+	EC	[14]
c-KIT	++	Variable	–	[12,23]
PLAP	++	++	EC	[13]

Abbreviation: EC, embryonal carcinoma.

According to the results for VASA, no difference in germ cell numbers between female patients and controls was observed. However, in males with trisomy 21, lower numbers of VASA-positive cells as compared with controls point at a disturbed development of maturing germ cells.

Testis-specific protein, Y-encoded, is expressed at a higher level, and the staining intensity is more pronounced in the germ cells of the males with trisomy 21 than in controls. Interestingly, in trisomy 21, TSPY expression is not only seen in prespermatogonia but is aberrantly expressed at a high frequency in gonocytes. In controls, TSPY expression is mainly confined to prespermatogonia; TSPY-positive gonocytes are only rarely encountered in this group. A summary of the expression profiles throughout pregnancy for the different markers in trisomy 21 and controls is presented in Fig. 9.

Prolonged expression of OCT3/4 and aberrant expression of TSPY as it is found in PGC/gonocytes of males with trisomy 21 may be related to tumorigenesis in these cells. Octamer binding transcription factor 3/4 is normally expressed in embryonic stem cells, regulating pluripotency and differentiation of these cells [24]. However, OCT3/4 expression in PGC is related to the survival of these cells, preventing them from premature apoptosis [25]. Moreover, OCT3/4 is consistently expressed in various germ cell tumors, including CIS and gonadoblastoma [14,21,24,26]. In an in vitro model investigating mouse embryonic stem cell–derived tumors, modulating the level of OCT3/4 expression changed the malignant phenotype of the tumor cells, thereby suggesting a pathogenetic relevance of OCT3/4 expression in these tumors [27].

The TSPY gene maps to the short arm of the Y chromosome, close to the centromeric region (the so-called GBY region or gonadoblastoma-susceptible region on the Y chromosome), where it is highly repeated [28]. Although the function of TSPY is not fully clarified, it is thought to be involved in premeiotic proliferation of male germ cells [15]. Aberrant (increased) expression of TSPY in patients with undervirilization syndromes and gonadal dysgenesis has been repeatedly related to the development of CIS and gonadoblastoma in these patients [9,15,22,26].

Increased apoptosis of germ cells has been described in sex chromosome aneuploid fetal human gonads [29]. Apparently, aneuploidy of autosomes does not provoke a similar apoptotic wave during fetal life because, in our study, no difference in apoptotic activity between patients and controls was observed. Yet, the mechanisms by which germ cell numbers in fetal human ovaries are regulated remain to be elucidated [30].

Taken together, our results suggest that trisomy 21 leads to delayed and possibly disturbed maturation of fetal germ cells. An effect of trisomy 21 on maturation of germ cells has been reported previously [8]. With this analysis, we present a detailed and differential expression profile in male and female individuals with trisomy 21 throughout preg-

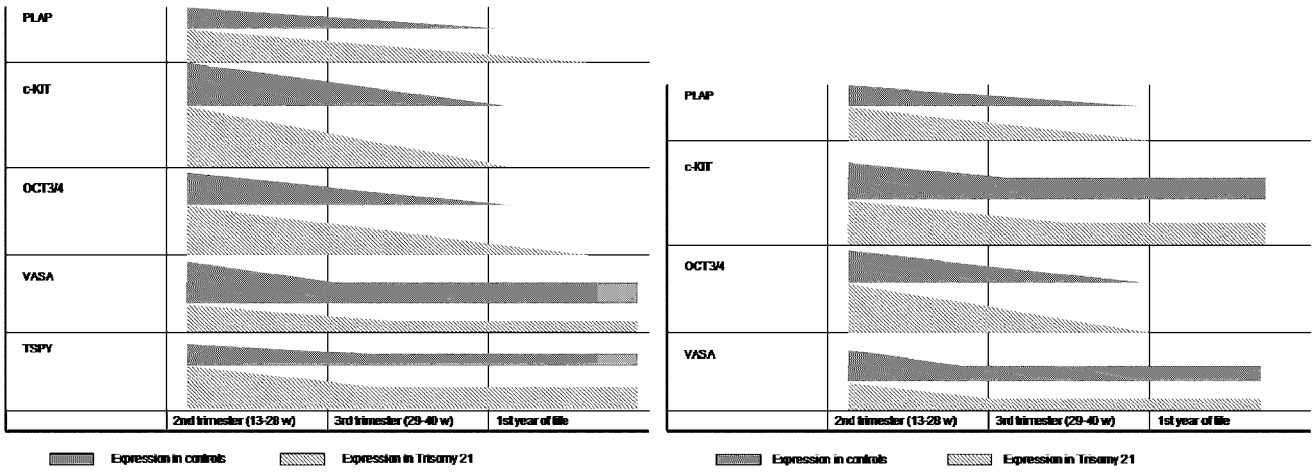

Fig. 9 Summary of the expression profiles for the different markers in male (left) and female (right) trisomy 21 gonads (light gray) and controls (dark gray). The PGC markers OCT3/4, PLAP, and c-KIT are expressed at a higher level throughout pregnancy, and the expression of OCT3/4 and PLAP is prolonged in trisomy 21 as compared with controls, pointing at a delay in the maturation of germ cells in trisomy 21. The delay is more pronounced in males than in females with trisomy 21. In males, VASA is expressed at a higher level in the control group, indicating that, in this group, more maturing germ cells can be found as compared with males with trisomy 21. Aberrant TSPY expression is observed in gonocytes of patients with trisomy 21, resulting in a higher total number of TSPY-positive cells in this group as compared with controls.

nancy for the first time. According to our results, the maturation delay of germ cells is more pronounced in males than in females. An increased incidence in TGCTs is only seen in males with Down syndrome. We hypothesize that the prolonged expression of OCT3/4, as is predominantly observed in male individuals with trisomy 21, in combination with an increased TSPY expression, could provide these PGC/gonocytes with an important advantage to survive and proliferate. Eventually, this might, after additional, still unknown pathogenetic hits, lead to clonal expansion of these cells and the development of CIS in the minority of cases. In contrast, earlier down-regulation of OCT3/4, possibly due to entry into meiosis, and the absence of TSPY expression might prevent female individuals with trisomy 21 from malignant transformation.

Moreover, trisomy 21 is characterized by male infertility, whereas female reproductive capacity seems to be preserved [31]. Whether the more pronounced maturation delay in males eventually accounts for the observed difference in gonadal function remains to be elucidated.

Finally, according to our data, identification of male germ cells with aberrant expression of markers such as PLAP or OCT3/4 in individuals with trisomy 21 during embryonic development or in the early postnatal period points at delayed germ cell development rather than plain CIS. Clearly, other pathogenetic hits must be involved because although an increased risk exists, only a minority of male individuals with trisomy 21 will eventually progress to CIS and the development of invasive germ cell tumors.

5. Conclusion

By comparing the expression of several immunohistochemical markers in normal fetal gonads with the presence of these markers in gonads of fetuses with trisomy 21, we were able to demonstrate that germ cell maturation is seriously delayed in the latter group. In contrast to conditions affecting the sex chromosomes, trisomy 21 does not lead to an increase in apoptosis during fetal germ cell maturation. For reasons that still need to be elucidated, the observed maturation delay is more pronounced in male than in female individuals with trisomy 21. The observed delay in maturation could result in a prolonged retention of germ cells in a phase vulnerable to further hits, thereby increasing the risk for the development of CIS.

References

[1] Satge D, Sommelet D, Geneix A, Nishi M, Malet P, Vekemans M. A tumor profile in Down syndrome. Am J Med Genet 1998;78:207-16.
[2] Dexeus FH, Logothetis CJ, Chong C, Sella A, Ogden S. Genetic abnormalities in men with germ cell tumors. J Urol 1988;140:80-4.
[3] Mann JR, Pearson D, Barrett A, Raafat F, Barnes JM, Wallendszus KR. Results of the United Kingdom Children's Cancer Study Group's malignant germ cell tumor studies. Cancer 1989;1963:1657-67.
[4] Satge D, Sasco AJ, Cure H, Leduc B, Sommelet D, Vekemans MJ. An excess of testicular germ cell tumors in Down's syndrome: three case reports and a review of the literature. Cancer 1997;80:929-35.
[5] Jacobsen GK, Henriques UV. A fetal testis with intratubular germ cell neoplasia (ITGCN). Mod Pathol 1992;5:547-9.
[6] Dieckmann KP, Rube C, Henke RP. Association of Down's syndrome and testicular cancer. J Urol 1997;157:1701-4.
[7] Smucker JD, Roth LM, Sutton GP, Hurteau JA. Trisomy 21 associated with ovarian dysgerminoma. Gynecol Oncol 1999;74:512-4.
[8] Rajpert-De Meyts E, Jorgensen N, Brondum-Nielsen K, Muller J, Skakkebaek NE. Developmental arrest of germ cells in the pathogenesis of germ cell neoplasia. APMIS 1998;106:198-204 [discussion 204-6].
[9] Cools M, van Aerde K, Kersemaekers AMF, et al. Morphological and immunohistochemical differences between gonadal maturation delay and early germ cell neoplasia in patients with undervirilisation syndromes. J Clin Endocrinol Metab 2005 [prepublished online] www.endojournals.org.
[10] Honecker F, Stoop H, de Krijger RR, Chris Lau YF, Bokemeyer C, Looijenga LH. Pathobiological implications of the expression of markers of testicular carcinoma in situ by fetal germ cells. J Pathol 2004;203:849-57.
[11] Stoop H, Honecker F, Cools M, de Krijger RR, Bokemeyer C, Looijenga LHJ. Differentiation and development of human female germ cells during prenatal gonadogenesis: an immunohistochemical study. Hum Reprod 2005;20:1466-76.
[12] Rajpert-De Meyts E, Skakkebaek NK. Expression of the c-kit protein product in carcinoma-in-situ and invasive testicular germ cell tumours. Int J Androl 1994;17:85-92.
[13] Hustin J, Collette J, Franchimont P. Immunohistochemical demonstration of placental alkaline phosphatase in various states of testicular development and in germ cell tumours. Int J Androl 1987;10:29-35.
[14] Looijenga LH, Stoop H, de Leeuw HP, et al. POU5F1 (OCT3/4) identifies cells with pluripotent potential in human germ cell tumors. Cancer Res 2003;63:2244-50.
[15] Schnieders F, Dork T, Arnemann J, Vogel T, Werner M, Schmidtke J. Testis-specific protein, Y-encoded (TSPY) expression in testicular tissues. Hum Mol Genet 1996;5:1801-7.
[16] Castrillon DH, Quade BJ, Wang TY, Quigley C, Crum CP. The human VASA gene is specifically expressed in the germ cell lineage. Proc Natl Acad Sci U S A 2000;97:9585-90.
[17] Duan WR, Garner DS, Williams SD, Funckes-Shippy CL, Spath IS, Blomme EA. Comparison of immunohistochemistry for activated caspase-3 and cleaved cytokeratin 18 with TUNEL method for quantification of apoptosis in histological sections of PC-3 subcutaneous xenografts. J Pathol 2003;199:221-8.
[18] Shi SR, Key ME, Kalra KL. Antigen retrieval in formalin-fixed, paraffin-embedded tissues: an enhancement method for immunohistochemical staining bases on microwave oven heating of tissue sections. J Histochem Cytochem 1991;39:741-8.
[19] Looijenga LH, Oosterhuis JW. Pathobiology of germ cell tumors: views and news. Anal Quant Cytol Histol 2002;24:263-79.
[20] Rajpert-De Meyts ER, Jorgensen N, Muller J, Skakkebaek NK. Prolonged expression of the c-kit receptor in germ cells of intersex fetal testes. J Pathol 1996;178:166-9.
[21] Rajpert-De Meyts E, Hanstein R, Jorgensen N, Graem N, Vogt PH, Skakkebaek NK. Developmental expression of POU5F1 (OCT3/4) in normal and dysgenetic human gonads. Hum Reprod 2004;19:1338-44.
[22] Lau Y, Chou P, Iezzoni J, Alonzo J, Komuves L. Expression of a candidate gene for the gonadoblastoma locus in gonadoblastoma and testicular seminoma. Cytogenet Cell Genet 2000;91:160-4.
[23] Strohmeyer T, Reese D, Press M, Ackermann R, Hartmann M, Slamon D. Expression of the c-kit proto-oncogene and its ligand stem cell factor (SCF) in normal and malignant human testicular tissue. J Urol 1995;153:511-5.

[24] Sperger JM, Chen X, Draper JS, et al. Gene expression patterns in human embryonic stem cells and human pluripotent germ cell tumors. Proc Natl Acad Sci U S A 2003;100:13350-5.

[25] Kehler J, Tolkunova E, Koschorz B, et al. Oct4 is required for primordial germ cell survival. EMBO Rep 2004;5:1078-83.

[26] Kersemaekers AMF, Honecker F, Stoop H, et al. Identification of germ cells at risk for neoplastic transformation in gonadoblastoma: an immunohistochemical study for OCT3/4 and TSPY. HUM PATHOL 2005;36:512-21.

[27] Gidekel S, Pizov G, Bergman Y, Pikarsky E. Oct-3/4 is a dose-dependent oncogenic fate determinant. Cancer Cell 2003;4:361-70.

[28] Vogel T, Schmidtke J. Structure and function of TSPY, the Y-chromosome gene coding for the "testis-specific protein". Cytogenet Cell Genet 1998;80:209-13.

[29] Modi DN, Sane S, Bhartiya D. Accelerated germ cell apoptosis in sex chromosome aneuploid fetal human gonads. Mol Hum Reprod 2003; 9:219-25.

[30] Abir R, Orvieto R, Dicker D, Zukerman Z, Barnett M, Fisch B. Preliminary studies on apoptosis in human fetal ovaries. Fertil Steril 2002;78:259-64.

[31] Johannisson R, Gropp A, Winking H, Coerdt W, Rehder H, Schwinger E. Down's syndrome in the male. Reproductive pathology and meiotic studies. Hum Genet 1983;63:132-8.

Journal of Pathology
J Pathol 2006; **208**: 395–400
Published online 4 November 2005 in Wiley InterScience (www.interscience.wiley.com). **DOI:** 10.1002/path.1872

Original Paper

Germ cell lineage differentiation in non-seminomatous germ cell tumours

Friedemann Honecker,[1,2] Hans Stoop,[1] Frank Mayer,[3] Carsten Bokemeyer,[2] Diego H Castrillon,[4] Yun-Fai Chris Lau,[5] Leendert H J Looijenga[1] and J Wolter Oosterhuis[1]*

[1]*Department of Pathology, Erasmus MC-University Medical Center Rotterdam, Daniel den Hoed Cancer Center, Josephine Nefkens Institute, Rotterdam, The Netherlands*
[2]*Department of Hematology/Oncology, University of Hamburg, Hamburg, Germany*
[3]*Department of Hematology/Oncology, University of Tübingen, Tübingen, Germany*
[4]*Department of Pathology, University of Texas Southwestern Medical Center, Dallas, TX, USA*
[5]*Division of Cell and Developmental Genetics, Department of Medicine, VA Medical Center, University of California, San Francisco, CA, USA*

**Correspondence to:*
J Wolter Oosterhuis, Department of Pathology, Erasmus MC-University Medical Center Rotterdam, Josephine Nefkens Institute, Room 430b, PO Box 1738, 3000 DR Rotterdam, The Netherlands.
E-mail:
j.w.oosterhuis@erasmusmc.nl

Received: 30 October 2004
Revised: 1 August 2005
Accepted: 23 August 2005

Abstract

Human germ cell tumours (GCTs) have long fascinated investigators for a number of reasons. Being pluripotential tumours, they can differentiate into both extra-embryonic and embryonic (somatic) tissues. However, it has never been shown convincingly that, in humans, these tumours are truly totipotent and can also give rise to the germ lineage, the third major differentiation lineage occurring early during embryonic life. Using a number of newly available, distinct, immunohistochemical markers, such as OCT3/4, VASA and TSPY, the occurrence of germ cells was investigated in a number of germ cell tumours. Development of germ cells was identified in three independent non-seminomas, including two pure yolk sac tumours and one mixed tumour composed of yolk sac tumour and immature teratoma. Our finding indicates a previously unknown totipotent potential of human GCTs and raises the question of whether, under certain culture conditions, primordial germ cells could be derived from human GCT cell lines.

Keywords: germ cell tumours; germ cell lineage; differentiation; totipotency; primordial germ cells

Introduction

Germ cell tumours of adolescents and adults (GCTs) are at the cross-roads of tumour and developmental biology. They are pluripotent tumours with multiple possible fates. Two subgroups can be distinguished, seminomatous and non-seminomatous GCTs (for review, see [1]), and Figure 1 shows their developmental potential schematically. Seminomas resemble early germ cells (primordial germ cells/gonocytes). They show limited capacity to differentiate into somatic or extra-embryonic tissues, although they can switch to a non-seminomatous phenotype [2]. Non-seminomas mimic early embryonic development. Embryonal carcinoma (EC) cells, the stem cells of non-seminomas, are highly similar to embryonic stem (ES) cells [3] and can give rise to embryonic endo-, meso- and ectoderm and/or differentiate into extra-embryonal yolk sac and trophoblast. As they have never been shown to give rise to the germ line in humans, they seem to fall one step short of totipotency.

Recent studies show that germ cells can be derived from mouse and human ES cells [4–6]. So far, it has been impossible to identify the development of germ cells in human GCTs. Recently, antibodies against several markers present in early germ cells of both sexes (OCT3/4, a marker for pluripotency, which is also expressed in ES cells, and VASA, a germ line-specific protein) or exclusively in male germ cells (TSPY, the testis-specific protein, Y-encoded), have been described [7–9]. Our search for germ cell development in non-seminomas was significantly supported by recent studies on the presence of these proteins during normal testicular development [10].

Materials and methods

Research on human tumour samples has been performed according to the *Code for Proper Secondary Use of Human Tissue in The Netherlands*, as developed by the Dutch Federation of Medical Scientific Societies (FMWV) (version 2002), and has been approved by an institutional review board (MEC 02.981).

Formalin-fixed, paraffin-embedded tissue blocks from germ cell tumours that had been collected between 1991 and 2003, in close collaboration with

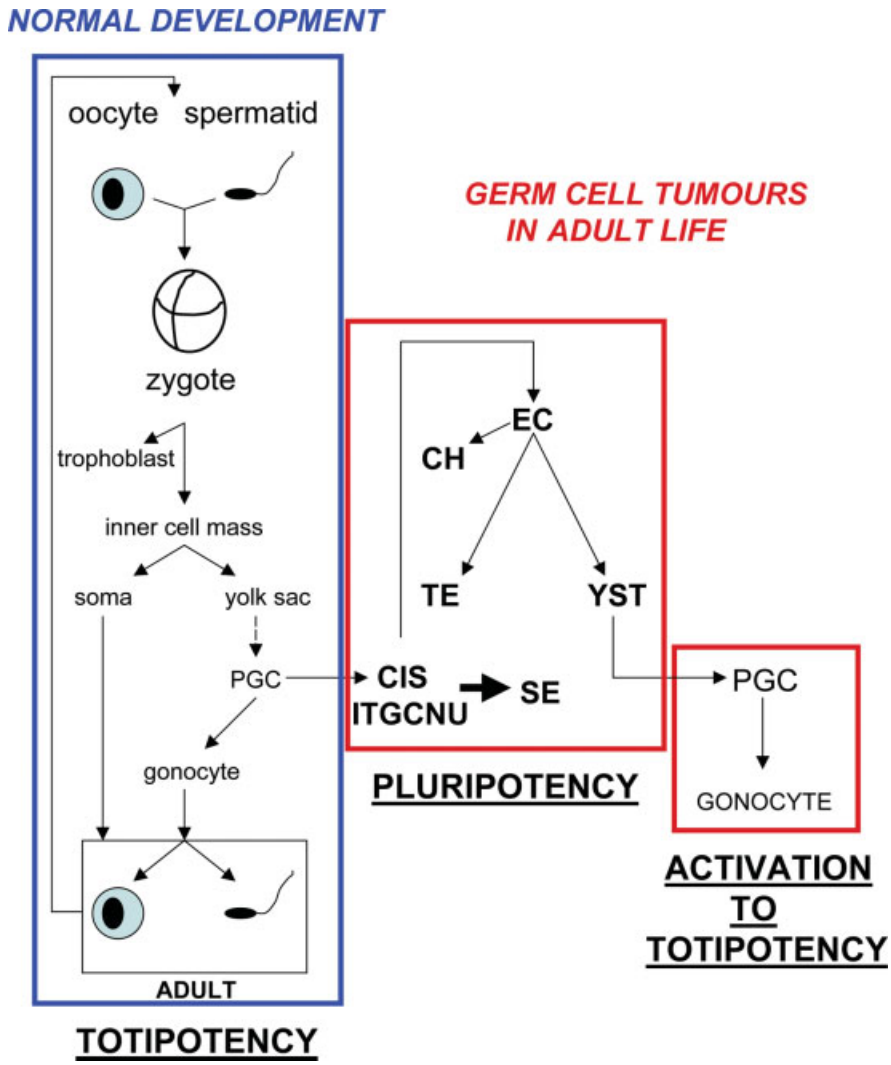

Figure 1. Developmental potential of normal and malignant germ cells. Normal development after fertilization is depicted in the boxed area on the left. Both embryonic (soma) and extra-embryonic tissues (trophoblast and yolk sac) develop from the zygote. Cells from the proximal region of the epiblast contribute to the primordial germ cell (PGC) pool, the allantois and the extra-embryonic mesoderm. The fate of epiblast cells becoming PGCs is not predetermined, but is specified by response to localized signals. After puberty, the derivatives of PGCs, known as spermatogonia, will eventually give rise to mature germ cells that can be fertilized and restart the life cycle (oocyte in females and spermatid in males). Due to as-yet unknown pathogenetic hits during intrauterine life, developmentally arrested germ cells can give rise to germ cell tumours. In the post-pubertal testis, this is thought always to involve an intermediate stage, termed carcinoma *in situ*/intratubular germ cell neoplasia unclassified (CIS/ITGCNU). Seminomas resemble early germ cells and CIS/ITGCNU, whereas embryonal carcinoma (EC) cells that originate after reprogramming of CIS/ITGCNU are highly similar to embryonic stem cells from the inner cell mass and can mimic early intrauterine development after fertilization (see boxed area in the middle). EC can differentiate into choriocarcinoma (CH), teratoma (TE) or yolk sac tumour (YST). Here we describe for the first time that tumour cells from non-seminomas containing yolk sac histology can re-activate totipotency and show properties of immature and more mature germ cells (see boxed area to the right)

urologists and pathologists in the south-western part of The Netherlands, were retrieved from our archive. In addition, tumour samples were obtained from patients treated according to protocols led by the Department of Hematology/Oncology, University of Tübingen. All cases were reviewed and diagnosed by J.W.O., according to the WHO classification.

Histochemical and immunohistochemical staining

For immunohistochemistry, 3 μm sections were incubated with the primary antibody, followed by biotinylated secondary antibodies for 30 min and a biotinylated streptavidin horseradish peroxidase- or alkaline phosphatase-coupled complex. The antibodies and conditions used are indicated in Table 1. All stains were counterstained with haematoxylin.

Double-staining was performed by using a combination of the same detection method but with different substrates: Fast Blue/Naphthol ASMX phosphate (F3378 and N500, Sigma, Steinheim, Germany) for blue staining and 3-amino-9-ethyl-carbazole (A.5754 and D4254, Sigma, Steinheim, Germany)/H_2O_2 for red staining, without counterstaining. Endogenous peroxidase activity and/or endogenous biotin was blocked using 3% H_2O_2 (for 5 min) and/or a blocking kit for

Table 1. Antibodies (source) and detection method used for immunohistochemistry

Antibody	Company	Clone, code	Pretreatment	Dilutions, incubation time and temperature	Secondary antibody (1 : 200) (biotinylated)	Visualization
PLAP	Cell Marque	CMC203	HIAR*	1 : 200, overnight (o.n.), 4 °C	Rabbit anti-mouse (Dako E0413)	ABCplx-ap[1]
c-KIT	DakoCytomation	A4502	HIAR	1 : 500, o.n., 4 °C	Swine anti-rabbit (Dako E0413)	ABCplx-ap
OCT3/4	Santa Cruz	sc-8629	HIAR	1 : 1000, 120 min, room temperature (RT)	Horse anti-goat (Vector BA9500)	ABCplx-hrp[2]
VASA	Provided by D. Castrillon		HIAR	1 : 2000, overnight (o.n.), 4 °C	Swine anti-rabbit	ABCplx-ap
TSPY	Provided by Y. Lau		None	1 : 3000, o.n., 4 °C	Swine anti-rabbit	ABCplx-ap
BMP4	Novocastra	3H2	None	1 : 100, o.n., 4 °C	Rabbit anti-mouse	ABCplx-ap
SCF	Santa Cruz Biotechnology	sc-1302	HIAR	1 : 400 o.n., 4 °C	Horse anti-goat	ABCplx-ap
CD30	DakoCytomation	Ber-H2	HIAR	1 : 100 o.n., 4 °C	Rabbit anti-mouse	ABCplx-hrp[2]
CD34	Neomarkers	QBEnd/10, MS-363-S	None	1 : 20, 30 min, RT	Rabbit anti-mouse	ABCplx-hrp[2]
CD61	Immunotech	SZ 21, 2116	HIAR	1 : 100, 30 min, RT	Rabbit anti-mouse	ABCplx-hrp[2]
Glycophorin C	DakoCytomation	M0820	HIAR	1 : 100, 120 min. RT	Rabbit anti-mouse	ABCplx-hrp[2]
Lysozyme	DakoCytomation	A0099	Pronase, 10 min	1 : 900, 30 min, RT	Swine anti-rabbit	ABCplx-hrp[2]
Myeloperoxidase	DakoCytomation	A0398	HIAR	1 : 5000, 30 min, RT	Swine anti-rabbit	ABCplx-hrp[2]

* Heat-induced antigen retrieval.
[1] ABCplx-ap, streptavidin–biotin–alkaline phosphatase complex.
[2] ABC-hrp, streptavidin–biotin–horseradish peroxidase complex.

endogenous biotin (Vector Laboratories, Burlingame, CA, USA) to prevent background staining.

Results

Detection of cells with germ cell characteristics in non-seminomas

Markers for immature germ cells and other factors involved in fetal germ cell differentiation, e.g. germ cell/placental-like alkaline phosphatases (PLAP), stem cell factor receptor (c-KIT) and glycogen, were studied in a series of 34 GCTs of pure non-seminomatous histology (YSTs, TEs and ECs): in other words, none of these tumours contained a seminomatous component, as judged by morphology and immunohistochemistry. In three cases, originating from the testis, the mediastinum and the pituitary gland, respectively, early germ cells were identified by morphology and marker expression (see Figure 2). In two cases, germ cells were found loosely distributed in clusters throughout the yolk sac component of the tumours (Figure 2A–E), whereas in the third case they were localized in tube-like structures (this tumour contained both yolk sac and immature teratoma components). The germ cells showed consistent staining for OCT3/4 (Figure 2C), PLAP (Figure 2D), c-KIT, TSPY (Figure 2E) and glycogen. CD30 was absent (Figure 2B insert), ruling out that these cells are EC cells rather than embryonic germ cells [11]. The presence of VASA (Figure 2F and lower insert), specific for late migratory and postmigratory germ cells [8], indicates that a number of these cells have progressed beyond the earliest stage of germ line commitment. While the majority of cells were positive for either OCT3/4 or VASA (Figure 2F), double staining revealed co-expression of both markers in only a minority of cells (lower insert), which was also the case for OCT3/4 and TSPY (Figure 2F, upper insert). The observation that the cells of interest are negative for OCT3/4 demonstrate that they are not seminoma cells.

Detection of cells with characteristics of early haematopoietic cells

Staining for c-KIT, CD34, lysozyme, myeloperoxidase, Glycophorin C and CD61 showed the presence of cells with characteristics of early haematopoiesis. In two cases, nests of cells resembling angiogenetic clusters (so-called haemangioblasts) could be identified by the presence of c-KIT, CD34 (Figure 2G insert), a marker for pluripotent haematopoietic stem cells, and glycophorin C, a marker for red cells and their precursors (Figure 2H insert). A number of other factors for haematopoietic differentiation (ie lysozyme, myeloperoxidase and CD61) were occasionally present. However, the cells lacked the morphological characteristics of haematopoietic differentiation, such as blast formation (data not shown).

All three cases showed the presence of bone morphogenetic protein 4 (BMP4) in the YST component (Figure 2G), mainly in areas showing hepatoid histology. BMP4 was not restricted to the areas containing germ cells. Moreover, BMP4 was also observed in non-seminomas (ie yolk sac tumours) without the presence of germ cell lineage differentiation (data not shown). Therefore it cannot be considered as a specific marker. Stem cell factor (SCF), the ligand for c-KIT, was found in the yolk sac component, most

often in close association with the developing germ cells (Figure 2H).

Discussion

An extensive immunohistochemical analysis was performed to study the developmental potential and cell fate commitment of non-seminomas. We describe the novel finding of germ cell development in non-seminomas. In three cases, small groups of cells showing characteristics of fetal germ cell differentiation, ie loss of OCT3/4 and increased staining for VASA and TSPY, were found. The same pattern of *OCT3/4* and *VASA* expression was recently described upon spontaneous differentiation of germ cells from human ES cells *in vitro* [6] and during normal germ cell development in humans [10]. Our findings indicate that germ cells can develop in non-seminomas, in particular YSTs showing expression of supporting factors, such as BMP4 and SCF. It is unknown whether the YST is the direct precursor of the germ cells or whether both lines co-develop from one common ancestor. This seems a rather semantic question; however, as all non-seminomas originate from a common stem cell, ie the EC cell (for review, see [1]; see also Figure 1).

Mammalian germ cells originate from the proximal region of the epiblast. In mouse experiments, ES cells can be stimulated to differentiate into germ cells and extra-embryonic mesoderm when grafted to the proximal epiblast [12]. This indicates that the potential to become a germ cell may not be restricted to predetermined progenitor cells but can be induced by extracellular factors [13]. The nature of these factors is largely unknown. Recent findings indicate that BMP4 might play a crucial role [4].

In two of the three cases, haematopoietic differentiation was found, underlining the close developmental relationship between germ cells and haematopoietic precursor cells. In fact, it has been hypothesized that primordial germ cells could be haematopoiesis-initiating cells [14], a process in which BMP4 could be an important signal [4,15]. Clinically, the relationship between mediastinal GCTs with yolk sac histology and acute myeloid leukemias is well established [16,17]. The haematopoietic precursor cells in these tumours are likely the origin of the leukaemias [18]. The clonal origin of mediastinal GCTs and haematological malignancies indicate a common malignant stem cell [19].

Failure to demonstrate germ cell development in non-seminomas so far might have been due to a number of reasons. It is probably a rare event (so far found in 3/34 non-seminomas), possibly due to the absence of crucial factors. Alternatively, development of germ cells may be hampered by the fact that these cells are highly susceptible to apoptotic stimuli, leading to early death. Most important, however, could be the fact that so far the markers to identify germ lineage differentiation were lacking. Only the use of a combination of the markers OCT3/4, VASA and TSPY has enabled us to identify germ cell development in non-seminomas. It is highly unlikely that the presence of these markers is due to aberrant expression, because of the consistency in loss of OCT3/4 and increase in VASA, as found during normal germ cell development. In addition, GCTs are known to show expression of various markers in accordance with their physiological pattern, dependent on their specific lineage of differentiation (for review, see [1]).

The fact that non-seminoma cells can differentiate into germ cells is exciting and should be exploited *in vitro* using pluripotent GCT cell lines, under culture conditions that enhance formation of germ cells [4,6,20]. The resulting germ cells could be traced using a specific reporter system [4,5] and studied for their expression profile [6].

Deriving germ cells from human GCTs would be more than a mere technical exercise. Even though the cells of origin show neoplastic properties (eg they are aneuploid), the system would clearly reflect many aspects of normal germ cell development. It could therefore provide a readily accessible tool for the investigation of mechanisms of human germ cell

Figure 2. Representative illustrations of the various immunohistochemical markers identified in the germ cell tumours showing germ cell differentiation. (A) Testicular yolk sac tumour, haematoxylin and eosin staining (magnification ×10; insert ×40). (B) Same case: α-fetoprotein (AFP) staining is seen as a red cytoplasmic signal. Note the stronger staining intensity in more solid yolk sac tumour areas, showing a hepatoid pattern (magnification ×10). Insert is staining for CD30, being negative (magnification ×20). (C) Same case: OCT3/4 (brown nuclear signal)-positive cells are scattered throughout the tumour (magnification ×10; insert ×40). (D) Same case: single cells show a red positive cytoplasmatic staining reaction for placental alkaline phosphatase (PLAP) (magnification ×10; insert ×40). (E) Same case: single cells show a red positive nuclear and cytoplasmic staining reaction for testis-specific protein on the Y chromosome (TSPY). Note also the weaker staining intensity in more solid yolk sac tumour areas, showing a hepatoid pattern (magnification ×10; insert 40×). (F) Same case: double staining for OCT3/4 (red nuclear signal) and VASA (blue cytoplasmic signal). Immature germ cells show strong signal intensity for OCT3/4, but are negative for VASA. This germ cell-specific marker is exclusively seen in more mature germ cells. The VASA-positive cells are negative for OCT3/4, and are therefore not seminoma cells (magnification ×40). Upper insert: double-staining for OCT3/4 (red nuclear signal) and TSPY (blue cytoplasmic signal). Note the double positive cells, and the single OCT3/4-positive cells (magnification ×40). Lower insert: double-staining for OCT3/4 (red nuclear signal) and VASA (blue cytoplasmic signal), showing some double positive cells for OCT3/4 and VASA. (G) Mediastinal yolk sac tumour, bone morphogenetic protein 4 (BMP4) staining (red cytoplasmic signal). Note the stronger staining intensity in more solid yolk sac tumour areas (magnification ×10). Insert: same case staining for CD34 (magnification ×20). (H) Testicular yolk sac tumour, same case as shown in A–F. Stem cell factor (SCF) is seen as a red cytoplasmic and membranous signal in the majority of yolk sac tumour cells (magnification ×10). Insert: same case, staining for glycophorin C (magnification ×40)

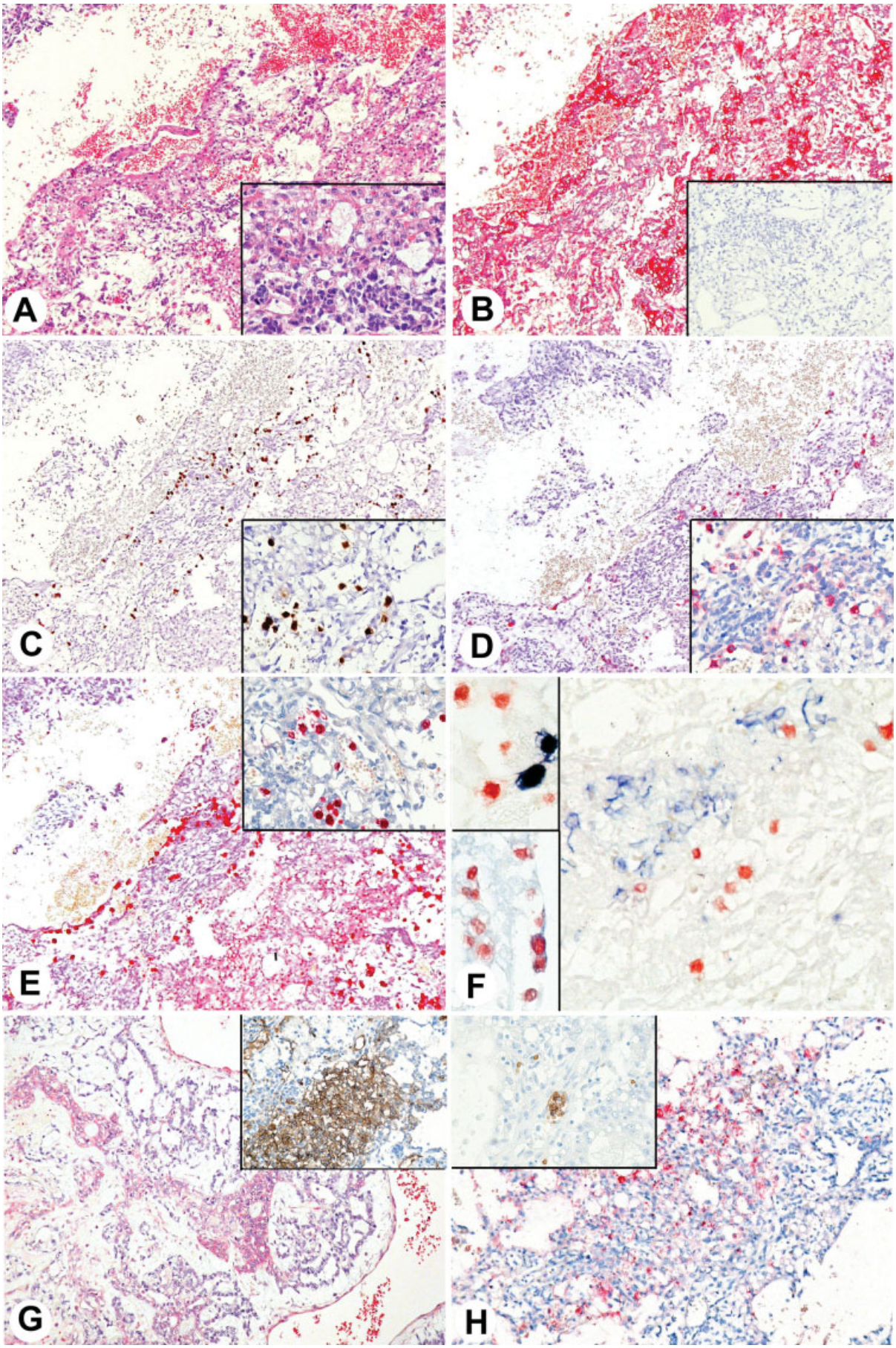
A
B
C
D
E
F
G
H

development, yet avoiding the ethical issues and legal restrictions associated with the use of normal primordial germ cells derived from human embryos or human ES cells.

Acknowledgements

We thank the urologists and pathologists in the south-western part of The Netherlands for their cooperation in collecting the tumour samples. This work was supported by the Dutch Cancer Society (H.S., J.W.O., L.H.J.L.) and the Deutsche Krebshilfe, Dr Mildred Scheel Stiftung (F.H.)

References

1. Oosterhuis JW, Looijenga LHJ. Testicular germ cell tumors in a broader perspective. *Nat Rev Cancer* 2005;**5:**210–222.
2. Oosterhuis JW, Kersemaekers AM, Jacobsen GK, Timmer A, Steyerberg EW, van Weeren PC, *et al*. Morphology of testicular parenchyma adjacent to germ cell tumours; an interim report. *APMIS* 2003;**111:**32–42.
3. Donovan PJ, de Miguel MP. Turning germ cells into stem cells. *Curr Opin Genet Dev* 2003;**13**(5):463–471.
4. Toyooka Y, Tsunekawa N, Akasu R, Noce T. Embryonic stem cells can form germ cells *in vitro*. *Proc Natl Acad Sci USA* 2003;**100:**11 457–11 462.
5. Hubner K, Fuhrmann G, Christenson LK, Kehler J, Reinbold R, De La Fuente R, *et al*. Derivation of oocytes from mouse embryonic stem cells. *Science* 2003;**300:**1251–1256.
6. Clark AT, Bodnar MS, Fox M, Rodriquez RT, Abeyta MJ, Firpo MT, *et al*. Spontaneous differentiation of germ cells from human embryonic stem cells *in vitro*. *Hum Mol Genet* 2004;**13:**727–739.
7. Looijenga LHJ, Stoop H, De Leeuw PJC, De Gouveia Brazao CA, Gillis AJM, Van Roozendaal KEP, *et al*. POU5F1 (OCT3/4) identifies cells with pluripotent potential in human germ cell tumors. *Cancer Res* 2003;**63:**2244–2250.
8. Castrillon DH, Quade BJ, Wang TY, Quigley C, Crum CP. The human VASA gene is specifically expressed in the germ cell lineage. *Proc Natl Acad Sci USA* 2000;**97:**9585–9590.
9. Lau Y, Chou P, Iezzoni J, Alonzo J, Komuves L. Expression of a candidate gene for the gonadoblastoma locus in gonadoblastoma and testicular seminoma. *Cytogenet Cell Genet* 2000;**91:**160–164.
10. Honecker F, Stoop H, De Krijger R, Lau Y-FC, Castrillon DH, Bokemeyer C, *et al*. Pathobiological implications of the expression of markers of testicular carcinoma *in situ* by fetal germ cells. *J Pathol* 2004;**203:**849–857.
11. Latza U, Foss H-D, Durkop H, Eitelbach F, Dieckmann K-P, Loy V, *et al*. CD30 antigen in embryonal carcinoma and embryogenesis and release of the soluble molecule. *Am J Pathol* 1995;**146:**463–471.
12. Tam PP, Zhou SX. The allocation of epiblast cells to ectodermal and germ-line lineages is influenced by the position of the cells in the gastrulating mouse embryo. *Dev Biol* 1996;**178:**124–132.
13. Lawson KA, Dunn NR, Roelen BA, Zeinstra LM, Davis AM, Wright CV, *et al*. Bmp4 is required for the generation of primordial germ cells in the mouse embryo. *Genes Dev* 1999;**13:**424–436.
14. Rich IN. Hemopoietic-initiating cells. *J Perinat Med* 1995;**23:**31–38.
15. Chadwick K, Wang L, Li L, Menendez P, Murdoch B, Rouleau A, *et al*. Cytokines and BMP-4 promote hematopoietic differentiation of human embryonic stem cells. *Blood* 2003;**102:**906–915.
16. Nichols CR, Roth BJ, Heerema N, Griep J, Tricot G. Hematologic neoplasia associated with primary mediastinal germ-cell tumors. *N Engl J Med* 1990;**322:**1425–1429.
17. Hartmann JT, Nichols CR, Droz JP, Horwich A, Gerl A, Fossa SD, *et al*. The relative risk of second nongerminal malignancies in patients with extragonadal germ cell tumors. *Cancer* 2000;**88:**2629–2635.
18. Lee KC. Hematopoietic precursor cells within the yolk sac tumor component are the source of secondary hematopoietic malignancies in patients with mediastinal germ cell tumors. *Cancer* 1994;**73:**1535.
19. Woodruff K, Wang N, May W, Adrone E, Denny C, Feig SA. The clonal nature of mediastinal germ cell tumors and acute myelogenous leukemia. A case report and review of the literature. *Cancer Genet Cytogenet* 1995;**79:**25–31.
20. Geijsen N, Horoschak M, Kim K, Gribnau J, Eggan K, Daley GQ. Derivation of embryonic germ cells and male gametes from embryonic stem cells. *Nature* 2004;**427:**148–154.

Journal of Pathology
J Pathol 2006 (in press)
Published online in Wiley InterScience (www.interscience.wiley.com). **DOI:** 10.1002/path.1948

Original Paper

New evidence for the origin of intracranial germ cell tumours from primordial germ cells: expression of pluripotency and cell differentiation markers

CE Hoei-Hansen,[1]* A Sehested,[2] M Juhler,[3] Y-FC Lau,[4] NE Skakkebaek,[1] H Laursen[5] and E Rajpert-De Meyts[1]

[1]*University Department of Growth and Reproduction, Rigshospitalet, Copenhagen, Denmark*
[2]*Department of Paediatrics, Rigshospitalet, Copenhagen, Denmark*
[3]*Department of Neurosurgery, Rigshospitalet, Copenhagen, Denmark*
[4]*VA Medical Center, University of California, USA*
[5]*Department of Neuropathology, Rigshospitalet, Copenhagen, Denmark*

**Correspondence to:*
CE Hoei-Hansen, University Department of Growth and Reproduction, Section GR-5064, Rigshospitalet, Blegdamsvej 9, DK-2100 Copenhagen, Denmark.
E-mail: chh@dadlnet.dk

Received: 12 October 2005
Revised: 18 November 2005
Accepted: 28 November 2005

Abstract

Primary intracranial germ cell tumours are rare neoplasms that occur in children and adolescents. This study examined both the biology and the origin of these tumours, as it has been hypothesized that they originate from a totipotent primordial germ cell. We applied recent knowledge from gonadal germ cell tumours and analysed expression of a wide panel of stem cell-related proteins (C-KIT, OCT-3/4 (POU5F1), AP-2γ (TFAP2C), and NANOG) and developmentally regulated germ cell-specific proteins (including MAGE-A4, NY-ESO-1, and TSPY). Expression at the protein level was analysed in 21 children and young adults with intracranial germinomas and non-germinomas, contributing to a careful description of these unusual tumours and adding to the understanding of pathogenesis. Stem cell related proteins were highly expressed in intracranial germ cell tumours, and many similarities were detected with their gonadal equivalents, including a close similarity with primordial germ cells. A notable difference was the sex-specific expression of TSPY, a gene previously implicated in the origin of gonadoblastoma. TSPY was only detected in germ cell tumours in the central nervous system (CNS) from males, suggesting that it is not required for the initiation of malignant germ cell transformation. The expression of genes associated with embryonic stem cell pluripotency in CNS germ cell tumours strongly suggests that these tumours are derived from cells that retain, at least partially, an embryonic stem cell-like phenotype, which is a hallmark of primordial germ cells.

Keywords: germ cell tumours; central nervous system; intracranial; germinoma; non-germinoma; NANOG; OCT-4; C-KIT; AP-2γ; TSPY

Introduction

Primary central nervous system germ cell tumours (CNS GCTs) are rare neoplasms occurring predominantly in children and adolescents. Nearly 3% of malignant paediatric tumours are GCTs, of which one fifth arise in the brain [1,2]. The incidence has apparently been at a steady level over the last decades [3]. GCTs comprise a large variety of histologically distinct tumours [4,5]. The germinomas (equivalents of testicular seminomas and ovarian dysgerminomas) have features of undifferentiated germinal epithelium. Embryonal carcinomas (ECs) represent tumours of immature totipotent cells. Yolk sac tumours (YSTs) and choriocarcinoma follow an extraembryonic differentiation pattern and secrete α-fetoprotein (AFP) or human choriogonadotropin (HCG), respectively. Teratomas display an embryonal differentiation mimicking organ structures of all germ layers, with varying histological grade of maturity and malignantly transformed elements. Clinical presentation, typical localisation, tumour imaging, and serum tumour markers can in most patients establish the diagnosis [1]. A correct histological diagnosis is of high priority in CNS GCTs as this determines the choice of treatment.

It was first proposed by Teilum [6] that all GCTs, irrespective of site, develop from a common precursor, a totipotent primordial germ cell (PGC) capable of embryonic and extraembryonic differentiation. As far as extragonadal tumours are concerned, it was later hypothesized that these tumours may originate from ectopic germ cells that failed to undergo apoptosis and are retained in fetal life in the midline of the CNS [7]. In testicular adult, but not paediatric, GCTs this precursor has been identified by Skakkebaek as the carcinoma *in situ* (CIS) cell [8,9]. For extragonadal GCTs, the simultaneous presence of testicular CIS has been reported only in adult male patients, primarily

those with assumed primary retroperitoneal GCTs, which probably are secondary extragonadal neoplasms [10,11]. To our knowledge, association of CNS GCTs with CIS has not been reported; however, testicular biopsies are hardly ever performed in these patients.

A common origin of gonadal and non-gonadal GCTs has been studied by several approaches. Analyses of imprinting status supported a common origin of paediatric gonadal and paediatric non-gonadal GCTs [7], but non-gonadal GCTs arising in children display different genetic aberrations than adult GCTs, for example they often lack amplification of 12p [12]. On the other hand, intracranial GCTs resemble very closely morphologically their gonadal counterparts.

We examined the biology and origin of intracranial GCTs. We applied recent knowledge from gonadal GCTs, and selected proteins with cell differentiation-related biological functions or developmentally regulated expression patterns. We focused on stem cell-related proteins (NANOG, OCT-3/4, AP-2γ, C-KIT), and germ cell-specific proteins, including cancer/testis antigens, which are aberrantly activated in various cancers (MAGE-A4, NY-ESO-1), and TSPY, which was implicated as a cause of gonadoblastoma in dysgenetic gonads [13,14]. Finally, we analysed markers of gonadal supportive cells (Sertoli or granulosa cells), some also identified as markers for the neuroectodermal stroma (AMH, MIC2, NSE), which could be considered possible pro-survival factors for primordial germ cells (PGCs) in the CNS.

Patients, materials, and methods

Tissue samples

We included 13 male and 8 female patients (male : female ratio 1.63 : 1), median age 12 years (range 0–30) diagnosed with CNS GCTs in Zeeland, Denmark (or Greenland, patient M12) in 1987–2004. Tumours were localized in the midline of the brain (Table 1). Our series of formalin-fixed tissue comprised: 11 germinomas, one embryonal carcinoma, one YST with polyembryoma, one mixed malignant GCT, one mature and three immature teratomas, and two malignant teratomas. One tumour was not classifiable with standard immunohistochemical staining, but had GCT morphology (M12). The project was approved by the Regional Committee for Medical Research Ethics in Denmark.

Clinical characteristics of the patients

Information on clinical symptoms was analysed by retrospective review of records and was available in most patients. Symptoms at diagnosis included weight loss, headache, and visual disturbances. Five patients displayed diabetes insipidus, one amenorrhoea, one growth retardation, and one precocious puberty. In two patients the tumour was evident at birth (large teratomas). HCG and AFP were measured in serum or cerebrospinal fluid (CSF) in most patients. HCG was elevated above 3 IU/l in serum in 6/15 patients and in CSF in 4/13 patients. AFP was elevated above 0.02 μg/l in serum in 4/17 patients and in CSF in 3/12 patients.

Treatment in most patients was guided by the 'SIOP CNS GCT 1996' protocol. All patients initially had surgery. Two patients had a partial and one a total tumour excision. In three patients additional surgery was necessary owing to increased intracranial pressure. Sixteen patients received surgery, chemotherapy, and radiotherapy, two had only surgery, two had surgery and radiotherapy, and one had surgery and chemotherapy. One patient received pre-operative chemotherapy. Chemotherapy consisted of 2–4 series of cisplatinum/etoposide/bleomycin or carboplatinum/etoposide/ifosfamide. Radiotherapy dosage was either 54 Grey (2×15 Grey to the entire CNS and 2×12 Grey to tumour) or 40–54 Grey ($1.6–1.8 \times 25–30$) for patients receiving craniospinal radiotherapy.

The following post-therapeutic complications occurred: requirement for ventriculo-peritoneal shunt ($n = 6$), cerebral haemorrhage ($n = 2$), impaired vision ($n = 4$), facial nerve paresis ($n = 2$), reduced hearing/tinnitus ($n = 2$), hypothyroidism ($n = 9$), low growth hormone levels/impaired growth ($n = 5$),

Table 1. Histological type and site distribution of the 21 intracranial GCTs

Histology/localisation	Pituitary+ pineal	Pituitary+ suprasellar	Suprasellar	Pineal	Pineal+ mesence-phalon	Orbit	Posterior fossa	Frontal and parietal lobe
Germinoma ($n = 11$)	M5, F6, F8	F1, F7	F2	M4, M9, M10, M11	M3			
Non-classified GCT ($n = 1$)				M12				
Embryonal carcinoma ($n = 1$)				M13				
YST + polyembryoma ($n = 1$)				M14				
Immature teratoma ($n = 3$)						M15	M16	F17
Mature teratoma ($n = 1$)				M18				
Malignant teratoma w/germinoma ($n = 2$)			F19	M20				
Mixed GCT ($n = 1$)							F21	

M, male; F, female.
Information about the staining results of each patient's tumour is found in Table 3.

adrenal insufficiency ($n = 8$), diabetes insipidus ($n = 4$), and low testosterone ($n = 2$). Two patients had no post-therapeutic complications.

One patient (M3) had a brother, who had a testicular GCT, and one patient (F19) had a chromosomal imbalance and was mentally retarded (45XX,-13,-22,-der(13),t(13;22)(q34;q11,21)mat). Patients were followed up until June 2005 or until death (mean follow-up 6.1 years, range 0–15). Four of the 21 patients died. One patient died 1 week after birth. Recurrence occurred in three patients, of whom one died. Additionally, two patients died in the follow-up period, but records on cause of death were unavailable.

Immunohistochemistry

Immunohistochemical staining was performed once for each of the antibodies (Table 2) using a standard indirect peroxidase method as previously published [15–22]. Briefly, most of the dewaxed and rehydrated sections were pre-treated in a microwave oven in a buffer (either TEG buffer = TRIS 1.21g/l, EGTA 0.19g/l, pH = 9.0; urea buffer = 5% carbamide, pH = 8.5; Citrate buffer = 10 mmol/l, pH = 6.0), or in protease (Sigma-Aldrich, St Louis, MO, USA). Subsequently, the sections were incubated with 0.5–1.5% H_2O_2 to inhibit the endogenous peroxidase, followed by non-immune goat serum or human serum to block unspecific binding sites. Incubation with the primary antibody was overnight at 4 °C. Positive and negative controls were run with every staining; for negative control, a serial section was incubated with dilution buffer. A secondary biotinylated goat anti-mouse, rabbit anti-goat or goat anti-rabbit link antibody was applied, followed by horseradish peroxidase–streptavidin complex. Between all steps, sections were thoroughly washed. Visualisation was with aminoethyl carbazole substrate (all reagents from Zymed Laboratories, San Francisco, CA, USA), and light counterstaining with Mayer's haematoxylin. Control slides containing testicular neoplasms were analysed concomitantly. Initial diagnostic pathological evaluation included staining of the following in selected samples: CK, PAS, GFA, NF, S-100, Vimentin, CEA, LCA, CD3, CD20, CD68, TRA-1-60, 43-9F, and M2A.

Sections were examined under a light microscope (Zeiss Oberkochen, Germany) and scored independently and systematically by two investigators (CEHH and HL). There were no major discrepancies. In a few cases, scoring was repeated. Staining was assessed using an arbitrary semi-quantitative score of the proportion of cells stained (Table 3).

Fluorescence *in situ* hybridisation (FISH)

Preparation of the sections was similar to that described above. Sections were deparaffinized, rehydrated, and pre-treated with proteinase K solution/phosphate buffered saline (20 μg/ml; Invitrogen, Carlsbad, CA, USA). Dehydration was applied before denaturation of the slides together with probes specific for the X-chromosome (Texas red-labelled) and the Y-chromosome (FITC-labelled, green fluorescence) (the probes were a gift from DakoCytomation, Glostrup, Denmark). Sections were hybridized for 2 h, washed, dehydrated, and mounted in Antifade with DAPI II (125 ng/ml; Vysis Inc, IL, USA). Sections were examined using an epifluorescence microscope (Leica Microsystems Wetzlar, Germany) with ×100 magnification, and analysed using CytoVysion software (Applied Imaging, Newcastle, UK).

Results

Based on knowledge obtained from studies of testicular germ cell neoplasms and normal germ cells during development, we have allocated all proteins/markers analysed in this study into functional groups. Table 3 presents the results, which are briefly summarized below.

Table 2. Characteristics of antibodies

Antibody	Type	Pre-treatment	Dilution	Details
PLAP	PAb rabbit	Protease	1:400	A0268, DakoCytomation, Glostrup, Denmark
HCG	PAb rabbit	Protease	1:8000	A0231, DakoCytomation, Glostrup, Denmark
AFP	PAb rabbit	Protease	1:400	A0008, DakoCytomation, Glostrup, Denmark
OCT-3/4	MAb mouse	TEG buffer	1:300	C-10, sc-5279, Santa Cruz Biotechnology Inc, CA, USA
C-KIT	PAb rabbit	TEG buffer	1:400	CD117, A4502, DakoCytomation, Glostrup, Denmark
AP-2γ	MAb mouse	Urea buffer	1:50	6E4/4:sc-12762, Santa Cruz Biotechnology Inc, CA, USA
NANOG	PAb goat	Citrate buffer	1:50	AF1997, R&D Systems, MN, USA
CDH1	MAb mouse	Urea buffer	1:100	13-1700, Zymed Laboratories, San Francisco, CA, USA
MAGE-A4	MAb mouse	Citrate buffer	1:200	Gift from Gulio Spagnoli, Ludvig Inst. for Cancer Research, Lausanne, Switzerland
NY-ESO-1	MAb mouse	None	1:50	Gift from Gulio Spagnoli, Ludvig Inst. for Cancer Research, Lausanne, Switzerland
TSPY	PAb rabbit	TEG buffer	1:7000	From Chris Lau, VA Med Center, Univ. California, USA
NSE	MAb mouse	Citrate buffer	1:80	M0873, DakoCytomation, Glostrup, Denmark
MIC2	MAb mouse	TEG buffer	1:50	CD99, M3601, DakoCytomation, Glostrup, Denmark
AMH	MAb mouse	Urea buffer	1:150	Gift from Richard L Cate, Biogen (R.C), MA, USA

MAb, monoclonal antibody; PAb, polyclonal antibody; TEG buffer: TRIS 6.06g/5l, EGTA 0.95g/5l, pH = 9.0; urea buffer: 5% carbamide, pH = 8.5; citrate buffer: 10 mmol/l, pH = 6.0.

Table 3. Immunohistochemical staining of the intracranial GCTs

Patient ID/Histology	PLAP	HCG	AFP	OCT-3/4	C-KIT	AP-2γ	NANOG	CDH1	MAGE-A4	NY-ESO-1	TSPY	NSE	MIC2	AMH
F1 GERM	++	+−*	−	++	+	++	++	−	+	−	−	+−	−	−
F2 GERM	++	+−*	−	++	++	++	++	−	−	−	−	+−	−	−
M3 GERM	+	−	−	++	+	++	+	−	−	−	+−	−		−
M4 GERM	++	−	−	++	+−	++	++	−	−	−	++	−	−	−
M5 GERM	+	+−*	−	++	++	++	+	−	+	−	+−	+−	−	−
F6 GERM	++	+−*	−	−	++	++	++	−	−	−	−	+−	−	+**
F7 GERM	++	−	−	++	+	++	+	−	+	−	−	−	−	−
F8 GERM	++	+−*	−	+	++	++	+	−	−	−	−	−	−	−
M9 GERM	+	+−*	−	++	++	++	+	−	+	−	++	−	−	−
M10 GERM	++	−	−	−	++	−	+	−	−	−	++	−	−	−
M11 GERM	+	−	−	++	++	++	++	−	+	−	−	−	−	−
M12 UNCL GCT	−	−	−	−	−	−	−	−	−	−	−	−	−	−
M13 EC	++	+−*	−	+−	−	+−	++	+	−	−	−	−	−	−
M14 YST + POLEMBR	−	−	+	+	+−	+	+	−	+	+	+−	+−	−	−
M15 IMM TERA	+−	−	−	−	+−	−	−	+	−	−	−	+−	−	−
M16 IMM TERA	−	−	−	−	+−	−	−	−	−	−	−	+−	+−	−
F17 IMM TERA	+	−	+	−	−	−	−	+	−	−	−	−	−	−
M18 MAT TERA	−	−	−	−	+−	−	−	+	−	−	−	−	+−	−
F19 MAL TERA + GERM	+	−	−	++ (germ)	+ (germ)	++ (germ)	++ (germ)	+	−	−	−	−	−	−
M20 MAL TERA + GERM	+	+−*	−	++ (germ)	+ (germ)	++ (germ)	++ (germ)	+	+	−	++	−	+−	−
F21 MIX MAL GCT	+	−	+	−	+−	−	−	+−	−	−	−	+−	+−	−
Testicular control tissues														
Normal testicular tissue****	−	+−*	−	−	−	−	−	−	++ (spg)	+ (spg/c)	+ (spg)	−	++(Sertoli)	++***
Carcinoma *in situ*	++	−	−	++	++	++	++	−	+	−	++	+	−	−
Seminoma	++	+−*	−	++	++	++	++	−	+	−	++	−	−	−
Non-seminoma (teratoma)	+−	+−*	+−	++	+−	+	++	+−	−	−	+−	+−	++	−

GERM, germinoma; UNCL GCT, unclassified germ cell tumour; EC, embryonal carcinoma; YST + POLEMBR, yolk sac tumour and polyembryoma; IMM TERA, immature teratoma; MAT TERA, mature teratoma; MAL TERA + GERM, malignant teratoma with germinoma component; MIX MAL GCT, mixed malignant germ cell tumour with endosomal sinus tumour; spg, spermatogonia; spg/c, spermatogonia and spermatocytes. Staining intensity = ++, the majority of tumour cells stained; +, staining in approximately 50% of tumour cells; +−, few cells stained; neg, no positive cells detected.

* Staining in syncytiotrophoblast cells; ** staining outside tumour; *** staining in pre-pubertal Sertoli cells; **** normal testicular control sections were from adult males, except for AMH, where pre-pubertal testis was analysed.

Re-examination of well-established GCT markers

Placental alkaline phosphatase (PLAP), a marker of GCTs and PGCs, was detected in 17/21 GCTs. HCG staining was only seen in scattered syncytiotrophoblasts, which were present in eight samples. AFP staining was seen in the tumour containing YST + polyembryoma, and in gut-derived components of two non-germinomas.

Expression of transcription factors related to stem cell characteristics

The results for three proteins associated with pluripotency, OCT-3/4, AP-2γ, and NANOG, were very similar. They were all positive in most germinomas, in the sample containing YST + polyembryoma, and in the two malignant teratomas with germinoma components. Small differences were noted, eg AP-2γ expression was detected in some glandular elements of the malignant teratomas (Figure 1 shows a serial section comparison). In addition, the expression of C-KIT, a marker of several tissue-specific stem cells, was detected in all germinomas and 7/10 non-germinomas.

Expression of developmentally regulated germ cell-specific proteins

MAGE-A4 (melanoma antigen-encoding gene-A4) was expressed heterogeneously in half of the samples containing germinoma. Our antibody may also detect expression of other MAGE family members. Expression of MAGE-A4 was also seen in the YST + polyembryoma, which was the only tumour sample where NY-ESO-1 (CTAG1B/lAGE) was expressed; expression of the two was overlapping but not identical (Figure 2). TSPY (TSPY1, the testis-specific protein, Y-encoded) was positive in 7/13 tumours from male patients and negative in tumours from female patients. In selected cases where material was available, presence of Y-chromosome material was analysed by FISH. Y-probe signals were only detected in tumour samples from male patients (Figure 2).

Expression of markers of gonadal stroma and neuroectoderm

AMH (anti-Müllerian hormone, also known as MIS, Müllerian-inhibiting substance) was detected in the vicinity of one germinoma sample in distinct groups of

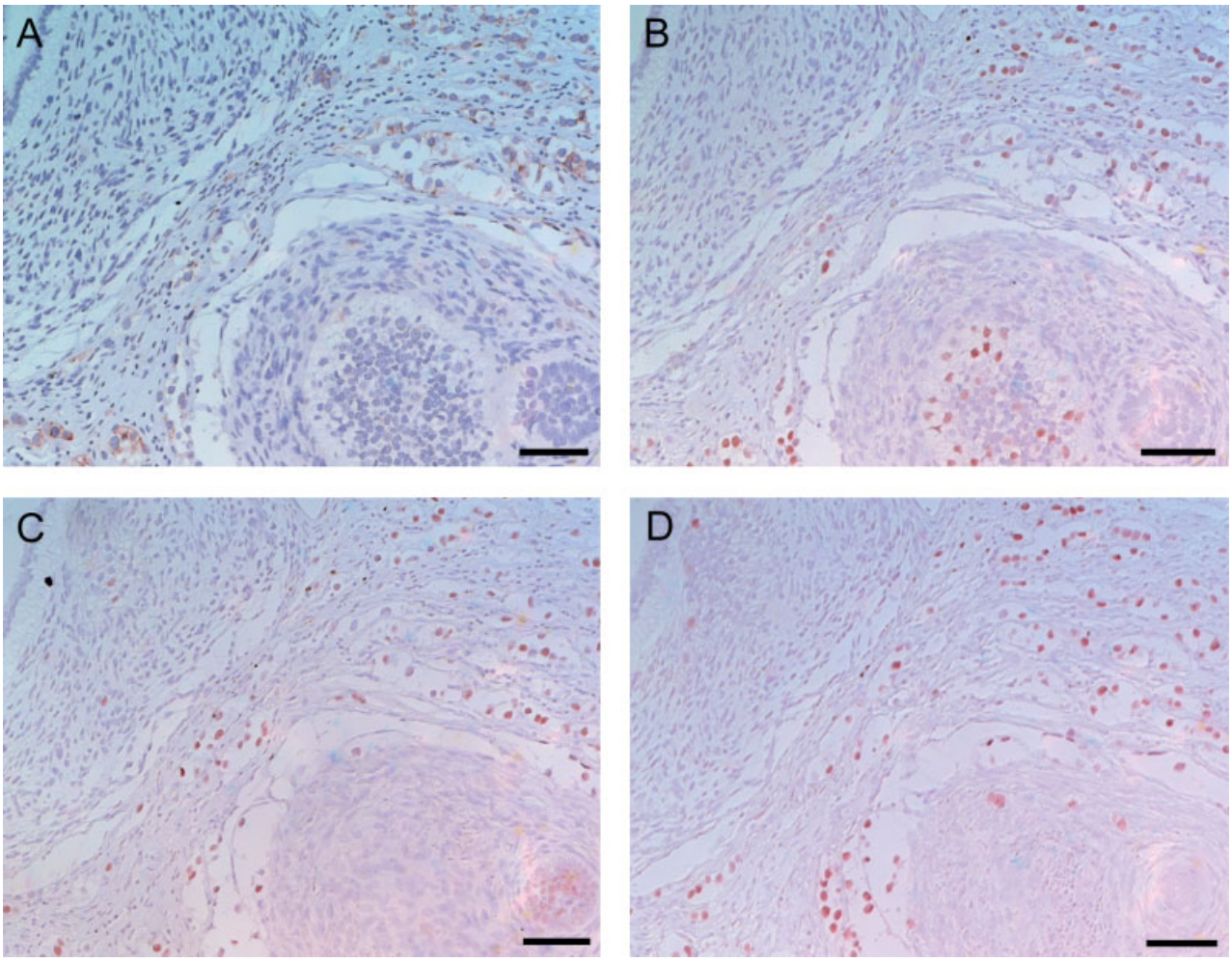

Figure 1. Expression pattern of four stem cell-related markers (C-KIT, OCT-3/4, AP-2γ, and NANOG) in serial sections of a malignant teratoma with germinoma component revealing many similarities. (A) C-KIT; (B) OCT-3/4; (C) AP-2γ; (D) NANOG. Scale bar = 50 μm

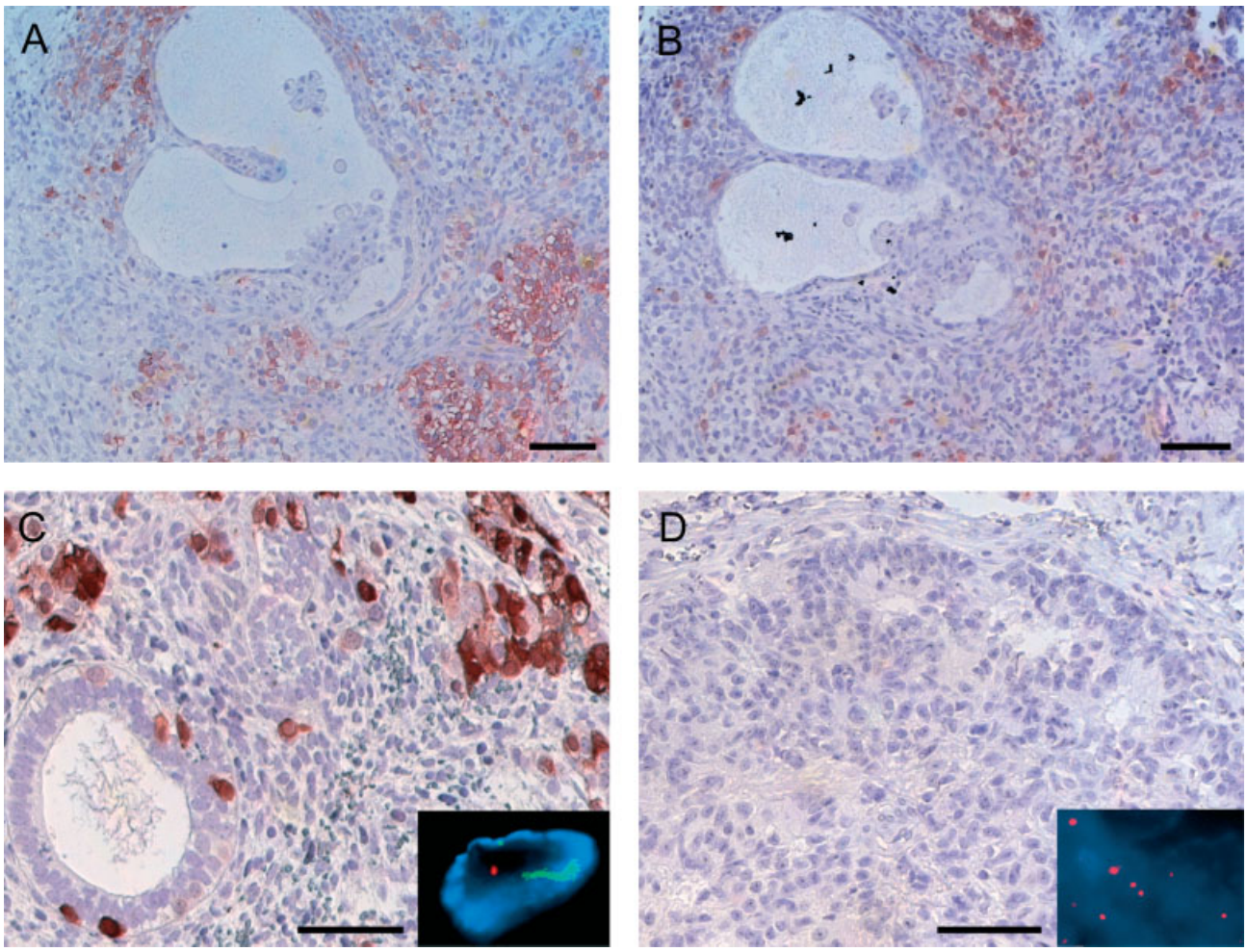

Figure 2. Examples of expression of genes related to germ cell properties. (A) MAGE-A4 and (B) NY-ESO-1 in YST + polyembryoma. (C) TSPY in a malignant teratoma (male patient). The inserted FISH image shows a cell from the same sample; chromosome X (red) and Y (green) material is present. (D) No TSPY staining in a mixed malignant GCT (female patient). The inserted FISH image from the same sample shows signal only from the chromosome X. Scale bar = 50 μm

cells, whereas all other samples were negative. MIC2 (CD99) staining was detected in a subset of the tumour samples in a small percentage of tumour cells, and also in neuroectodermal components. NSE (neuron-specific enolase) was first described as a marker of neuroendocrine tumours [23], but high levels have also been described in testicular GCTs and CIS, where NSE expression may be due to the increased gene dosage effect associated with the overrepresentation of isochromosome 12p [16,24,25]. CDH1 (E-cadherin) expression was seen in a subset of non-germinomas in epithelial elements. CDH1 is an adhesion glycoprotein primarily expressed in epithelial tissues that in testis is expressed in fetal gonocytes, seminomas, and non-seminomas, but not in adult testes [26].

Discussion

The pathogenesis of the rare intracranial GCTs remains poorly understood. We performed an extensive analysis of a panel of proteins in a series of 21 tumour samples of intracranial GCTs, which is one of the largest series ever examined in detail. Our patients had representative tumour types, age and sex distribution compared with previously published groups of patients.

The most important findings of this study concern the pattern of expression of genes associated with embryonic stem cell pluripotency and germ cell-specific genes, the majority never previously studied in CNS GCTs. We examined the question of whether CNS GCTs originate from displaced PGCs or rather from more undifferentiated stem cells, which for unknown reasons directly form embryonic-like tumours or tumours with a germinoma phenotype. The latter may be caused by the presence of factors facilitating germ cell specification in the midline area of the body. Our choice of genes was based on studies reporting their expression in testicular GCTs and in their precursor cell, CIS [27,28]. *OCT-3/4* (*POU5F1*, a POU-family transcription factor), and *NANOG* (a homeobox gene) are recently described key regulators of self-renewal and pluripotency features of embryonic stem cells [29–31]. Outside early embryonic development, OCT-3/4 and NANOG are only expressed in

PGCs, oogonia, and gonocytes, and are not expressed in spermatogonia or later stages of germ cell differentiation [20,22,32]. Therefore both proteins, but in particular OCT-3/4 for which excellent antibodies exist, are good markers for neoplastic germ cells in any location in the body, including CIS, gonadoblastoma, germinoma/dysgerminoma/seminoma, and ECs [20,22,32,33]. The presence of OCT-3/4 and NANOG in CNS GCTs suggests that some components of these tumours retain embryonic stem cell-like pluripotency, probably explaining the frequent presence of teratomatous somatic components.

We examined two representatives of the 'cancer/testis' gene family located on the X-chromosome, MAGE-A4 and NY-ESO-1 [34], which normally are germ cell-specific but reappear in various somatic cancers. Both are expressed in testis in spermatogonia/primary spermatocytes, but appear in gonocytes first around weeks 17–18, when they begin to differentiate into pre-spermatogonia [18,19,35]. They are heterogeneously expressed in CIS and classical seminoma (MAGE-A4) or spermatocytic seminoma (NY-ESO-1) [18,19]. In accordance with this pattern, we found heterogeneous staining of MAGE-A4 in some germinomas, but hardly any NY-ESO-1. We did not detect any sex-specific differences, as NY-ESO-1 was positive in only one (male) patient, and MAGE-A4-positive samples were detected in both sexes.

The results of the expression of another germ cell-specific gene, *TSPY* [36], provided a novel functional insight. It has been hypothesized that TSPY may be the gene in the Y chromosome GBY locus disposing dysgenetic gonads to gonadoblastoma [14]. It is expressed in gonocytes, spermatogonia, CIS, gonadoblastoma, and seminoma [14,26,37,38]. In a recent study of gonadoblastomas, the authors suggested that TSPY may be a marker of cells with invasive potential [37]. Another study detected the expression of TSPY in hepatocellular carcinoma, suggesting that it may be a novel cancer/testis antigen [39]. We did not find evidence supporting TSPY involvement in the malignant transformation, as it was only expressed in tumours from male patients. As germinomas in males and females exhibited virtually identical phenotype and clinical aggression, involvement of TSPY in intracranial GCT development can be excluded, and TSPY expression in gonadal tumours may simply be associated with presence of the Y-chromosome (or a part of it) in germ cells, thus reflecting the physiological phenotype of male germ cells.

We also investigated two proteins associated with various tissue-specific stem cells: AP-2γ (TFAP2C) and C-KIT tyrosine kinase receptor for stem cell factor (SCF). Both have a developmentally regulated expression pattern in the gonads (present only in immature gonocytes/oogonia) and are highly expressed in CIS, seminoma, and dysgerminoma [15,40,41]. Previously, a study reported AP-2γ expression in six germinomas [42]. Our analysis in a large series of CNS GCTs showed an AP-2γ expression pattern in CNS GCTs identical to that seen in gonadal tumours. The KIT/SCF system is of particular interest, because it was reported to have an anti-apoptotic function during PGC migration [43]. High expression of KIT detected in our study and in a previous study [44] is consistent with a hypothesis that KIT/SCF may be involved in survival of ectopic PGCs. Recently, a gain-of-function mutation in the *KIT* gene was found in bilateral testicular GCTs [45]. To our knowledge, similar studies have not yet been performed in CNS GCTs.

We were curious whether the presence of ectopic germ cells in the CNS would be associated with stromal cells having phenotypic features of cells physiologically accompanying and nourishing germ cells in the gonads. Therefore, we examined two markers for Sertoli/granulosa cells, MIC2 and AMH. MIC2 is a pseudoautosomal glycoprotein with functions related to cell adhesion and apoptosis. However, in addition to Sertoli cells, granulosa cell tumours, Sertoli cell tumours, and Leydig cell tumours, MIC2 is also expressed by T-cells, Ewings sarcoma, and is considered a marker for primitive neuroectodermal cells [46–49]. In accordance with that, we detected MIC2 in some neuroectodermal-like components of a subset of tumours. AMH (MIS) is a glycoprotein causing involution of Müllerian ducts in the fetus leading to male differentiation. AMH is expressed by immature Sertoli cells, granulosa cells, and by sex cord-stromal tumours [17,50]. No tumour samples were AMH positive, but we detected small groups of AMH-stained cells in the vicinity of one germinoma sample. We do not presently have an explanation for this, and cannot exclude the possibility of a genuine AMH expression in CNS or a cross-reaction with a related protein.

Expression of the classical markers of GCTs (PLAP, HCG, and AFP) was as expected. Most of the samples were PLAP positive, confirming its value as a good marker for CNS GCTs, mainly germinomas. Comparison of germinoma markers revealed that PLAP, C-KIT, and NANOG recognized all germinomas in our series, while AP-2γ recognized 91% and OCT-3/4 recognized 82%. We found no association of any of the studied markers with the clinical history and tumour progression.

In summary, analysis of the immunohistochemical expression pattern of a panel of classical and novel testicular GCT markers contributed to a careful description of their intracranial equivalents, and provided additional tools for differential diagnosis of rare intracranial tumours. We have improved phenotype characterization of these special tumours, and demonstrated that they retain several features of pluripotent embryonic stem cells, resembling in this respect testicular GCTs. As immature germ cells are the only cell type that retains pluripotency outside early embryonic life, our findings are consistent with the currently prevalent hypothesis that CNS GCTs originate from PGCs displaced during migration. It is, however, still not clear why a subset of the PGCs can survive and

later develop into tumours. In the testis, the dysgenetic and oncogenic development seems likely to be caused in part by exogenous, hormonal-like factors acting upon a genetically susceptible fetus [51]. Different mechanisms could lead to the intracranial GCTs, which apparently have not increased in incidence, as has been seen for testicular GCTs [3]. At present, a disturbance in the control of germ cell migration appears to be the most probable cause of CNS GCTs. The mechanisms are unknown and may include a mutation in one of the genes involved either in an anti-apoptotic or a pro-survival pathway during migration. Epigenetic changes leading to aberrant gene expression and protein dysfunction may also be involved. The presence of embryonic pluripotency genes along with germ cell-specific markers in CNS GCTs confirms their similarity to gonadal GCTs, with one important difference in the lack of precursor lesions, CIS/gonadoblastoma, which require the presence of male-specific genes. The combined results of this study argue against a role for TSPY in the pathogenesis of CNS GCTs and provide new evidence for the origin of these tumours from PGCs.

Acknowledgements

We thank H Kistrup, ID Garn, L Andersen, and A Meisler for skilful technical assistance, and M Ifversen for contribution to the initiation of the project. We also thank G Spagnoli and RL Cate for a generous gift of antibodies, and DakoCytomation for providing FISH probes.

This work was supported by grants from the Danish Cancer Society, Svend Andersen's Foundation, the Vissing Foundation, the Kirsten and Freddy Johansen's Foundation, and the Danish Medical Research Council.

Y-FC Lau is a research career scientist of the US Department of Veterans Affairs.

References

1. Gobel U, Schneider DT, Calaminus G, Haas RJ, Schmidt P, Harms D. Germ cell tumours in childhood and adolescence. GPOH MAKEI and the MAHO study groups. *Ann Oncol* 2000;**11:**263–271.
2. Felix I, Becker LE. Intracranial germ cell tumours in children: an immunohistochemical and electron microscopic study. *Pediatr Neurosurg* 1990;**16:**156–162.
3. Dreifaldt AC, Carlberg M, Hardell L. Increasing incidence rates of childhood malignant diseases in Sweden during the period 1960–1998. *Eur J Cancer* 2004;**40:**1351–1360.
4. Rosenblum MK, Matsutani M, VanMeir EG. CNS germ cell tumours. In *Pathology and Genetics of Tumours of the Nervous System*, Kleihues P, Cavanee WK (eds). IARC Press: Lyon, France, 2000; 208–214.
5. Friedman NB. The comparative morphogenesis of extragenital and gonadal teratoid tumours. *Cancer* 1951;**4:**265–276.
6. Teilum G. Classification of endodermal sinus tumour (mesoblatoma vitellinum) and so-called "embryonal carcinoma" of the ovary. *Acta Pathol Microbiol Scand* 1965;**64:**407–429.
7. Schneider DT, Schuster AE, Fritsch MK, Hu J, Olson T, Lauer S, *et al*. Multipoint imprinting analysis indicates a common precursor cell for gonadal and nongonadal pediatric germ cell tumours. *Cancer Res* 2001;**61:**7268–7276.
8. Skakkebaek NE. Possible carcinoma-in-situ of the testis. *Lancet* 1972;**2:**516–517.
9. Hawkins E, Heifetz SA, Giller R, Cushing B. The prepubertal testis (prenatal and postnatal): its relationship to intratubular germ cell neoplasia: a combined Pediatric Oncology Group and Children's Cancer Study Group. *Hum Pathol* 1997;**28:**404–410.
10. Bohle A, Studer UE, Sonntag RW, Scheidegger JR. Primary or secondary extragonadal germ cell tumours? *J Urol* 1986;**135**: 939–943.
11. Daugaard G, Rorth M, von der Maase H, Skakkebaek NE. Management of extragonadal germ cell tumours and the significance of bilateral testicular biopsies. *Ann Oncol* 1992;**3:**283–289.
12. Bussey KJ, Lawce HJ, Olson SB, Arthur DC, Kalousek DK, Krailo M, *et al*. Chromosome abnormalities of eighty-one pediatric germ cell tumours: sex-, age-, site-, and histopathology-related differences — a Children's Cancer Group study. *Genes Chromosomes Cancer* 1999;**25:**134–146.
13. Page DC. Hypothesis: a Y-chromosomal gene causes gonadoblastoma in dysgenetic gonads. *Development* 1987;**101:**151–155.
14. Lau Y, Chou P, Iezzoni J, Alonzo J, Komuves L. Expression of a candidate gene for the gonadoblastoma locus in gonadoblastoma and testicular seminoma. *Cytogenet Cell Genet* 2000;**91:**160–164.
15. Rajpert-De Meyts E, Skakkebaek NE. Expression of the c-kit protein product in carcinoma-in-situ and invasive testicular germ cell tumours. *Int J Androl* 1994;**17:**85–92.
16. Kang JL, Rajpert-De Meyts E, Skakkebaek NE. Immunoreactive neuron-specific enolase (NSE) is expressed in testicular carcinoma-in-situ. *J Pathol* 1996;**178:**161–165.
17. Rajpert-De Meyts E, Jorgensen N, Graem N, Muller J, Cate RL, Skakkebaek NE. Expression of anti-Mullerian hormone during normal and pathological gonadal development: association with differentiation of Sertoli and granulosa cells. *J Clin Endocrinol Metab* 1999;**84:**3836–3844.
18. Aubry F, Satie AP, Rioux-Leclercq N, Rajpert-De Meyts E, Spagnoli GC, Chomez P, *et al*. MAGE-A4, a germ cell specific marker, is expressed differentially in testicular tumours. *Cancer* 2001;**92:**2778–2785.
19. Satie AP, Rajpert-De Meyts E, Spagnoli GC, Henno S, Olivo L, Jacobsen GK, *et al*. The cancer-testis gene, NY-ESO-1, is expressed in normal foetal and adult testes and in spermatocytic seminomas and testicular carcinoma in situ. *Lab Invest* 2002;**82:**775–780.
20. Rajpert-De Meyts E, Hanstein R, Jorgensen N, Graem N, Vogt PH, Skakkebaek NE. Developmental expression of POU5F1 (OCT-3/4) in normal and dysgenetic human gonads. *Hum Reprod* 2004;**19:**1338–1344.
21. Hoei-Hansen C, Nielsen JE, Almstrup K, Graem N, Skakkebaek NE, Leffers H, *et al*. Transcription factor AP-2gamma is a developmentally regulated marker of testicular carcinoma in situ and germ cell tumours. *Clin Cancer Res* 2004;**10:**8521–8530.
22. Hoei-Hansen CE, Almstrup K, Nielsen JE, Brask SS, Graem N, Skakkebaek NE, *et al*. Stem cell pluripotency factor NANOG is expressed in human foetal gonocytes, testicular carcinoma in situ and germ cell tumours. *Histopathology* 2005;**47:**48–56.
23. Kaiser E, Kuzmits R, Pregant P, Burghuber O, Worofka W. Clinical biochemistry of neuron specific enolase. *Clin Chim Acta* 1989;**183:**13–31.
24. Niehans GA, Manivel JC, Copland GT, Scheithauer BW, Wick MR. Immunohistochemistry of germ cell and trophoblastic neoplasms. *Cancer* 1988;**62:**1113–1123.
25. Kawata M, Sekiya S, Hatakeyama R, Takamizawa H. Neuron-specific enolase as a serum marker for immature teratoma and dysgerminoma. *Gynecol Oncol* 1989;**32:**191–197.
26. Honecker F, Kersemaekers AM, Molier M, Van Weeren PC, Stoop H, De Krijger RR, *et al*. Involvement of E-cadherin and beta-catenin in germ cell tumours and in normal male foetal germ cell development. *J Pathol* 2004;**204:**167–174.
27. Skakkebaek NE, Berthelsen JG, Giwercman A, Muller J. Carcinoma-in-situ of the testis: possible origin from gonocytes and precursor of all types of germ cell tumours except spermatocytoma. *Int J Androl* 1987;**10:**19–28.
28. Almstrup K, Hoei-Hansen C, Wirkner U, Blake J, Schwager C, Ansorge W, *et al*. Embryonic stem cell-like features of testicular

carcinoma in situ revealed by genome-wide gene expression profiling. *Cancer Res* 2004;**64:**4736–4743.
29. Scholer HR, Hatzopoulos AK, Balling R, Suzuki N, Gruss P. A family of octamer-specific proteins present during mouse embryogenesis: evidence for germline-specific expression of an Oct factor. *EMBO J* 1989;**8:**2543–2550.
30. Chambers I, Colby D, Robertson M, Nichols J, Lee S, Tweedie S, *et al*. Functional expression cloning of Nanog, a pluripotency sustaining factor in embryonic stem cells. *Cell* 2003;**113:**643–655.
31. Mitsui K, Tokuzawa Y, Itoh H, Segawa K, Murakami M, Takahashi K, *et al*. The homeoprotein Nanog is required for maintenance of pluripotency in mouse epiblast and ES cells. *Cell* 2003;**113:**631–642.
32. Looijenga LH, Stoop H, de Leeuw HP, Gouveia Brazao CA, Gillis AJ, van Roozendaal KE, *et al*. POU5F1 (OCT3/4) identifies cells with pluripotent potential in human germ cell tumours. *Cancer Res* 2003;**63:**2244–2250.
33. Hattab EM, Tu PH, Wilson JD, Cheng L. OCT4 immunohistochemistry is superior to placental alkaline phosphatase (PLAP) in the diagnosis of central nervous system germinoma. *Am J Surg Pathol* 2005;**29:**368–371.
34. Boon T, Coulie PG, Van den EB. Tumour antigens recognized by T cells. *Immunol Today* 1997;**18:**267–268.
35. Takahashi K, Shichijo S, Noguchi M, Hirohata M, Itoh K. Identification of MAGE-1 and MAGE-4 proteins in spermatogonia and primary spermatocytes of testis. *Cancer Res* 1995;**55:**3478–3482.
36. Lau YF. Gonadoblastoma, testicular and prostate cancers, and the TSPY gene. *Am J Hum Genet* 1999;**64:**921–927.
37. Kersemaekers AM, Honecker F, Stoop H, Cools M, Molier M, Wolffenbuttel K, *et al*. Identification of germ cells at risk for neoplastic transformation in gonadoblastoma. *Hum Pathol* 2005;**36**: 512–521.
38. Schnieders F, Dork T, Arnemann J, Vogel T, Werner M, Schmidtke J. Testis-specific protein, Y-encoded (TSPY) expression in testicular tissues. *Hum Mol Genet* 1996;**5:**1801–1807.
39. Yin YH, Li YY, Qiao H, Wang HC, Yang XA, Zhang HG, *et al*. TSPY is a cancer testis antigen expressed in human hepatocellular carcinoma. *Br J Cancer* 2005;**93:**458–463.
40. Jorgensen N, Rajpert-De Meyts E, Graem N, Muller J, Giwercman A, Skakkebaek NE. Expression of immunohistochemical markers for testicular carcinoma in situ by normal human foetal germ cells. *Lab Invest* 1995;**72:**223–231.
41. Strohmeyer T, Reese D, Press M, Ackermann R, Hartmann M, Slamon D. Expression of the c-kit proto-oncogene and its ligand stem cell factor (SCF) in normal and malignant human testicular tissue. *J Urol* 1995;**153:**511–515.
42. Pauls K, Jager R, Weber S, Wardelmann E, Koch A, Buttner R, *et al*. Transcription factor AP-2gamma, a novel marker of gonocytes and seminomatous germ cell tumours. *Int J Cancer* 2005;**115:**470–477.
43. Molyneaux K, Wylie C. Primordial germ cell migration. *Int J Dev Biol* 2004;**48:**537–544.
44. Takeshima H, Kaji M, Uchida H, Hirano H, Kuratsu J. Expression and distribution of c-kit receptor and its ligand in human CNS germ cell tumours: a useful histological marker for the diagnosis of germinoma. *Brain Tumour Pathol* 2004;**21:**13–16.
45. Looijenga LH, de Leeuw H, van Oorschot M, van Gurp RJ, Stoop H, Gillis AJ, *et al*. Stem cell factor receptor (c-KIT) codon 816 mutations predict development of bilateral testicular germ cell tumours. *Cancer Res* 2003;**63:**7674–7678.
46. Visfeldt J, Cortes D, Thorup JM, Byskov AG. Anti-MIC2 as a tool in examination of testicular biopsies. *APMIS* 1999;**107:**631–635.
47. Kommoss F, Oliva E, Bittinger F, Kirkpatrick CJ, Amin MB, Bhan AK, *et al*. Inhibin-alpha CD99, HEA125, PLAP, and chromogranin immunoreactivity in testicular neoplasms and the androgen insensitivity syndrome. *Hum Pathol* 2000;**31:**1055–1061.
48. Al Bozom IA, El Faqih SR, Hassan SH, El Tiraifi AE, Talic RF. Granulosa cell tumour of the adult type: a case report and review of the literature of a very rare testicular tumour. *Arch Pathol Lab Med* 2000;**124:**1525–1528.
49. Comperat E, Tissier F, Boye K, De Pinieux G, Vieillefond A. Non-Leydig sex-cord tumours of the testis. The place of immunohistochemistry in diagnosis and prognosis. A study of twenty cases. *Virchows Arch* 2004;**444:**567–571.
50. Matias-Guiu X, Pons C, Prat J. Mullerian inhibiting substance, alpha-inhibin, and CD99 expression in sex cord-stromal tumours and endometrioid ovarian carcinomas resembling sex cord-stromal tumours. *Hum Pathol* 1998;**29:**840–845.
51. Skakkebaek NE, Rajpert-De Meyts E, Main KM. Testicular dysgenesis syndrome: an increasingly common developmental disorder with environmental aspects. *Hum Reprod* 2001;**16:**972–978.